TÉCNICO LISBOA

Synthesis of PE-based nanoparticles from an original surfactant-free emulsion polymerization process of Ethylene using RAFT technique

Ricardo Luís Ferreira da Silva

Thesis to obtain the Master of Science Degree in

Chemical Engineering

Supervisors:

Prof. Dr. Maria do Rosário Gomes Ribeiro

Dr. Frank D'Agosto

Dr. Muriel Lansalot

Dr. Vincent Monteil

Examination Committee

Chairperson: Prof. Dr. Maria Filipa Gomes Ribeiro

Supervisor: Prof. Dr. Maria do Rosário Gomes Ribeiro

Member of the Committee: Prof. Dr. Ana Margarida Sousa Dias Martins

2015

This page was left intentionally in blank.

Acknowledgments

Foremost, I would like to express my gratitude to my supervisor Prof. Dr. Maria do Rosário Ribeiro for accepting my internship, all the guidance and support and for examining my Master thesis. Besides my advisor, I would like to thank the rest of my thesis committee, Prof. Dr. Ana Margarida Sousa Dias Martins for accepting to examine my thesis and Prof. Dr. Maria Filipa Gomes Ribeiro, chairperson of the jury.

I am extremely grateful to Dr. Vincent Monteil, Dr. Frank D'Agosto and Dr. Muriel Lasanlot for accepting me in this research project and providing all the conditions that allowed me to work on it. I would like to thank them for their support, motivation, and fruitful discussions, sharing their immense scientific knowledge. Furthermore, their guidance and patience helped me in all stages of the research project and specially when writing this thesis.

My sincere thanks also goes to all the LCPP team, who kindly supported and provided me knowledge that allowed me to perform the experimental procedures and analyse the data acquired in this project. In particular, I would like to thank to Arthur Zarrouki, Thiago Guimarães, Islem Belaid, Manel Taam, Pierre-Yves Dugas and Ming Koh.

A special thanks to Mathieu Fuentes for his friendship and all the help in this project, to Matthieu Humbert and all the Portuguese co-workers and friends for providing me unforgettable moments during my stay in Lyon.

Lastly, and most important, I would like to thank my family: to my mother, my brother and Catarina for their endless love and support in every moment of my life.

This page was left intentionally in blank.

Abstract

Taking advantage of the recently established controlled radical polymerization of ethylene mediated by xanthates and the expertise of the C2P2 team in the emulsion polymerization of ethylene, this thesis is a contribution to the study of the synthesis of polyethylene-based nanoparticles by implementation of reversible addition-fragmentation chain transfer (RAFT) polymerization of ethylene in the emulsion process from water-soluble functional polymers. The mechanism of particle formation proceeds without surfactants by polymerization-induced self-assembly of amphiphilic block copolymers (PISA process).

This project was divided into four sections. The first part of this project consisted in the synthesis and purification of the macroRAFT (polyethylene glycol end-functionalized with xanthate, PEG-X) used in the polymerizations mediated by xanthates, which was prepared by post-modification of an existing polymer. The characterization of the resulting product validated its properties, which allowed to proceed to the polymerization procedures.

The second section consisted in the acquisition of experimental data to evaluate the effect of the presence of PEG-X in the ethylene polymerization. Thus, several polymerizations were performed at 70°C and 100 bar of ethylene pressure, with and without surfactant, in the presence of either the macroRAFT agent or its non-functional counterpart (PEG-OH). It was found that indeed the polymerizations were strongly influenced by the presence of the macroxanthate.

The third part consisted in the study of the influence of the macroRAFT/initiator molar ratio on the polymerization. This study was carried out at 70°C and 100 bar maintaining the standard initiator concentration, varying the quantity of the macroRAFT. It appeared that the ratio strongly influenced the yield of PE.

The last part involved the kinetic study of the polymerization in the presence of the macroRAFT agent (at 70°C) and inherently a study on the effect of the pressure on this polymerization given that this study was performed at two different pressures (100 and 200 bar). The increase in pressure appeared to affect the stabilization of the obtained latexes, particularly for long polymerization times.

Key words: Polyethylene, free radical emulsion polymerization, RAFT, MADIX, PISA.

This page was left intentionally in blank.

Resumo

Tendo por base a polimerização controlada do etileno mediada por xantatos estabelecida recentemente pela equipa de investigação do C2P2 e beneficiando do vasto conhecimento da equipa na polimerização em emulsão do etileno, esta tese é uma contribuição para o estudo da síntese de nano-partículas baseadas em polietileno. A síntese ocorreu através da implementação da técnica de controlo de polymerização *reversible addition-fragmentation chain transfer (RAFT)* em emulsão, a partir de polímeros funcionais solúveis em água. O mecanismo pelo qual as partículas se formam ocorre sem surfactante pelo processo *polymerization-induced self-assembly (PISA),* onde se dá a formação das nanopartículas por auto-assemblagem de copolímeros anfifílicos em bloco.

Este projeto foi dividido em quatro secções. A primeira consistiu na síntese e purificação do agente macroRAFT (polietileno glicol funcionalizado com xantato na terminação da cadeia, PEG-X) usado nas polimerizações mediadas por xantatos, que foi preparado por funcionalização de uma cadeia polimérica pré-existente. A caracterização do produto resultante validou as suas propriedades (estrutura, massa molar, etc.), o que permitiu prosseguir para os procedimentos de polimerização.

A segunda parte consistiu na aquisição de dados experimentais de forma a avaliar o efeito da presença de PEG-X na polimerização de etileno. Assim, as polimerizações foram efetuadas a 70℃ e 100 bar (pressão de etileno), com e sem surfactante, na presença de macroRAFT (PEG-X) ou na presença do seu homólogo não funcional (PEG-OH). Ficou demonstrado que as polimerizações são fortemente influenciadas pela presença do macroxantato.

Na terceira parte do projeto foi realizado um estudo da influência do rácio molar entre o agente macroRAFT e a espécie iniciadora da polimerização. Este estudo foi novamente realizado a 70℃ e 100 bar mantendo a concentração inicial de iniciador e variando a quantidade de macroRAFT. Aparentemente o rácio entre estas espécies influenciou fortemente o rendimento da polimerização em PE.

A quarta e última parte deste projeto consistiu no estudo cinético da polimerização em presença do agente macroRAFT PEG-X (a 70℃) que envolveu intrinsecamente um estudo do efeito da pressão no sistema, realizado a duas pressões diferentes (100 e 200 bar). A polimerização aparentou ser afetada pelo aumento da pressão, originado latexes menos estáveis, principalmente a elevados tempos de reação.

Palavras Chave: Polietileno, polimerização radicalar em emulsão, RAFT, MADIX, PISA

This page was left intentionally in blank.

Table of contents

List of tables

List of figures

Glossary

AA	Acrylic Acid
ACPA	4,4′-Azobis(4-cyanovaleric acid
AIBA	2,2′-Azobis(2-methylpropionamidine) dihydrochloride
AIBN	2,2'-Azobisisobutyronitrile
APS	Ammonium Persulfate
CMC	Critical micelle concentration
Cryo-TEM	Cryogenic transmission electron microscopy
CRP	Controlled radical polymerization
CTAB	Cetyl trimethylammonium bromide
Đ	Dispersity
D_2O	Deuterium oxide
DCM	Dichloromethane
DEC	Diethyl carbonate
DLS	Dynamic light scattering
DMC	Dimethyl carbonate
DSC	Differential scanning calorimetry
FREPE	Free radical emulsion polymerization of ethylene
FRP	Free radical polymerization
FRPE	Free radical polymerization of ethylene
IPA	Isopropyl alcohol
HDPE	High density polyethylene
LCB	Long chain branching
LDPE	Low density polyethylene
LLDPE	Linear low density polyethylene
M_n	Number-average molar mass
M_w	Weight-average molar mass
MWD	Molar weight distribution
MADIX	Macromolecular Design via the Interchange of Xanthates
NMR	Nuclear magnetic resonance
P	Pressure
PAA-X2	Polyacrylic acid end-functionalized with xanthate
PC	Polymer content
P_{crit}	Critical pressure
PDI	Polydispersity index
PE-X	Polyethylene-xanthate
PEG-OH	Poly(ethylene glycol)
PEG-X	Xanthate-functionalized polyethylene glycol
$P_{ethylene}$	Ethylene pressure
PE	Polyethylene
PISA	Polymerization-induced self-assembly
RAFT	Reversible addition-fragmentation chain transfer
SCB	Short chain branching
SDS	Sodium dodecylsulfate
SEC	Size exclusion chromatography
SC	Solid content
T	Temperature
T_c	Crystallization temperature
T_{crit}	Critical temperature
TCB	1,2,4-trichlorobenzene

TEA	Triethylamine
TEM	Transmission electron microscopy
THF	Tetrahydrofuran
T_m	Melting temperature
UHMWPE	Ultra-high molecular weight polyethylene
VAc	Vinyl acetate
VLDPE	Very low density polyethylene
VOCs	Volatile organic compounds
X_c	Crystallinity percentage
Z_{av}	Average particle size, obtained by DLS

Introduction

Scope & Aim

Being the most produced polymer in the world, polyethylene (PE) success is due mainly to its low production cost, easy processability, chemical inertia and mechanical properties, which provides it with a wide range of applications. PE is produced via two types of processes: a catalytic way, under mild conditions (T<150°C and P>40 bar) and through a radical process under harsh conditions (T>200°C and P>40 bar).

Additionally, PE can be used in an aqueous dispersion form, with application such as in coatings (e.g. for papers). After more than 70 years since its industrial production started, the team of C2P2 showed that it was still possible to innovate in free radical polymerization of ethylene (FRPE), recently reporting the free radical emulsion polymerization of ethylene (FREPE) under mild conditions (T<100°C and P<250 bar).

Taking advantage of the progress in FRPE under mild conditions, the team investigated the controlled radical polymerization (CRP) of ethylene in an organic solvent through *reversible addition-fragmentation chain transfer* (RAFT) polymerization mediated by xanthates, presenting the first example of a controlled radical polymerization (CRP) of ethylene using RAFT.

The emulsion polymerization (EP) process requires the use of surfactants that may sometimes be detrimental to the final application. Hence, it was appealing to find alternatives in which surfactants, such as amphiphilic di-block copolymers, are both produced in situ and covalently anchored at the surface of the final particles. With the developments of the CRP in water, FREPE was performed according to the polymerization-induced self-assembly (PISA) process – in which basically a hydrophilic living polymer chain is grown in a first step and chain-extended in water with a hydrophobic monomer, creating block copolymers that will self-assemble into nano-sized self-stabilized particles. The C2P2 team recently managed to perform PISA using RAFT according to a one pot process where the hydrophilic and the hydrophobic block are formed successively in the same reactor in water.

Gathering the recently established CRP of ethylene mediated by xanthates and the expertise of the C2P2 team in the emulsion polymerization of ethylene, the PISA process of ethylene achieved through RAFT mediated by xanthates was found to be a very interesting research area to investigate. This constitutes the aim of this project: develop the synthesis of PE-based nanoparticles from an original surfactant-free emulsion polymerization of ethylene using RAFT technique.

Outline of the manuscript

This thesis comprises three chapters. The first chapter (chapter I) corresponds to an up-to-date bibliographic review of the most relevant aspects of polymerization to this project.

Chapter II presents the experimental part, including materials, experimental set-up, polymerization procedures and polymer characterization methodologies.

Chapter III concerns the experimental results and the discussion of the different polymerizations studies, with the possible conclusions from these studies.

This page was left intentionally in blank.

Chapter I - Literature Review

This page was left intentionally in blank.

1 - Polyethylene

Polyethylene, PE, is the most produced polymer in the industry of synthetic polymers. Being considered a commodity, the production of this highly demanded polymer reached around 78 Million tons in 2012. Furthermore, its consumption continues to show a clear increase in the world every year. [1]

PE is produced from ethylene, a gaseous monomer obtained predominantly from the petrochemical industry, by thermal cracking of natural gas or crude oil, however other sources independent from the latter, such as bioethanol, are acquiring an increasing importance. [2], [3]

A great number of reasons can be enumerated to explain the enormous commercial success of polyethylene in the world and its day-to-day use. One of these main reasons is the low production cost of PE, being one of the least expensive polymers in the market, about 1500 $ m^{-3} in 2012. [1]

Polyethylene is the simplest polymer that can be produced, if considered that it is only composed by carbon and hydrogen atoms. They can be arranged in the simplest structure of polyethylene, a long backbone formed of an even number of covalently bonded carbons with a pair of hydrogen atoms linked to each carbon, except for the chain ends that are terminated by methyl groups. [1], [2]

In the simplest PE structure, the absence of large pendant groups and short chain grafts on the main backbone structure allows it to fold in an organized manner leading to the crystallization of the polymer, a phenomenon that occurs when a solid domain is created. Even though this phenomenon is very common in the PE formation, not all the chains segments comply with this arrangement. Some of them are not perfectly linear, with the presence of short chain branches and chain-end groups, which hinder the crystallization and lead to the formation of amorphous domains, flexible areas wherein the chains can move with a certain freedom degree. In terms of morphology, that is, the molecular organization in a solid or molten polymer, PE can thus be categorized as semi-crystalline: parts of its chains are in crystalline domains and others are in amorphous areas, providing the latter with three zones, i.e. crystalline and amorphous domains as well as an interfacial region between the first two, as seen in Figure 1.

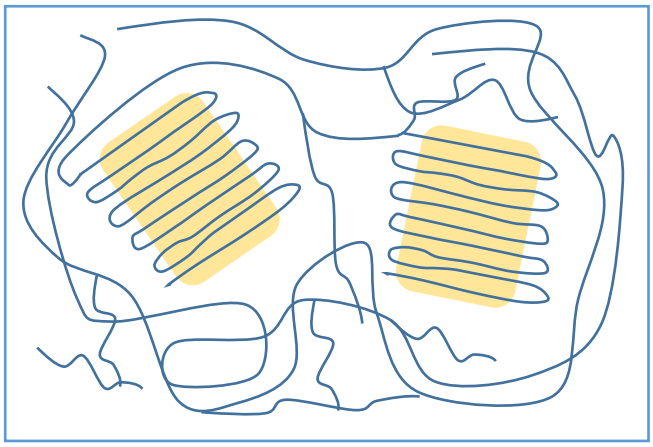

Figure 1-Cristalline (orange background), amorphous, and interfacial domains of PE.

The structure of polyethylene provides it with a great thermal stability and low toxicity. In addition, considering that the branching (long and short) in PE can be modified with relative ease, via the selection of the process of production, different crystallinities, rheological behaviours and related properties will be obtained leading, consequently, to a wide selection of commercial applications. [2], [3]

1.1 – Polyethylene properties

As it will be shown below, two main synthetic routes can be considered to produce polyethylene, radical and catalytic, yielding, consequently, different kinds of polymer. The polymerization via a radical process, which is largely employed in industry, operates under harsh conditions (high pressure of ethylene, $P \approx 1000 \text{ to } 4000 \text{ bar}, T \approx 300°C$) generating high branching degree with large amounts of long-chain (LCB) and short-chain branches (SCB). On the other hand, the conditions involved in the catalytic route are much milder (relative low pressure of ethylene $P \approx 30 - 40 \text{ bar}, T < 100°C$). The polymers produced via this route are provided with a controlled branching degree and basically, at the industrial scale, only the short chain branching occurs with controlled branches' lengths. [2], [4]

Depending on the synthetic route of production of polyethylene different kinds of PE will be yielded. A common way to classify these kinds of PE consists in sorting them by density, i.e., low and high density, polyethylene grades. The density is tightly linked to the branching type of the polymer (and branching degree) and to the crystallinity, which allows to predict the physical properties of the PEs fairly well.

Additionally, polyethylene is by its nature relatively chemically inert. [2] Among the inherent properties of the different types of PE, this particular characteristic provides a broad range of applications to PE, because it presents a good resistance to environmental degradation and solvents, which allows it to be used in packaging for example (films, containers, etc.). However, the advantage of these properties can raise environmental concerns, given that if not treated properly, wastes of PE can accumulate for long periods of time. [5]

1.1.1 – Polyethylene specific properties

As said above polyethylene can be divided in two main categories, low and high density PEs, which include different types of PE that have their own properties. Herein are presented, for each kind of PE, some of the properties that have a particular importance to this polymer, such as density, crystallinity and melting temperature.

1.1.1.2 Low Density Polyethylene

The low density category includes several types of PE, such as the low density polyethylene, LDPE (density of 0.91-0.94 g cm^{-3} -Figure 2), linear low density polyethylene LLDPE (density of 0.90-0.94 g cm^{-3} - Figure 3) and for last, very low density polyethylene, VLDPE (density = 0.86-0.90 g cm^{-3} - Figure 4). [2], [4] These low densities are due to the high degree of short chain branching exhibited by these types of PE which, as said before, also hinders the formation of crystalline domains. This last characteristic is related to the macroscopic properties of PE, in particular the rigidity, leading for example to the high flexibility of low density polyethylenes.

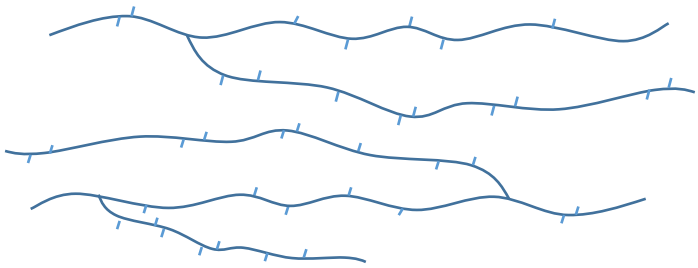

Figure 2- LDPE.

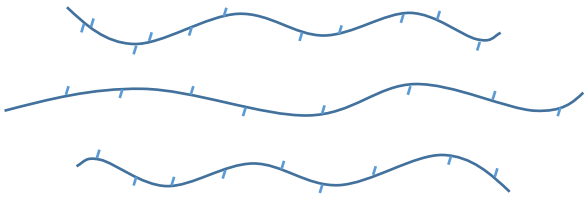

Figure 3- LLPE.

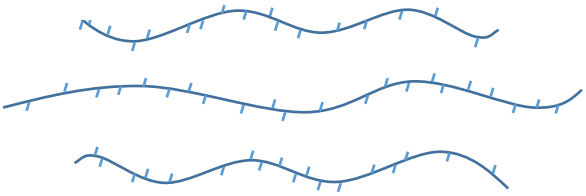

Figure 4- VLDPE.

LDPE, also called *high-pressure polyethylene*, [6] is synthesized through a free radical polymerization process unlike the other low density PEs. Due to existence of a high density of both long and short-chain branches, along the main backbone LDPE is characterized by having low tensile modulus, being extremely ductile and generally translucent and easily pliable - a films of LDPE can deform uniformly when stretched, with little (if any) whitening in the strained regions, showing substantial deformation before the onset of tearing, which does not proceed readily – this characteristic provides it with several applications in the packaging field (films, bags, etc.). [2] The degree of crystallinity of LDPE varies between 42 and 62% and its melting temperature, T_m, which ranges from 98 to 115℃.

Unlike LDPE, LLDPE contains only SCB, and is characterized by having a broad molar mass distribution. LLDPE is produced through a catalytic process and when made using Ziegler-Natta catalysts tends to have more polymer of the lower molar mass fraction and less of the high molar mass fraction. [4] The tensile modulus of LLDPE is higher than LDPE and usually has lower values of crystallinity, ranging from 34 to 62% and its melting temperature is comprised between 100 and 125℃. [2] LLDPE can have applications similar to the ones of LDPE, being produced in thin transparent films that are highly resistant to puncture or tear.

At last VLDPE presents similar characteristics to LLDPE, although it has a higher density of short chain branching that, once again prevents the formation of large crystalline domains, decreasing its crystallinity. The degree of crystallinity varies between 4 and 34% and its melting temperature ranges from 60 to 100℃. [2] In terms of applications it can be used in packaging films but has a lower tensile strength. Thus these films are very soft and are readily deformed. [2], [4]

In this group (low density PEs), LDPE differs from the other low density PEs mainly due to the presence long chain branches that strongly affect the rheological behaviour of the polymer, in both shear and extension. This has a significant importance in the processing of LDPE, mainly in the shear thinning and strain hardening phenomena, allowing the better performance of the extrusion process at low temperature and requiring less power to operate. [3]

1.1.1.2 – High density polyethylene

High density polyethylene, HDPE, alongside LDPE, represents the majority of the thermoplastic world market, [7] being the most produced PE in the world, with around 36 Mtons in 2012. [1] HDPE is synthesized through a catalytic route using coordination catalysts. [6] This type of polyethylene is a predominantly linear polymer being chemically the closest in structure to pure PE (i.e. linear PE chain). As seen in Figure 5, HDPE is basically unbranched (low degree of short chain branching). Consequently, with a very low level of defects to hinder organization, a very high degree of crystallinity can be achieved, resulting in PE that has high density. [4] When compared to LDPE, HDPE has increased tensile strength, stiffness and chemical resistance. In addition, most HDPEs have number-average molar masses ranging from 50 to 250 kDa. The produced materials have a wide range of applications, being mainly used in containers, housewares, industrial wrappings, pipes etc., complementing the applications of LDPEs category. The density of HDPE ranges from 0.94 to 0.97 g cm^{-3}, the degree of crystallinity varies in the range from 62 to 82% and its melting temperature, T_m, varies from 125 to 135°C. [2], [4]

Figure 5 - HDPE

Besides the typical HDPE there are various specialty types of HDPEs, such as high and ultra-high molecular weight. Materials with such types of PE have some interesting/peculiar characteristics, like increased tensile strength, elongation, etc. High-molecular-weight high-density, HMWPE polyethylene (0,25 to 1,5 MDa) for instance, is used for pressure piping in mining, industrial, oil, and water applications. Ultrahigh-molecular-weight high-density polyethylene (>1.5 MDa) has very high abrasion resistance and impact strength, the highest of any thermoplastic material with applications in the mining and freight industries as well as in agricultural and earthmoving machinery. [6]

In sum, low density polyethylenes are characterized by having low molar mass, exhibiting a rather low degree of crystallinity and flexibility. The higher density PEs are prone to have higher crystallinity, with their main features being the combination of light weightiness and strong mechanical properties, which allows to complement the applications of low density PEs.

Knowing the enormous commercial importance of polyethylene and properties of the several polyethylene grades it is found relevant to briefly describe the synthesis routes that lead to the different types of PE mentioned above, with particular interest in the free radical process, used in this study, before reviewing the underpinning concepts of this project.

2- Synthesis routes of Polyethylene

The polymerization of ethylene can be performed via two main routes. Either by a free radical polymerization process, which requires the use of radical initiators being normally performed at high pressure and relative high temperature, or by the catalytic route, which involves the use of organometallic catalysts (coordination insertion polymerization) and normally requires much lower pressures than the free radical process. [8] As mentioned before, the two production methods influence the structure of the obtained polymer, yielding different types of polyethylene. The free radical process originates branched polymer chains, exhibiting long and short chain branches, whereas organometallic coordination catalysts leads to the synthesis of linear or regularly branched polymer chains. The polymerization of ethylene can be carried out either in solution, slurry or in bulk, given that at pressures above 100MPa, ethylene is in its supercritical state (T_{crit}= 9,2°C, P_{crit}=50,4 bar) [9] acts as solvent for polyethylene. [8], [10]

This section is not meant to provide the reader with an accurate review of all possible production processes, which would be out of scope of this work, and will thus focus on the description of the free radical process used in this project.

2.1 Free radical polymerization of ethylene – LDPE

Historically, the development of PE, nowadays, a highly demanded polymer and an integral part of everyday life did not proceed smoothly. As many other scientific discoveries polyethylene was produced serendipitously several times before the utility of synthetic polymer field was appreciated. Thus, the production of polyethylene can be separated in several distinct periods. It was not until the 1930s that chemists, attempting to produce an entirely different product, inadvertently created polyethylene and recognized its potential. However, previously to that period, the (pre-1930's) incidental production of PE took place with the first record of the preparation being reported in 1898 by H. von Pechmann, followed shortly after by his colleagues, E. Bamberger and F. Tschirner, that characterized the white, waxy substance that was produced, recognizing that it contained long -CH_2- chains and termed it *polymethylene*. [11] In both cases PE was produced by the decomposition of a diazomethane mixture. However the commercial significance of this discovery was unappreciated at the time and further investigations were only resumed in the early 30's of the twentieth century. [12]

Alongside other studies being realized in the 1930s, the British company Imperial Chemical Industries, ICI, set a great research program in order to investigate the high pressure chemistry of some organic compounds, including ethylene. Where other contemporaries ended-up failing to understand, once again, the potential of the obtained material, the researchers of ICI, E. Fawcett and R. Gibbon, after several attempts of an experiment that failed in its intended purpose[1], they noticed that a small quantity of a white waxy solid was found lining the reaction vessel. The product was later identified as a polymer of ethylene, being this the first time that its existence was recognized. [12]

The reaction was not reproducible and after several attempts that led to uncontrollable outcomes especially in terms of exothermicity, accompanied by the inherent increase of pressure, in 1935 the proper conditions that would allow the consistent polymerization of ethylene to take place were set. In 1936 ICI took out the first patent on the manufacture of polyethylene. [13]

[1] High pressure reaction of ethylene with benzaldehyde (the benzaldehyde was recovered unchanged).

The materials yielded by this process were ductile with melting temperature of about 115°C and had some of the characteristics of the PE type that we call today LDPE. [14] These properties were investigated and some of them like their flexibility and chemical inertness led to the recognition of these materials as a great electric insulators for coaxial cables aiming at the commercialization in the open market.

Great efforts to scale up the production of PE were made, involving the design of a reaction vessel capable of withstanding a pressure over 1500 bar. However, at the time that the production lines were ready to produce PE and to commercialize it, the Second World War, WWII, broke out and the British government kept PE a secret in order to use it as electrical insulating material in their military equipment. [2]

After WWII the production of PE went to full commercial scale with American companies such as Union Carbide, Du Pont and the Bakelite Corporation taking under license the method developed by ICI. Within 10 years the variety of products made from polyethylene expanded dramatically and the total amount of produced PE reached 7500 tons, demonstrating the enormous commercial success of polyethylene. In the following decades, the development of LLDPE in the 1960's and the oil crises in the 1970's, led to the development of large capacity and high pressure polymerization plants. Nowadays, around 20 million tons of PE are obtained each year by high pressure polymerization ($P_{ethylene}$ ≈ 1000-4000 bar, T ≈ 300°C). [10]

2.1.1 – Free Radical polymerization of ethylene - General mechanism

Currently, free radical polymerization represents approximately 50% of the production of all synthetic polymers. This particular process has been changing people's lives, providing access to materials that otherwise would not be available to the average consumer, even though that, at the time of its commercialization, the proper scientific understanding of the concepts involved in FRP was lacking. [15], [16]

Furthermore, the commercial success of free radical polymerization can be attributed to the broadness of monomers available to perform this kind of polymerization, mainly due to the tolerance of radicals to several functionalities (acidic, hydroxyl, etc.), [15] and their ability to copolymerize, giving a wide variety of produced materials and leading, consequently, to a large range of applications. [15], [16]

Conventional free radical polymerization proceeds via a chain growth mechanism. [17] The FRP of ethylene occurs in the same way as other typical liquid monomers which basically consists of different types of reactions involving free radicals. [18] These elementary reactions are the initiation, where occurs the radical generation from non-radical species and their subsequent addition to the monomer (Figure 6), the propagation step where the propagating (oligo or macro)radicals continue the addition to the monomer (Figure 7), promoting the chain growth and the termination reactions giving that the latter one can be divided in two sub-types as bimolecular termination between two radical centres consisting in disproportionation (Figure 8) (atom transfer and atom abstraction reactions) and combination (Figure 9) (radical–radical recombination reactions). In the free radical polymerization of ethylene, there are other reactions, such as transfer reactions that will be deepen below. [18]

- Initiation

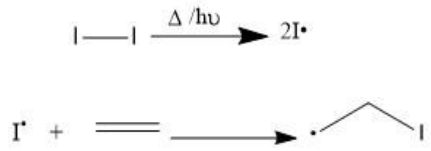

Figure 6-FRP initiation reaction.

In this first reaction radicals are generated (and can continue to do so during the polymerization) by the decomposition of the initiator species either by thermal cleavage, by redox reactions or by the effect of an incident radiation. [18] As seen in Figure 6 after the first step, the primary or initiator radicals will react with the carbon-carbon double bond of the monomer, setting what is called the initiation reaction. In the industrial field, the initiation reaction for the polymerization of ethylene that is frequently used is the thermal decomposition of initiator species, such as peroxides or oxygen. [8]

- Propagation

Figure 7 - FRP propagation step.

The propagation reaction is responsible for the growth of the polymer chains by the successive addition of monomer, end to end, to a radical centre, extending the oligomer chain - Figure 7.

- Termination

In the case of ethylene the termination step is frequently obtained by the combination of two propagating macroradicals generating one larger unreactive chain – Figure 8.

Figure 8 - Combination reaction in FRP.

On the other hand it is possible to proceed with termination step by disproportionation, where one oligomer chains abstracts one hydrogen atom from another chain, producing two polymers that present different chain ends. One of them is going to have an unsaturated end and the other a saturated end.

Figure 9- Disproportionation in FRP.

Between the two types of termination, the combination mechanism is the most common for the ethylene free radical polymerization.

- Chain transfer

Chain transfer reactions are processes that involve the termination of the propagation of macroradical in such way (like abstracting an hydrogen to another molecule) that the free radical associated with it transfers to another molecule (solvent, polymer, monomer, chain transfer agent) on which further chain growth occurs, maintaining the number of free radicals and growing chains. When the transfer occurs to a polymer (intra or inter-molecularly), this reaction has a major role in the polymer branching and chain extension. As exhibited above, the type and degree of chain branching strongly affects the properties of the produced PE, such as the crystallinity and the density and, subsequently, the properties of the final materials. The addition of a chain transfer agent can be used to control the molar mass of the final polymer. [10] [16]

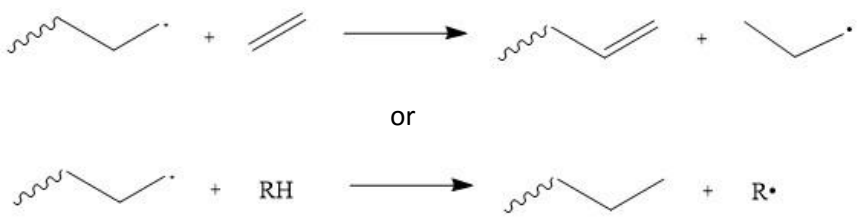

Figure 10 -Example of chain transfer in FRPE, with R= alkyl or aryl group or some other organic moiety. [10]

In the case of free radical polymerization of ethylene, transfer reactions mainly occur through intra or inter-molecular transfer reaction to the polymer, leading to the chain branching of polyethylene. Indeed, the resulting polymer chain from this reaction can be divided in two categories according to the branching type: short chain branching (SCB) or long-chain branching (LCB). It will depend whether if the reaction happens intra or intermolecularly, respectively. [10]

In Figure 11 is shown an example of intermolecular transfer reaction, where a hydrogen atom present on a PE chain is abstracted by a propagating macroradical producing a LCB. The probability of intermolecular hydrogen abstraction from a given molecule leading to LCB, is proportional to the length of the molecule, which means that long-chain branching is more prevalent at higher molecular weights. [17], [12]

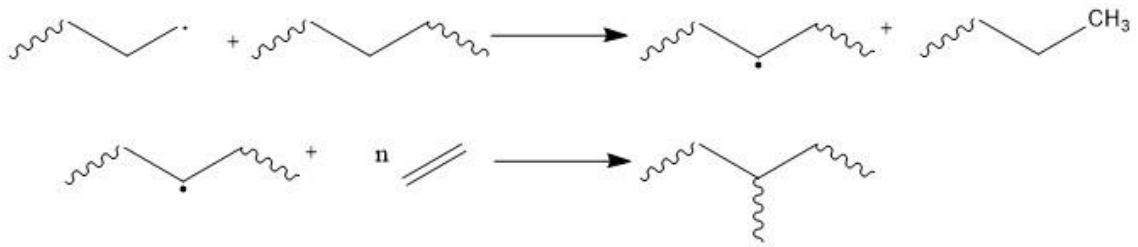

Figure 11 - Example of intermolecular chain transfer in FRPE.

Short-chain branching is due to the intramolecular reaction known as *backbiting* that occurs when the growing end of a chain turns back on itself, allowing the abstraction of a hydrogen atom only a few bonds away from the active chain-end. Chain growth continues from the location of the new radical, leaving the original chain end as a short branch. As a result of the approximately tetrahedral arrangement of the bonds linking carbon atoms to neighbouring atoms, ethyl and butyl branching is prevalent, even if more complex branches can also be formed, however to a lesser extent. Figure 12 exhibits an example of such reaction and further extension from the new polymerization site. Consecutive backbiting reactions may happen as well, generating short chain branching.

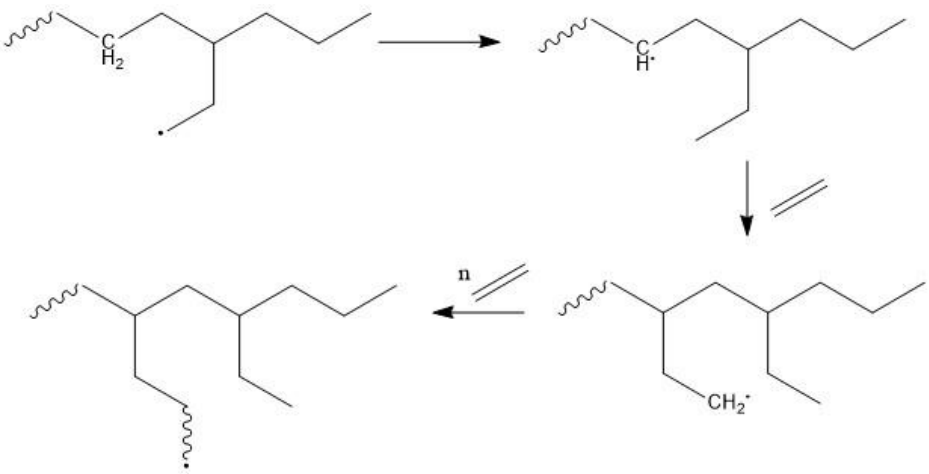

Figure 12 -Example of intramolecular chain transfer in FRPE.

As seen before SCB has a major influence on crystallinity and consequently in the density and melting temperature, whereas LCB will influence the rheological behaviour, affecting the viscosity and thus the processability of the polymer.

The polymerization conditions define the type of branching and its frequency, yielding different properties for the resulting product. Therefore, the material properties can be modified and adjusted to the needs of the final application, by setting the proper polymerization conditions being that, usually, higher temperatures will lead to a higher branching degree. [12], [8]

2.2 - Industrial production of LDPE

Even though this study was performed at a laboratory scale it was thought relevant to mention the industrial process used for LDPE production. As said before, the low density PE has a major role in the polymer industry, its consumption is disseminated through the world, something that can be easily backed-up by its share in the plastics market- 9 % of the total polymer demand in 2012 (from 211 Million metric tons). [19]

This radical process is frequently known as the *high pressure polymerization* process due to the high pressure (i.e. 1100-3000 bar) and relative high temperatures that are required to perform the polymerization and produce LDPE (i.e. 140-300℃). However, to prevent explosive self-decomposition the temperature should not exceed 350℃. [20]

These harsh conditions are necessary due to the high activation energy of the propagation step, since this monomer is considered as a "non-activated" one, given that it does not have substituents on the double bond to stabilize the formed radicals. The reactivity of ethylene will be influenced only by its surroundings. Indeed, the propagation step activation energy, E_a, of ethylene is 34,3 kJ mol^{-1}, higher than the ones of other well-known and used monomers like styrene, methyl methacrylate and vinyl acetate (32,5, 22,3 and 20,4 kJ mol^{-1}, respectively). [21] Thus, the reaction environment plays a major role in the reactivity of the monomer. This statement can be supported by the experimental rate constants for the propagation and termination reactions of ethylene from kinetic studies that have been made – The $k_p k_t^{-1/2}$ values show that the propagation reaction is favoured over the termination reaction by very high pressures and temperatures as seen in Table 1 which shows the dependence of the $k^p k^{t-1/2}$ values on those parameters. [22]

Table 1-$k_pk_t^{-1/2}$ values for dependence of: i) pressure at 129°C ii) Temperature (pressure reduced at 1 atm).

i)

P(atm)	$k_pk_t^{-1/2}$ (l $mol^{-1/2}s^{-1/2}$)
750	0.22
1000	0.30
1500	0.4
2000	0.54
2500	0.73

ii)

T(°C)	$k_pk_t^{-1/2}$ (l $mol^{-1/2}s^{-1/2}$)
-20	0.009
83	0.150
129	0.170
130	0.210
250	1.700

Frequently in this process, before the introduction into the reactor, ethylene is combined with the polymerization initiator (such as peroxides) in a mixture that is compressed either by a series piston or in a membrane compressor. [8] Commonly there are two types of reactors that are used to produce LDPE: a continuous-flow mechanically stirred autoclave (originally developed by ICI) and a tubular reactor (originally developed by BASF) as can be seen in Figure 13 (adapted from [23]). Either way, the process scheme for both reactors is very similar and there are some considerations to take into account when the polymerization conditions are chosen. In these systems, the pressure of the reactor has to be high enough to allow the dissolution of the polymer in its monomer, often being higher than 2000 bar. [24] As said before, the control of these conditions (temperature, pressure, addition of chain transfer agent, etc.) is very important given that they have a great influence on the resulting properties of the products.

Given that the residence time in the polymerization reactor is quite short, in the range of 10 to 60 s, and that the conversion of ethylene to LDPE is incomplete, around 15-25 % per pass for the autoclave and 20 to 40% for the tubular type, the reactor effluent has to be flashed in separators, releasing the LDPE from the unreacted ethylene. Afterwards the unreacted monomer is cooled and recycled by being added to the make-up stream of ethylene. [10], [23], [20]

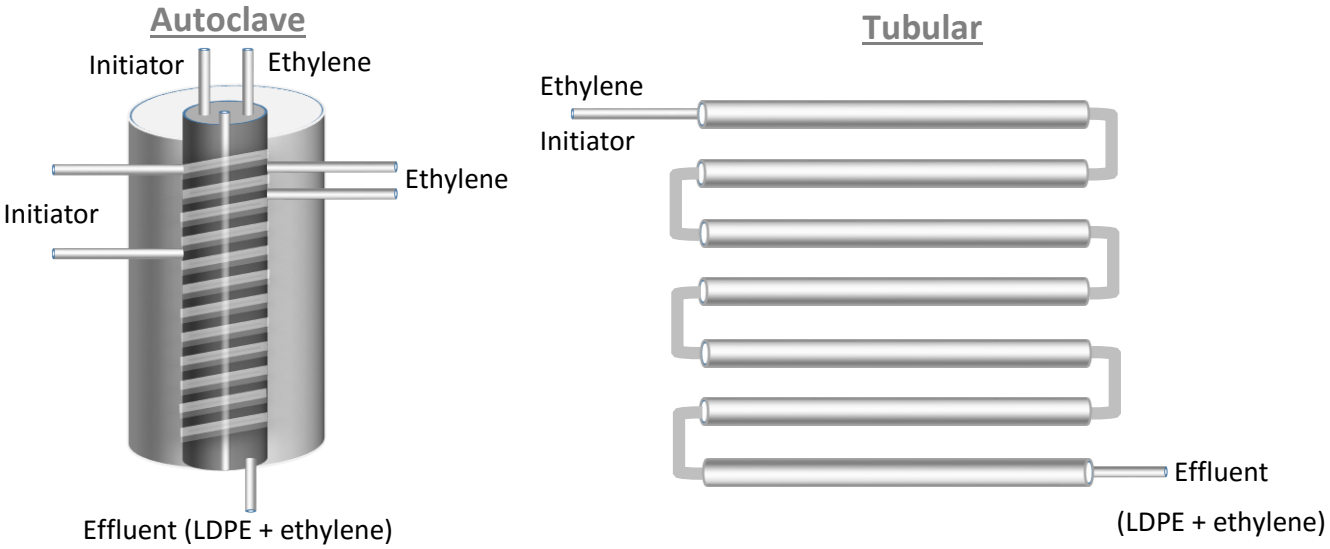

Figure 13- Autoclave (left) and Tubular (right) high pressure reactors.

2.3 - Free radical ethylene Polymerization at C2P2 - LCPP

As stated above, the polymerization of ethylene via a free radical process occurs under very harsh condition that can be potentially unsafe if not well controlled. Although feasible, these polymerization condition are very difficult to reproduce on a research laboratory scale. Indeed, free radical polymerization processes of ethylene involving relatively low pressures and temperatures were, for a very long time, considered to be inefficient.

At C2P2 laboratories, an apparatus was design to perform the polymerization of ethylene under mild conditions (pressure and temperature). Originally, the reactor was designed to study catalytic or hybrid radical/catalytic homo- and co polymerization of ethylene under temperatures up to 150°C and 250 bar within safe conditions – the description of the reactor and auxiliary equipment is presented in the following chapter (experimental chapter). [25] Until recently, it was common knowledge that the LDPE production process could only be performed efficiently under very harsh condition. However, during a blank experiment using a thermal initiator and an unusual solvent in that reactor, it was found that indeed, the free radical polymerization of ethylene was possible under much lower temperatures and pressures than the ones used in the industrial production if an unusual solvent was used. [25]

Similar observations were reported in the 1970s when performing the polymerization of ethylene in the pressure range from 100 to 500 bar in organic solvent or in water using a thermal initiator or (gamma) radiation. [26] The results from the recent experiments allowed the C2P2 team to reassess these researches considering the advances in the field of polymer chemistry since then, re-opening a field of free radical polymerization of ethylene under a low pressure range ($P_{ethylene}$< 300 bar). This allowed studying ethylene polymerizations using classical radical initiators, such as diazo compounds (2,2'-Azobisisobutyronitrile (AIBN) for example). [27], [28]

Indeed, the effect of the solvent in the FRP of ethylene was notably studied at the C2P2. It was shown that the solvent has a major influence on the polymerization activity and on the molecular weight of the obtained polyethylenes. PE with either low molecular weight and high chain-end functionality or non-functional/higher molecular weight can be synthesized according to the solvent used. [27], [28] A number of organic solvents were thus studied, solvents including toluene, dialkylcarbonates (Diethyl Carbonate, DEC and Dimethyl Carbonate, DMC) and Tetrahydrofuran, THF. However, all the solvents did not lead to the same activation. It was found that the nonpolar ones were less efficient than the polar ones. Some of the solvents (particularly THF, DMC and DEC) showed interesting properties in terms of yield or molar masses.

The experiments of FRP of ethylene in toluene were performed at 70°C in the range 10 to 250 bar using the diazo compound, AIBN, as initiator. This solvent was used in a first approach given that it is a typical solvent for the slurry catalytic process under similar polymerization conditions. PE was not formed for ethylene pressures under 50 bar and from 50 to 250 bar, the polymerization yielded a very low quantity of PE (3% of conversion) with molar masses around 2300 $gmol^{-1}$. [28]

When THF, was used as solvent at 100 bar of ethylene pressure, 3.9 g of PE were recovered (in a system with 50 mg of AIBN and 50 mL of THF at 70°C in 4 hours) and the molar mass was low, around 1200 g mol^{-1}. [27]

In both solvents the obtained PE was fairly branched (7 branches/1000C in toluene and 9/1000C in THF) as evidenced by ^{13}C NMR. It was observed that in those solvents the chain transfer reaction to solvent was significant and led to phenyl-ended and THF-ended PE, in the case of toluene and THF, respectively. In the case of transfer to THF two different structures were identified (1- and 2-polyethylenyl-THF) as shown in Figure 14. [27]

Figure 14 - Transfer to THF in radical polymerization of ethylene (2-polyethylenyl-THF).

As mentioned above, the solvent effect in the radical polymerization of ethylene is very significant, in opposition to what frequently occurs to other typical monomers in the radical process. This is illustrated in Figure 15, which shows the dependence of yield with ethylene pressure.

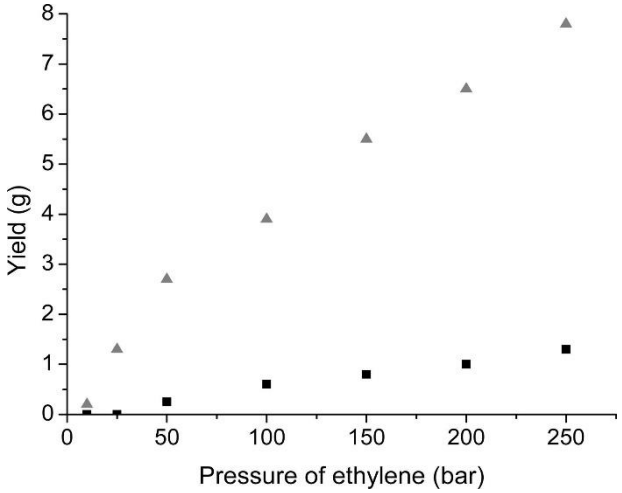

Figure 15- Pressure influence on ethylene radical polymerization (4h, 70°C, 50 mg AIBN and 50 mL solvent). ■ toluene, ▲ THF.

The polymerizations with dialkylcarbonates, DEC and DMC were performed at the same reaction conditions as THF and toluene (pressure of ethylene at 100 bar, 70°C, 50 mg of AIBN and 50 mL of DEC or DMC). However, transfer reactions events were lowered in these solvents. In both cases high molar masses were obtained, 7000 $gmol^{-1}$ for DEC and 12000 $gmol^{-1}$ for DMC. Moderate yields were achieved, between the ones from toluene and THF, 1.2 and 1.6 g of PE for DEC and DMC, respectively.

The radical ethylene polymerization was also carried out in bulk (supercritical ethylene) under the same mild conditions ($P_{ethylene}$=100 bar at 70°C with 50 mg AIBN). It was confirmed to be ineffective yielding a very low quantity of PE, 0.1 g, with a molar mass around 3000 g mol^{-1}.

The polymerization kinetics have been studied and compared for toluene, THF and DEC (Figure 16) confirming the strong effect of solvents on yields. The polymerizations in the presence of these three solvents followed a first order kinetics, since ln[1/(1-x)] increased linearly (x – is the normalized yield based on the highest yield of the series). The yield increased much faster in the case of THF when compared to the other solvents.

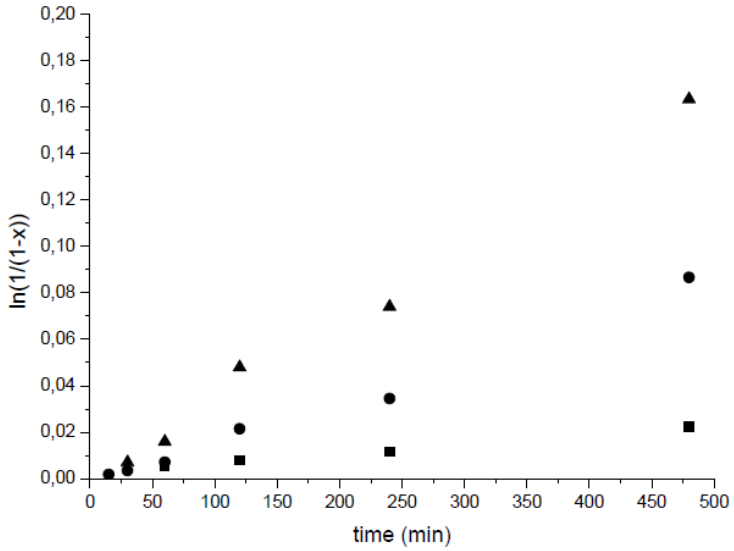

Figure 16 -Kinetic study of the effect of the solvent on polymerization yield (x). ▲THF ● DEC ■ toluene

The study of the pressure influence on the polymerization supports the activating character of these solvents. Whatever the polymerization ethylene pressure, higher yields were systematically obtained when THF was used, in comparison to the polymerizations performed with toluene and the dialkylcarbonates.

These studies clearly show that the solvent strongly influences the radical polymerization of ethylene dictating the characteristics of the obtained PE, such as molar mass and yield. Hence, the choice of the solvent is a very important parameter. As seen above, THF generated the highest yields, while DMC produced the highest molar masses. The origin of the "activation phenomenon" has been investigated by extending the study to other organic solvents, showing that in fact only the average physical properties of the solvents (or from their mixtures) influence the activation of the FRP of ethylene. [27], [28]

Other studies were performed at C2P2, investigating the potential transposition of this free radical process polymerization of ethylene to low transferring solvents (including water), while keeping activity as high as possible. Indeed, the particular case of DMC showed to be an excellent compromise for this process, since it was the less transferring polar solvent involved in these studies, being more efficient than nonpolar solvents and avoiding the chain transfer reactions, leading to high molar mass polyethylenes and acceptable yields (2g in 4h). [28] [29]

As a non-transferring and polar solvent, water was investigated to increase the yield and molar mass of the produced PEs. The transposition to an emulsion polymerization in aqueous dispersed would also benefit from the compartmentalization of radicals. Furthermore, the use of water as solvent would be environmental friendly and open a way to reduce the utilization of volatile organic compounds, VOCs. The experiments actually led to the formation of PE latexes, with the polymer being insoluble in water. The investigation of these emulsion polymerization systems was initially carried out

at C2P2 by *E. Grau* with a cationic system using a (cationic) water-soluble initiator, 2,2-azobis(2-amidinopropane)dihydrochloride (AIBA) in water at 70 °C, with and without a cationic surfactant (cetyltrimethylammonium bromide, CTAB), which was used to help nucleation and particle stabilization. [30]

Further studies in emulsion polymerization were then undertaken at C2P2 by *G. Billuart* who performed additional characterization of PE nanoparticles obtained in the cationic systems and worked on the development of anionic polymerizations systems. [30] [31] These studies will be detailed in the next section of this manuscript.

2.4 - Emulsion polymerization: general mechanism

Emulsion polymerization leads to the production of a fine dispersion of a polymer in a continuous medium, which most often is water; the dispersion is called latex. This type of polymerization plays a major role in the free radical process.

Emulsion polymerization was first developed in industrial laboratories in the late 1920s for the production of synthetic rubber latexes as an alternative to the use of natural rubber latexes in tyre manufacture. With the WWII came the need to have a synthetic alternative to the highly demanded natural rubber, and the emulsion process became a technology of great importance to the world. Since then, with a worldwide annual production of around 20 Mtons this process has been applied to the production of a wide range of products, from commodities to specialty polymers, including adhesives, paints, textiles, construction materials, high-end medical products etc. [32], [33]

The reason for the great acceptance of synthetic polymer dispersions and its ubiquitous use relies on the flexibility related to this process. Latex properties can be tailored to the application. Indeed, the use of various types of monomers, processing methods, and additives during emulsion polymerization, allows the synthesis of a wide variety of products with specialised properties. Emulsion polymerization thus allows for the production of a broad range of particles in terms of size, particle morphology, molecular weight, composition of the polymer and the surface functionality. These features will define the properties of the final product.

In most other types of polymerizations, the rate of polymerization is inversely proportional to the molar mass due to the large number of radicals necessary to produce a high polymerization rate, which results in the formation of low molar mass polymers. However, in the case of emulsion polymerization, the rate of polymerization and the molar mass can be simultaneously high as a result of the segregation of radicals by compartmentalization within polymerizing particles. [31]

The low viscosities of polymer latexes permit a high rate of heat transfer during polymerization and allow the latexes to flow over a substrate to be coated. Water can then be rapidly evaporated so that the latex particles can coalesce to form a continuous polymer film. Water-based emulsion polymer coatings are commonly used in the paper and pulp industry as a mean to reinforce and protect paper from water (a study was performed on this subject at C2P2 with PE produced via emulsion polymerization). These type of coatings are environmentally friendlier than solvent-based coatings. Environmental regulations limit the release of VOCs, which discourages the use of solvent-based polymer applications. [31] [34]

As first introduced and defined by Harkins in 1945 in the theory of the mechanism of emulsion polymerization (with studies of nucleation in presence of surfactant) this process can be theoretically

divided into three intervals. [35] Later on, these ideas have been modified by *Gardon, Harada, Stokmayer* and others. [36] Even if this model of emulsion has some limitation it offers sufficient information to allow a better understanding of this subject.

An emulsion polymerization medium is mainly composed by a hydrophobic monomer, surfactant and a water-soluble initiator. Before the beginning of the polymerization, there is an initial state, where the monomer is dispersed in water in large droplets stabilized by the surfactant and the initiator is dissolved in the continuous phase.

As it is well-known, surfactants are amphiphilic molecules. When the concentration of such species is above some critical value, called the critical micelle concentration (CMC), they will assemble into micelles - structures where the water-soluble (hydrophilic) part is oriented outwards and the hydrophobic inwards.

In Figure 17 is presented a schematic of the possible initial state of an emulsion polymerization with concentration of surfactant above the CMC. Note that the surfactant micelles (nanometre scale) are much smaller than the monomer droplets (micrometre order) and the initiator is dissolved in the aqueous phase.

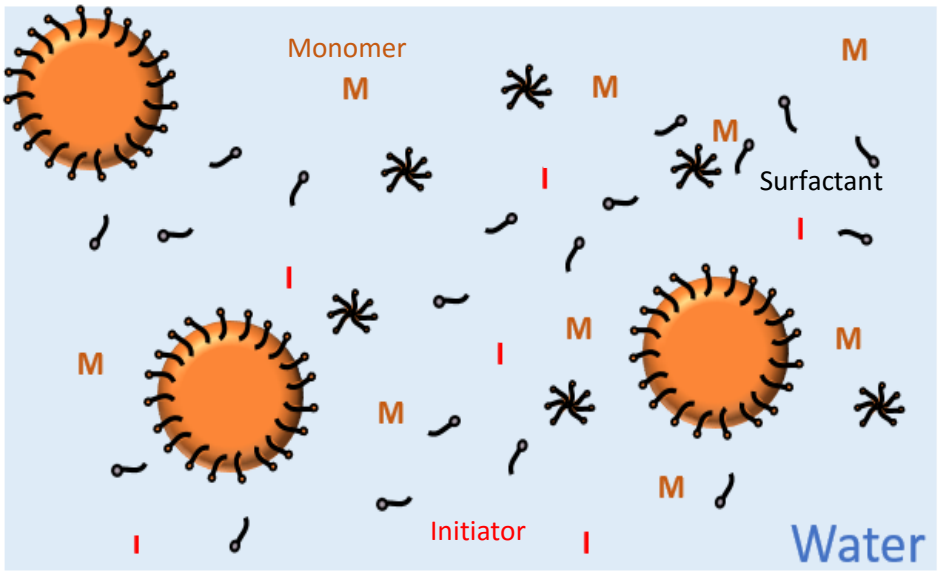

Figure 17- Initial state of Emulsion polymerization (surfactant concentration above cmc).

Figure 18 presents a schematic view of this process and the polymerization rate versus time for each interval defined by Harkins, which will be described below.

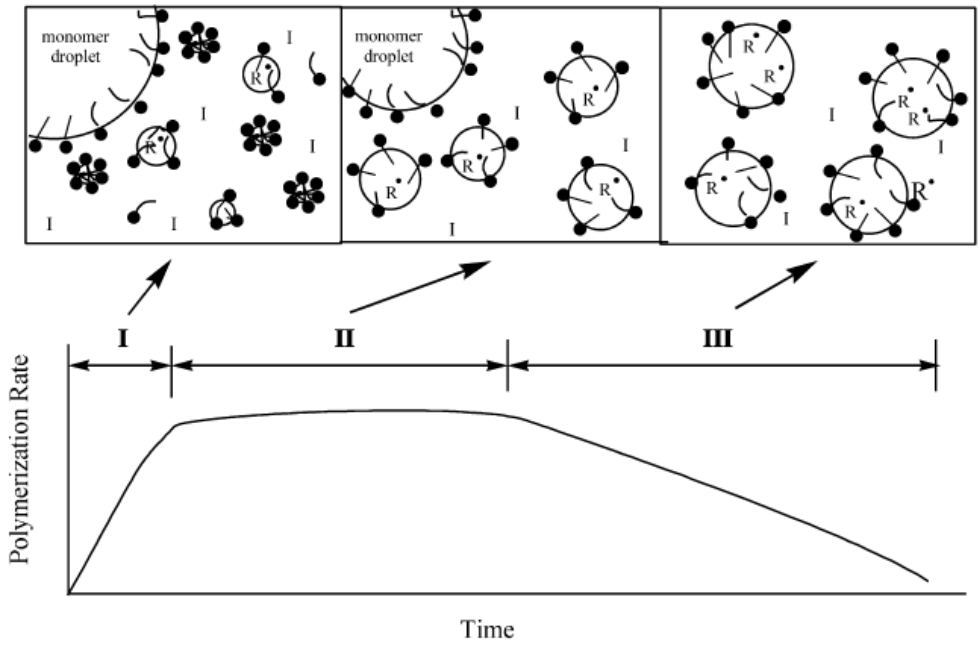

Figure 18- Intervals in emulsion polymerization (from [34]).

- Interval I –Nucleation

Polymerization occurs when an initiator-derived radical reacts with the monomer that is present in the water phase and continues to propagate until it reaches a critical chain length where its solubility in water diminishes greatly and it is forced to enter in a monomer-swollen micelle. In this monomer-rich environment, the oligomer can rapidly propagate once that there is an enormous quantity of monomer molecules.

This fast polymerization step requires a large consumption of surfactant molecules to stabilize the formed particle surface, with the great majority of the micelles being consumed at this step. If the surfactant concentration is above its CMC, the nucleation will cease when the surface area of the particles is sufficient to reduce the amount of free surfactant below the CMC. In these systems, particle formation thus occurs via micellar nucleation.

If the solubility of the hydrophobic monomer is high and/or in the absence of micelles, the oligoradical chains can precipitate with themselves to form polymer particles. This is referred to as homogeneous nucleation. [34]

- Interval II – Particle growth

This is the stage where the particles grow by consumption of the monomer present inside the particles. Monomer droplets act as reservoirs, feeding the particles by monomer diffusion through the aqueous phase, keeping the monomer concentration high and constant inside the particles. The initiation is still taking place in water, with the formation of oligoradicals, which are constantly entering the particles. The end of this interval occurs when all the monomer droplets have disappeared. [32]

- Interval III – Terminal phase of polymerization

Interval III starts when there are no more monomers droplets in the system, leading to a decrease in the monomer concentration in the growing particles, which means that the rate of polymerization tends to slow down. The remaining monomer molecules are consumed in the viscous organic particle core-phase. Consequently, sometimes a reaction called the *Trommsdorf effect* or *gel effect* [37] can occur and is related to this increase in viscosity that leads to a very rapid increase of the molar masses, which may lead to possible runaway of the polymerization that can alter the characteristics of the produced polymers. [34]

2.5 - Free radical emulsion polymerization of ethylene

2.5.1 – First studies on free radical emulsion polymerization of ethylene

Some studies of free radical polymerization of ethylene in aqueous dispersed media have been previously reported. However they were performed under relatively high pressures (P> 300 bar) and for a wide range of temperatures. Furthermore, the interpretation of the results from these studies was difficult due to the lack of analytical tools available at the time to study the colloidal properties of the obtained polymer dispersions.

Early studies have been reported in the 1940s In 1943, *Kern* and *Hopff* polymerized ethylene under relative high pressures (600 to 800 bar), using persulfates as initiators in basic and acidic conditions obtaining PE latexes of high solids content (≈ 40 %). [38] [39] In the 1960s several studies on the emulsion polymerization of ethylene were performed by *Stryker* and *Mantell.* These authors used aqueous solutions with potassium persulfate as initiator, potassium myristate as surfactant in the presence of potassium hydroxide and tert-butyl alcohol (used for regulation of particle sizes) under ethylene pressures ranging from 200 to 1400 bar and investigated the factors that affect the stability of polyethylene latexes. [40], [41], [42]

As mentioned before, in the 1970s the research group of *Takehisa et al.* performed studies in emulsion polymerization of ethylene. [43] These polymerizations were induced by gamma radiation under ethylene pressures ranging from 100 to 200 bar (at 80 to 100°C), in the presence of potassium myristate, in the presence of potassium hydroxide. Solid contents up to 15% were obtained in these studies and the radiation effect, surfactant concentration, stirring rate and polymerization pressure were investigated. However, at the time particle sizes and morphologies were not studied. Similarly to former studies, transfer reactions to the surfactant were evidenced. [44]

Machi et al. studied the bulk polymerization of ethylene at low temperature (T<100°C), which evidenced the existence of long-lived radicals. Differential scanning calorimetry (DSC) investigations showed that higher polymerization temperature would lead to lower crystallinity and melting temperature values. This is in accordance with the fact that transfer reactions, responsible for branching, occur more frequently with higher temperatures as stated before. [45]

2.5.2 - Free radical emulsion polymerization of ethylene at C2P2

As stated in the previous section, free radical emulsion polymerization of ethylene, FREPE, under mild conditions (at 70°C in the range 50 to 250 bar) using diazo compound as initiator (AIBN) has recently been studied at C2P2 by *Monteil et al.* studied. Indeed, the DMC showed to be an excellent compromise for this process, since it was the less transferring polar solvent avoiding the chain transfer reaction, leading to high molar mass polyethylenes while keeping acceptable yields (2g in 4h). [28], [29]

On the other hand, using water would benefit from advantages of this solvent mentioned before. *Grau et al.* first investigated the FRP of ethylene in emulsion under mild conditions using a cationic water-soluble initiator, 2,2-azobis(2-amidino-propane) dihydrochloride (AIBA). The polymerizations were performed at 70°C, with and without a standard cationic surfactant (cetyltrimethylammonium bromide, CTAB), which helped to promote the nucleation and particle stabilization. The stabilization of PE particles in the system without surfactant was ensured by the cationic fragments of the initiator, which induced electrostatic repulsion. [30]

In all cases, ethylene was polymerized with significant yields, and stable PE latexes were recovered for ethylene pressures from 50 up to 250 bar. For the standard polymerization time (4h) the surfactant-free system yielded a quantity of PE (1.3 g) lower than the values obtained using the same amount of initiator in THF and DMC but was higher than in toluene. The average particle diameters (Dp) measured by dynamic light scattering, DLS, increased with the ethylene pressure from 30 to 110 nm with very low polydispersity indexes (≈0.05), with a spherical particle morphology.

When the polymerizations were performed in the presence of surfactant (CTAB, 1 g L^{-1}), the yield increased to 4.6 g of PE for the standard polymerization time at 100 bar of ethylene and the solids content reached up to 40 %. The average particle size seemed to reach a plateau at 50 nm with increasing ethylene pressure, and polydispersity indexes were close to 0.1. In this case, the particles showed a disc-like morphology.

In both polymerization cases (with/without surfactant) the yield and molar masses increased with the increase in ethylene pressure. However the activities observed with surfactant were much higher than the surfactant-free polymerization and were found to be even higher than the ones achieved in THF. [27] Particle sizes increased, but their shape remained unchanged. Similar effects were observed when stirring rate was increase. [30] The following figure presents the evolution of yield and particle size measured by DLS with the increase in ethylene pressure for both cases.

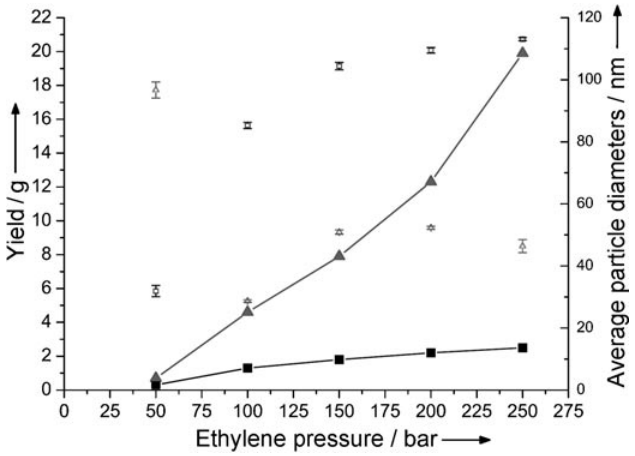

Figure 19 –FREPE ■ yield and □ average particle diameter vs ethylene pressure (80 mg AIBA, 50 mL water, 4h at 70 °C); ▲ yield and Δ average particle diameter vs ethylene pressure (80 mg AIBA, 50 mL water, 4h at 70 °C and 1 gL^{-1} CTAB).

Both systems of polymerizations (with or without surfactant) produced PE with low melting point (Tm around 100°C) and low crystallinity (30–40%), with the highest values obtained for the surfactant-free process. As expected, the emulsion polymerization process yielded PEs with high molar masses ($M_n \approx 10^4$ *to* 10^5 gmol^{-1}). The PEs were moderately branched in both polymerization conditions, which is in agreement with the measured crystallinities and melting temperatures. The higher branching level in water than in an organic solvent was explained by the compartmentalization of the radicals, which increased the possibility of transfer reactions to the polymer.

The PE latexes were also characterized by transmission electron microscopy (TEM), which allowed to observe spherical particles for the surfactant-free process, and disk-like shapes for the polymerizations with surfactant. [30]

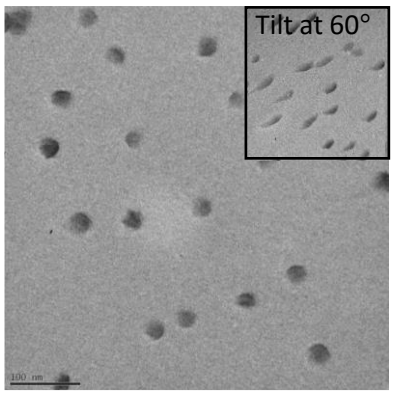

Figure 21- TEM of PE particles synthesized by FREPE in the presence of surfactant (AIBA, 100 bar of ethylene at 70 °C and CTAB – 2 gL^{-1}). [30]

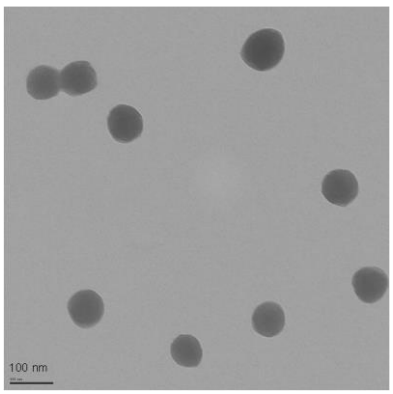

Figure 20 - TEM of PE particles synthesized by FREPE (AIBA, 100 bar of ethylene and 70 °C). [30]

In line with the studies performed at C2P2 on free radical emulsion polymerization of ethylene using cationic systems, it was found interesting to explore the synthesis of negatively charged PE latexes using a conventional anionic initiating and stabilizing system. Such work was carried out by *Billuart et al.* [31]

The initial experiments were performed using 4,4'-azobis(4-cyanopentanoic acid), ACPA (1 gL^{-1}), as initiator. Since ACPA has two carboxylic acid functions, the pH of the polymerization medium needed to be slightly basic to dissolve it. Thus, $NaHCO_3$ (1 g L^{-1}) was introduced in the system and the polymerizations were performed with or without surfactant - sodium dodecyl sulfate, SDS. The polymerization yielded a stable latex, however with a very low quantity of PE (the polymer content, PC, was around 0.5%). Different experimental conditions were investigated in order to increase the yield, varying the ethylene pressure, surfactant concentration and pH. Nonetheless, despite producing stable latexes, the yields remained low (PC$\leq$ 0.5%).

Hence, the feasibility of anionic FREPE was then investigated using a more common initiator, ammonium persulfate (APS). The polymerizations in the presence of APS (0.84 g L^{-1}) and SDS (3 g L^{-1}) yielded a low quantity of PE (0.59 g) with particles around 95 nm and the pH dropped from 5.4 to 2.8 during the polymerization. When pH regulators were used, such as $NaHCO_3$, K_2CO_3, or NaOH, the resulting latexes were stable and exhibited a greater amount of PE (PC$\geq$4%) with no significant pH variation observed. [31]

In fact, the pH sensitivity of persulfate initiators is well-known and the requirement of using pH regulators in emulsion polymerization of monomers such as butadiene and ethylene-vinyl acetate mixtures has been reported in the literature. [46], [47] Thus, the FREPE needs a medium with a steady basic pH in order to obtain significant amounts of polymer. Particle sizes remained around 25 nm, and DLS evidenced high polydispersity indexes (>0.1), indicating nonspherical, disklike particle morphologies as observed in the cryo-TEM analyses (Figure 22). Despite the possible transfer reactions to SDS, high molar masses were obtained (in the range of 10^5 g mol^{-1}).

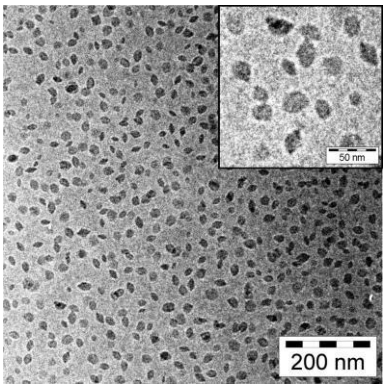

Figure 22 - Cryo-TEM picture of a PE latex synthesized with 3 g L^{-1}.

Ethylene pressure and stirring rate were then varied in order to increase the solids contents of the latexes. Increasing ethylene pressure led to higher solids contents, larger particles, and higher molar masses, up to 2.5×10^6 g mol^{-1}. The stirring rate in the presence of surfactant seemed to have no influence on particle sizes, but the polymer content drastically increased resulting in an increase of the particle number. Both parameters (pressure and stirring rate) appeared to improve the monomer feed to the growing chains, leading to slightly less branched and thus more crystalline PEs. Combining higher pressures and stirring rates, stable latexes with PC up to 30% were obtained.

2.6 – Controlled Radical Polymerization

As mentioned in the previous sections, free radical polymerization has many advantages. This process can be used to (co)polymerize a large variety of monomers with a large range of polymerization conditions. However, FRP provided a poor control on some of the parameters that allow the synthesis of well-defined macromolecular architectures, namely, the molar mass of the polymer and its dispersity, the end functionality and the architecture of the chains. [8], [48]

The discovery and the implementation of the controlled/living polymerization permitted to overcome that major issue and represented a great impact in polymer science. Given the large implementation of free radical polymerization, the control over structural parameters prepared by FRP turned accessible the production of a wide range polymers with well-defined molecular architectures and structural morphologies, having a significant impact in material science. [49]

2.6.1 – General comments on controlled Radical Polymerization

In this section is present an introduction to the controlled radical polymerization, CRP, and its relation with ethylene.

The CRP could not be approached without referring to the first reported living polymerization systems. The term *living polymer* was first introduced by *Michael Szwarc* to describe the products of the anionic polymerization of styrene initiated by electron transfer in THF. With experiments where block copolymers were synthesized via sequential monomer addition, *Szwarc* inspired many more to proceed with studies in this field. [49] As defined by *Szwarc*, the term *living* refers to a chain growth process without chain breaking reactions, such as transfer and termination reactions. This living state provides the ability to polymer chains to further add another monomer after the prior monomer batch is consumed, allowing the synthesis of block copolymers. [8] In reality, it is difficult to completely suppress those reactions so the subject has been discussed in terms of how rigorous it should be. Later on *Szwarc* modified his definition to: "*A polymerization is living when the resulting polymer retains its integrity for a sufficiently long time to allow the operator to complete its task, whether a synthesis or any desired observation or measurement. Even in that time some decomposition or isomerization may occur, provided it is virtually undetectable and does not affect the results*". [49]

Hence, the living polymerization does not necessarily implies that the resulting polymer has a controlled molar mass and a narrow molar mass distribution (low dispersity, *Đ*), with some additional conditions being needed to actually achieve those objectives, such as the total consumption of initiator in the early stage of polymerization and the fast exchange between several species of different reactivities (at least as fast as the propagation step).

The term *Controlled polymerization* rose from the achievement of those criteria, being suggested in 1987 by *A. Müller and K. Matyjaszewski*, and is defined *as "a synthetic method to prepare polymers, which are well-defined with respect to topology (e.g., linear, star-shaped, comb-shaped, dendritic, and cyclic), terminal functionality, composition, and arrangement of comonomers (e.g., statistical, periodic, block, graft, and gradient), and which have molecular weights predetermined by the ratio of concentrations of reacted monomer to introduced initiator, as well as a designed (not necessarily narrow) molecular weight distribution, MWD"*. [49]

Hence, even that in the ideal case a living polymerization should be controlled as well, that does not necessarily always happens. On other hand, a controlled polymerization is also not always a living polymerization.

This is particularly true in the field of CRP where bimolecular termination cannot be avoided. The main methods of achieving CRP can be divided into two categories, through the mechanism responsible for the reversible deactivation of the propagating radicals, which are balanced in an equilibrium between the active and the dormant species, either via reversible termination or via reversible (degenerative) chain transfer.

The most common techniques to control free radical polymerization are the *Nitroxide-Mediated Polymerization* (NMP) and the *Atom Transfer Radical Polymerization* (ARTP) that belong to the first category and the *Degenerative Transfer polymerization* (DT) or the *Reversible Addition-Fragmentation Chain Transfer* (RAFT) *polymerization* belonging to the latter one. This last technique, which has been used in the frame of this work, is detailed in the following paragraphs.

2.6.2 - Reversible addition-fragmentation chain transfer polymerization (RAFT)

Since its disclosure in the open literature in 1998, the RAFT process has been the most versatile of the controlled radical polymerization techniques. As *Chiefari et al*. stated, the characteristic that distinguishes the RAFT polymerization from all the other CRP methods is that it can be used with a large range of monomers resulting in polymers with controlled molar masses and very narrow molar mass distributions (Đ< 1.2). [50]

This process requires the use of an organic molecule called RAFT agent, or RAFT chain-transfer agent (CTA). As seen in Figure 23 the CTA has an activating group denominated by Z and a leaving group by R, and the corresponding structure is a thiothiocarbonylated compound (ZC(=S)SR) including trithiocarbonate (where the Z = -S-R'), dithioester (Z = -R), dithiocarbamate (Z = -NR'R'') or a dithiocarbamate (also called xanthate) (Z = -OR'). The use of xanthates as a controlled free radical polymerization technique has also been described as MADIX (Macromolecular Design via Interchange of Xanthate) by the *Rhodia* Company simultaneously to RAFT. [51]

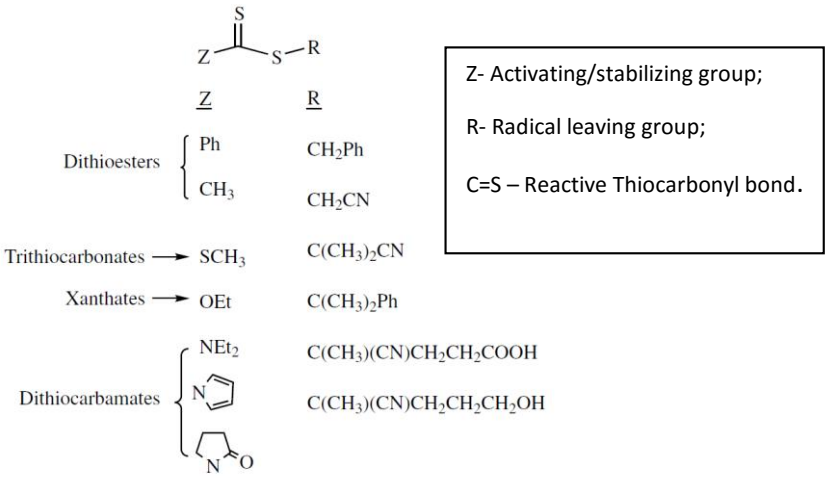

Figure 23- Examples of Thiocarbonylthio RAFT agents [53].

The mechanism of RAFT polymerization involves the typical reactions of a conventional free radical polymerization, plus additional addition-fragmentation steps, starting by the initiation step with the decomposition of an initiator. There is practically no limitation for the radical initiators, however the use of peroxides may oxidize RAFT reagents. Furthermore, the concentration of the initiator has to be tuned in order to provide the system with the adequate ratio between the CTA and initiator to ensure that the large majority of polymer chains were originated from the transfer agent and not from the radical initiator. [52]

After the initiation, in the early stages of the polymerization, the addition of the propagating radical ($P_n^{\cdot}$) to the RAFT agent followed by the fragmentation of the intermediate radical species, gives rise to a polymeric RAFT agent, or macroRAFT agent, and a new radical ($R^{\cdot}$). These steps form the pre-equilibrium.

Afterwards, the radical $R^{\cdot}$ reinitiates the polymerization by addition to the monomer leading to the formation of new propagating radical ($P_m^{\cdot}$). This step continues in the presence of the monomer, generating an equilibrium between the active species that carry on with the polymerization ($P_n^{\cdot}$ and $P_m^{\cdot}$) and with the dormant ones, allowing the polymeric chains to grow at the same rate. This characteristic of the RAFT process is the one responsible for the narrow molar mass distribution of the resulting polymers.

The polymerization continues following the same procedure, with the polymer chains growing, until some irreversible termination or transfer reaction occurs. For instance, the combination of two polymer chains will cease the propagation by a bi-molecular coupling reaction. [53]

- Initiation:

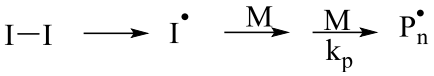

Figure 24- Initiation step in RAFT.

- Addition to RAFT agent:

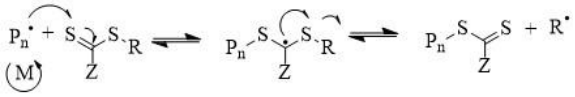

Figure 25- Addition to RAFT agent.

- Reinitiation

Figure 26- Reinitiation step in RAFT polymerization.

- Chain equilibrium by reversible addition fragmentation:

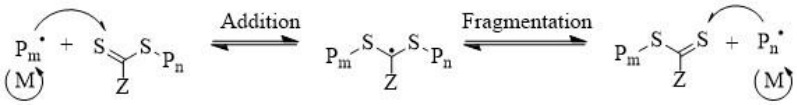

Figure 27 - Chain equilibration by reversible addition fragmentation.

- Termination (Combination):

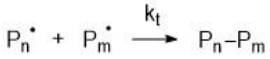

Figure 28 - Termination by the combination of 2 active polymer chains.

Selection of transfer agent

The CTA is thus responsible for the equilibrium between the dormant and active chains by a reversible transfer reaction through addition and fragmentation (Figure 25 to Figure 27). The CTA choice is a critical point in RAFT polymerization, given that there is no universal chain transfer agent. A proper selection of an adequate RAFT agent should be made depending on the monomer to polymerize in order to achieve a well-controlled polymerization. [54]

According to their reactivity, monomers can be divided into two groups: more-activated monomers (MAMs) and less-activated monomers (LAMs). The first group typically include monomers with vinyl groups conjugated with a carbonyl group or an aromatic ring (for example, (meth)acrylates, (meth)- acrylamides, and styrenics), while the second group typically contains a saturated alkene or oxygen/nitrogen lone pair adjacent to the vinyl group. In LAM group are included such monomers as ethylene and vinyl acetate (VAc). Several reviews have provided guidance for selecting the ideal RAFT agents for most monomers. [55], [56]

The reactivity of a CTA during RAFT is strongly affected by both the Z and R groups. The structure of the Z group is indeed very important. It governs the general reactivity of the C=S bond toward radical addition and affects the lifetime/fate of the resulting intermediate radical. Concerning

the R group, should be a good homolytic leaving group, being more stable than $P_n^{\cdot}$, in order to be formed and be able to reinitiate the polymerization. [49]

The RAFT agents such as dithioesters or trithiocarbonates suitable for controlling polymerization of more-activated monomers inhibit or retard polymerizations of less-activated monomers. Similarly RAFT agents suitable for controlling polymerizations of LAMs, such as xanthates, tend to be ineffective with MAMs. The reduced effectiveness of the dithiocarbamate RAFT agents with MAMs relates to their lower reactivity toward radical addition and consequent smaller transfer constants. The double-bond character of the thiocarbonyl is reduced by the contribution of zwitterionic canonical forms that localize a positive charge on nitrogen and a negative charge on sulfur. [55]

On the other hand, the tendency of dithioesters or trithiocarbonates to inhibit polymerization of LAMs is due to the poor ability of the radical leaving-group to propagate species with a terminal LAM unit. Dithiocarbamates that possess electron-withdrawing groups adjacent to nitrogen or where the nitrogen lone pair is part of an aromatic ring system are effective with MAMs but inhibit polymerizations of LAMs. [54], [55]

Hence, if the stabilizing effect of the Z groups is strong, as the one of phenyl groups, they will be very efficient for such monomers as styrene and methacrylate. However, the Ph groups have a setback because they will stabilize the intermediate radical, resulting in the retardation of the polymerization of acrylates, for example, and the inhibition of the polymerization of vinyl esters, such as vinyl acetate, and ethylene. On the other hand, very weakly stabilizing groups, such as –OR in xanthates can have the opposite effect in styrene although they perform well with vinyl esters. [49]

2.7 - Controlled radical polymerization of ethylene by RAFT at C2P2

As seen in this section a controlled radical polymerization can be achieved from various techniques. However, none of these techniques were successfully applied to control ethylene polymerization. As previously mentioned, the FRP of ethylene typically yields PE with large molar mass distributions and results in branching via backbiting. This, combined with the unstabilized nature of ethylene makes difficult the control of ethylene polymerization via RAFT. Furthermore, the conditions that are normally involved in the synthesis of PE through radical polymerization are very harsh, which increases the difficulty to control the macromolecular architecture. Thus, it was appealing to identify original ways to polymerize ethylene under conditions that allow the fine control of the chain growth through a free radical process. [57]

Indeed, taking advantage of the recent progress from the C2P2 team in efficiently performing the free radical polymerization of ethylene under mild conditions, and considering ethylene as a LAM, the team investigated the RAFT polymerization of ethylene mediated by xanthates. [27], [28] This study was carried out by Dommanget et al. constituting the first example of a controlled radical polymerization of ethylene using RAFT in the presence of xanthates. [57]

The selected xanthates are shown in Figure 29. Relying on the knowledge gained from the studies on the FRP of ethylene, dimethylcarbonate, DMC was chosen as the solvent. Indeed it was demonstrated that in order to minimize irreversible chain-transfer reactions while maintaining an acceptable yield, the use of DMC, was essential. The polymerizations were thus performed in this solvent in the presence of AIBN as initiator at 200 bar and 70°C. [27], [29]

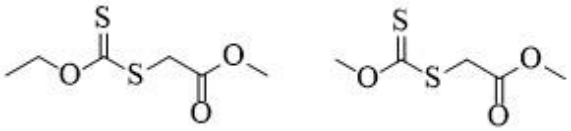

1 2

Figure 30 - Xanthates used in CRP of ethylene. [57]

O-ethyl xanthate 1 (Figure 29) was first selected to mediate the RAFT polymerization using CTA/initiator ratio of 10:1. In these polymerizations, a linear increase of M_n versus the yield was observed and much narrower molar mass distributions were obtained when compared to the blank experiments (Figure 30). These findings evidencing a living character showed that the polymerization of ethylene was effectively controlled by the xanthate-1.

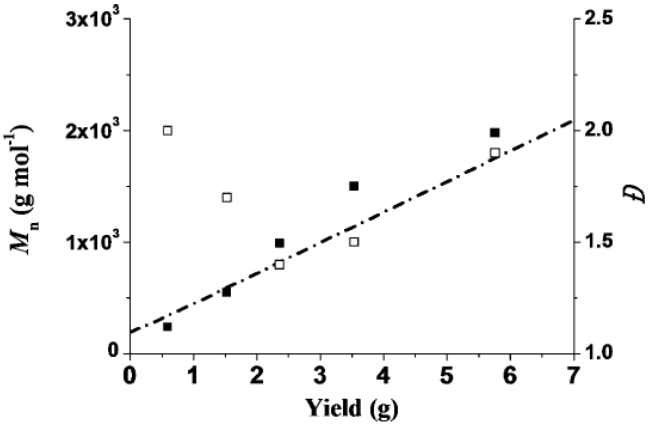

Figure 29 - Evolution of M_n (experimental: ■, theoretical:· — · —) and MWD (□) with the polymerization yield .

The polyethylene obtained after 7 h of polymerization, evidenced a melting temperature, T_m, of 116℃ and a crystallinity of 50%. To evaluate the living character of the obtained PE, chain-extension experiments with ethylene were performed from polyethylene–xanthate (PE-X, M_n=550 gmol^{-1}, $Đ$=1,7, functionalization rate 80%) in DMC under the same previous reaction conditions, while keeping the molar ratio between PE-X and AIBN at 9. The peak corresponding to the final polymer was shifted towards higher molar masses when compared to the chromatogram of the initial PE-X (Figure 31). However a broader molar mass distribution due to the presence of the initial PE-X is observable in the final product. Indeed, this result showed the livingness of the majority of PE-X chains. [57]

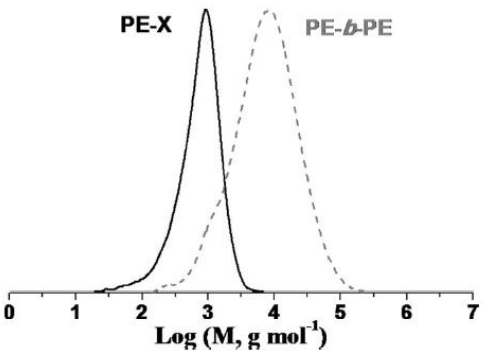

Figure 31 - Evolution of MWD during the chain-extension reaction of PE-X with ethylene.

3 – CRP in emulsion through PISA

As seen above, the emulsion polymerization process requires the use of surfactants that may sometimes be detrimental to the final application due to their propensity of migrating within the final dispersion of materials. Among those surfactants, amphiphilic block copolymers are sometimes employed.

Hence, it was very appealing to find alternatives to emulsion polymerization system in which surfactant is both produced in situ and covalently anchored at the surface of the final particles. With the developments of the CRP in water, emulsion polymerization can be now performed according to the polymerization-induced self-assembly (PISA) process. The basic principle behind the PISA process is to grow a hydrophilic living polymer chain in a first step and chain-extend it in water with a hydrophobic monomer, creating block copolymers that will self-assemble into nano-sized self-stabilized particles. [58] This original way of performing surfactant free emulsion polymerization brings the additional advantage of forming amphiphilic di-block copolymers in high yield that self-assemble during their formation and that can lead to various morphologies (worms, rods, fibers, etc.). [59] , [60]

The C2P2 team recently managed to perform PISA using RAFT according to a one pot process where the hydrophilic and the hydrophobic block are formed successively in the same reactor in water (Figure 32). [61]

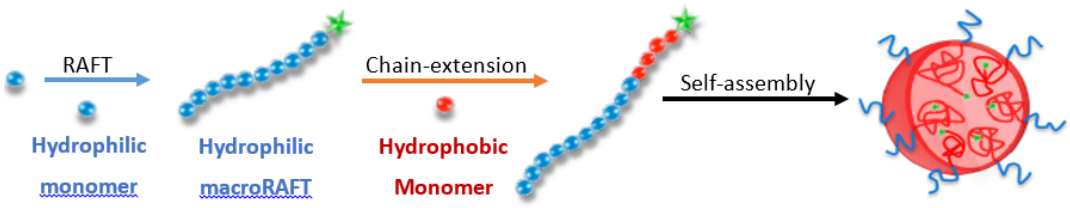

Figure 32 - PISA using RAFT in aqueous system.

First developed with trithiocarbonate chain transfer agents, suitable to polymerize more-activated monomers [55] such as styrene, n-butyl acrylate and methyl methacrylate as hydrophobic monomers, *Binauld et al*.[62] recently showed that a xanthate-based PISA process could also be performed and LAMs such as VAc could be employed as hydrophobic monomer. In such work, the emulsion polymerization of vinyl acetate was carried out in the presence of different hydrophilic Polymers obtained by RAFT/MADIX.

With the recently established CRP of ethylene mediated by xanthates and the expertise of the C2P2 team in the emulsion polymerization of ethylene, the PISA process of ethylene achieved through RAFT polymerization by using hydrophilic macroxanthates as CTA was found to be an interesting research area to investigate, considering that stable PE particles could be synthesized without surfactant and that original PE-based block copolymer structures could be formed.

Conclusions

After more than 70 years of industrial production, polyethylene still is one of the most produced polymers, the C2P2 team has nevertheless demonstrated that it is still possible to innovate in free radical polymerization of ethylene.

Gathering the knowledge that was developed at C2P2 in the chemistry fields presented above, namely the FRP of ethylene under mild condition, its controlled polymerization by RAFT technique, the polymerization-induced self-assembly (PISA) process and the emulsion polymerization of ethylene, the foundations were laid for the project investigated in this work: The synthesis of PE-based nanoparticles from an original surfactant-free emulsion polymerization of ethylene using RAFT technique.

This page was left intentionally in blank.

Chapter II – Experimental part

This page was left intentionally in blank.

In order to achieve the objectives of this work there were various techniques, materials and experimental devices that needed to be studied. This chapter presents the materials, reagents, experimental set-up and all the procedures involved in this work such as the analytical ones used to characterize the obtained samples.

1- Materials

The majority of the experiments were performed in aqueous medium, and the water used in these studies was deionized in an ELGA® PURELAB Classic by ultrafiltration.

Depending on the systems (cationic or anionic), the chosen initiators were the 2,2'-Azobis(2-methylpropionamidine) dihydrochloride (AIBA granular, Sigma-Aldrich®, 97%), 4,4'-azobis(4-cyanopentanoic acid) (ACPA, Sigma-Aldrich®, ≥ 98 %) and Ammonium Persulfate (APS, Sigma-Aldrich®, 98 %). The initiators were used as they were received.

Despite the main objective that was the development of surfactant-free emulsion polymerization some experiments were performed using a surfactant, namely, cetyl trimethylammonium bromide (CTAB Sigma-Aldrich®, ≥ 99 %). In addition, a pH buffer was used in some of the experiments: - Sodium hydrogen carbonate ($NaHCO_3$, Sigma-Aldrich®, 99.4 %).

The macroRAFT agent used in this work, namely the namely the poly(ethylene glycol) functionalized with a xanthate chain end (PEG-X) was obtained by post-modification of a commercial polymer, poly(ethylene glycol) methyl ether (PEG, number-average molar mass, M_n, of around 2000 g mol^{-1}, Sigma-Aldrich®), by a xanthate extremity. 2-bromopropionyl bromide (97%) and triethylamine (≥99.5%) from Sigma-Aldrich® were also used in this process.

The monomer used in the polymerizations was ethylene from Air Liquide (99.95 %).

2- Procedures

2.1 - Synthesis of the macroRAFT agent – PEG-X

This work required the use of a hydrosoluble macroRAFT agent, which was prepared before the polymerization of ethylene.

Due to its high efficiency in other polymerization systems [62], the macroRAFT agent used in this study was the xanthate-functionalized polyethylene glycol (PEG-X). The synthesis of this macroRAFT agent was achieved by post-modification of a commercial polyethylene glycol methyl ether ($M_n \approx 2000$ g mol^{-1}, Sigma-Aldrich®) and was performed in two steps detailed below.

The first step involved the dissolution of the PEG-OH (20 g, 1×10^{-2} g L^{-1}) in dichloromethane (DCM, 80 mL) and after 2.7 g (2.7×10^{-2} g L^{-1}) of triethylamine (TEA) were added to the mixture. Then, around 5 g (2.3×10^{-2} g L^{-1}) of 2-bromopropionyl bromide were added drop-by-drop, with the flask in an ice bath. After this addition, the flask was removed from the ice bath and left under stirring for 16 h.

As secondary products of the first step of this reaction salts of hydrobromic acid (HBr) that were separated from the (intermediate) product by filtration. The intermediate was then washed with a series of solutions: first a saturated aqueous solution of NH_4Cl (15 mL), followed by a $NaHCO_3$ (15 mL) and then by water (15 mL). The aqueous and the organic phases were separated, and the latter was further dried out using anhydrous magnesium sulphate and filtered. The solvent was evaporated and the residue dried up to constant weight.

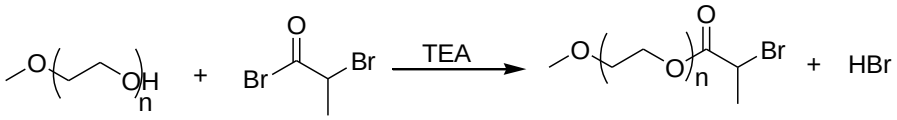

Figure 33 - 1st step of PEG-X synthesis.

In the second step, the product from the first step was dissolved in DMC (55 mL) and 3.2 g (2.0×10^{-2} g mol^{-1}) *O*-ethyl xanthic acid potassium salt were slowly added and left overnight for stirring.

The resulting product was purified, removing the formed KBr by filtration and sequentially washed two times with a saturated aqueous solution of NH_4Cl (15 mL), followed by a $NaHCO_3$ (15 mL) and after with water (15 mL). Similarly to the first step the phases were separated and the organic one was dried using magnesium sulphate. After filtration the resulting solution was precipitated in petroleum ether in an ice bath and the recovered product was dried under vacuum.

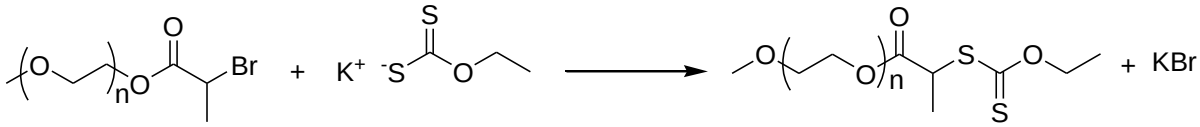

Figure 34 - 2nd step of PEG-X synthesis.

After the polymerization, M_n was determined by size exclusion chromatography analysis in THF solvent (after methylation) and, subsequently, the dispersity, *Đ,* was obtained. These variables were around 2300 g mol^{-1} and 1.03, respectively (Figure 42).

The product was also analyzed by ^{1}H NMR in $CDCl_3$ (presented in following chapter), which confirmed the structure of the PEG-X.

2.1 - High pressure polymerization

The polymerization of ethylene involved several procedures that had to be made previously to it. The initial aqueous solutions were prepared in a *Schlenk*, the desired quantities of initiator (around 50 mg of AIBA or ACPA, or 44 mg of APS) were added to 50 mL of deionized water. Depending on the system, 50 mg of surfactant (CTAB) or different amounts of macroRAFT agent (PEG-X) could be introduced in the solution. After, the solution was degassed for around 15 minutes by bubbling under an inert gaseous atmosphere (argon) before its injection in the reactor.

2.1.1 - High pressure polymerization apparatus

The polymerizations were performed in an apparatus designed at C2P2 with a reactor from *Parr Instrument Company* as seen in Figure 35. The reactor used was a 160 mL stainless steel autoclave capable of withstanding temperatures of 150°C and pressure up to 250 bar. These variables acquired by temperature and pressure sensors in the reactor connected to a computer, allowing the in-line acquisition from the software. For safety reasons an *Inconel* rupture disk, with rupture at 340 bar, and a relief valve were added to the reactor in case of overpressure. The stirring inside the reactor was achieved by a *Rushton* turbine and the temperature control was ensured by a jacket that could be heated or cooled down.

In order to inject the solution into the reactor, an injection chamber of 50 mL of capacity was connected to the latter, allowing the injection in one step even when the reactor was under pressure as seen in the following figure.

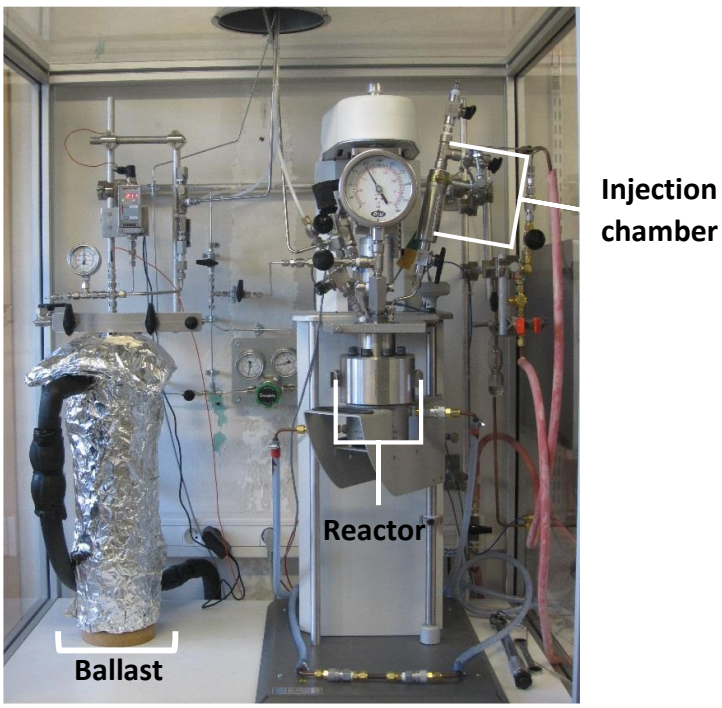

Figure 35- Ethylene high pressure polymerization apparatus (C2P2) - Ballast (left) and reactor (right).

2.2 - Free radical emulsion of ethylene

Before starting the polymerization, the reactor undergoes successive cycles of argon pressurization and vacuum atmospheres. Meanwhile the reactor was preheated to the desired polymerization temperature. The initial solution, which previously had been under an argon atmosphere, was transferred to the injection chamber through a *cannula*, pushed by argon.

After the injection chamber was filled with the solution and the inert conditions were set, the solution was loaded into the reactor and the ethylene was immediately introduced in order to initiate the polymerization. Since it was a semi-batch polymerization system, the pressure of ethylene decreased as the reaction went on, so it was necessary to frequently add ethylene to keep the reactor in isobaric conditions.

To provide the necessary ethylene pressure for the experiments, a 1.5 liter steel ballast (on the left of Figure 35) was used in this apparatus instead of high pressure compressors (ethylene was supplied to the laboratory in a bottle at 70 bar). Thus, to guarantee the desired pressure, the ballast had a jacket with a cooling or heating system, which would be cooled down to -20°C by a cryostat liquid and fed with ethylene coming from the bottle at around 40 bar, conditions under which ethylene is in liquid state. When the pressure inside the ballast reached 40 bar, the system would be in equilibrium and ethylene feed valve would be closed. Afterwards the ballast was heated until room temperature, reaching around 200 bar of ethylene, normally sufficient to maintain the differential in pressure between the ballast and the reactor. Whenever higher pressures were needed, the ballast had to be heated, getting pressures up to 300 bar.

After the desired polymerization time was reached, the reactor was cooled down and slowly degassed until atmospheric pressure. Then the reactor was opened in order to collect the resulting latex. Samples from these latexes were taken to perform colloidal characterizations and other fractions of these latexes were dried to determine the solids content, which was used to calculate the polymer content after subtracting the non-polymeric components such as the initiator and surfactant.

3 - Polymer characterization

3.1 - Gravimetry

The characterization of the polymers was divided in several categories. The first one was the gravimetric analysis where a set of analytic methods were performed based on the mass of the sample. The solids content (SC) of each polymerization was measured by drying a known mass of the obtained latex (m_{latex}) at 70°C and under vacuum. After total evaporation of the solvent (water) the remaining mass ($m_{dry\ extract}$) was weighted and the solids content in mass was determined by the equation below:

$$SC\ (\%) = \frac{m_{dry\ ext.}}{m_{latex}} \times 100$$

To determine the polymer content (PC) of the latex, the masses of the other species (i.e. initiator, PEG-X and surfactant, if present) were subtracted from the total mass and this was taken into account in the determination of the polymerization yield. On the other hand, in the case of formation

of coagulated polymer the yield was calculated from the polymer content of the latex part and the mass of coagulated polymer.

The yield (%) given by the polymer content, in this case is just PE content, was obtained by following equation:

$$Yield\ (\%) = \frac{m_{polymer}}{m_{latex}} \times 100$$

3.2 – *Molar mass measurements - Size Exclusion Chromatography (SEC)*

Polymer molar masses were measured in a Viscotek Malvern® HT-GPC Module 350 A (Figure 36) by Size Exclusion Chromatography (SEC) - to obtain the number-average molar mass, M_n and the weight-average molar mass, M_w and subsequently the *dispersity* ($Đ = M_w/M_n$). This determination was based on a triple detection system: viscosimeter, refractometer (RI), light scattering at a low angle (7° –LALS) and a right angle (90° – RALS) at a 1 mL min^{-1} elution rate.

This equipment had 3 standard columns (300×7.8 mm -PPS POLEFIN® with the single porosity of $1,0 \times 10^6$Å, $1,0 \times 10^5$Å and 1000 Å) with different separation ranges. As the obtained polymers were in a latex form they needed to be dried and further dissolved at 150℃ in 1,2,4-trichlorobenzene (TCB) stabilized with 2,6-di(tertbutyl)-4-methylphenol (200 mg L^{-1}) with the resulting concentration in the optimal range between 3 and 5 mg mL^{-1}.

The software used for data acquisition and treatment was the *OmniSEC* from *Malvern*. The molar mass distribution values were calculated with a calibration curve based on narrow polyethylene standards or on the Universal calibration – based on refractometer and viscometer data.

Figure 36- Viscotek Malvern® HT-GPC Module 350 A used to determine polymer molar masses and dispersities by SEC.

3.3 - Differential Scanning Calorimetry (DSC)

To obtain the melting temperature (T_m), crystallization temperature (T_c) and crystallinity (X_c and Xm) Differential Scanning Calorimetry (DSC) analyses were performed on an equipment from Mettler-Toledo (DSC-1) where a crucible ($40\mu L$, aluminum) was filled with the previously dried samples. These samples were submitted to two successive heating and cooling cycles (from 10℃ to 160℃ at a 5℃ min^{-1} rate and from 160℃ to 10℃ at a rate of 20 ℃ min^{-1}).

DSC was performed on the latexes as well. However the temperatures of the cycles were different – heating from 0℃ to 130℃ and then back to 0℃ at a rate of 5℃ min^{-1} in both cases. In this case 120µL stainless steel crucibles sealed with a Viton O-ring were employed.

3.4 - Colloidal analyses - Dynamic Light Scattering (DLS)

The study of the colloidal properties of the obtained latex was carried out by Dynamic Light Scattering (DLS) using a Malvern® Zetasizer Nano ZS (Figure 37). With this study it was possible to determine the particle size through the hydrodynamic particle diameter (Z_{av}) using the software of the Zetasizer Nano ZS that also allowed the determination of the particle size distribution given by the polydispersity index, *PDI*, value. Usually, a higher the PDI value implies a broader particle size distribution. However, these analyses are suitable for spherical particles. The analyses were made by non-invasive method, with a 633 nm wavelength laser beam being sent to an infinitely diluted sample. The scattered signal intensity was analysed at a 173° angle, at 25 °C.

Figure 37 - Malvern® Zetasizer Nano ZS used in the DLS analyses (determine Z_{av} and PDI).

3.5 - Nuclear Magnetic Resonance (NMR)

To analyse the structure of the products obtained in this work such as macroRAFT, the polymers, ^{1}H NMR analyses in $CDCl_3$ were performed on a Bruker Avance II (400 MHz) available at the C2P2 laboratory.

Figure 38 - Bruker® Avance II (400 MHz).

3.6 – Transmission Electron Microscopy (TEM)

The electronic microscopy analyses were performed at the *Centre Technologique des Microstructures, Ctμ, Platform of the campus Lyon 1 - Université Claude Bernard (Villeurbanne, France*) on a Philips CM120 transmission electron microscope capable of supplying tensions between 60 and 120 kV (Figure 39).

Transmission electron microscopy (TEM) was performed on the samples, which were prepared by diluting a fraction of the latexes. A drop ($30\mu L$) of the diluted solution was then deposited onto a Formvar/carbon-coated copper grid and left to dry at room temperature for several minutes. Afterwards, the excess solution was removed by using a filter paper and the grid was isolated and left for further drying at room temperature.

The cryogenic transmission electron microscopy (cryo-TEM) analyses were performed in order to preserve the latex in its original structure, unlike TEM analyses. This process would allow trapping the particles in amorphous ice allowing them to keep their morphology. The samples were prepared on site. Similarly to the procedure for TEM, the latex sample was diluted to an appropriate concentration. After, a drop from this solution was deposited on the grid surface (Quantifoil® R2/1 copper grid with 100 Holey carbon film) and the grid was submerged in a liquid ethane container to freeze the latex as fast as possible.

Figure 39 - Philips CM120 transmission electron microscope in Ct*µ.*

Chapter III – Results and Discussion

This page was left intentionally in blank.

1 - Introduction

As introduced during this report, the present work resulted from the knowledge developed at the Laboratory of Chemistry Catalysis, Polymers and Processes (C2P2) in the last few years. The work developed that team showed that the harsh polymerization conditions, mainly used in industry, for the free radical polymerization process of ethylene were not necessarily unavoidable. [30] Indeed, it was evidenced that the polymerization could proceed under mild conditions. However, the solvent choice played a major role in the polymerization of ethylene. [27], [28] These experiments were performed in organic solvent and transfer to solvent reactions were the main concern.

As a non-transferring polar solvent, water was then an interesting case to study. This was carried on using commercial 2,2'-azobis(2-methylpropionamidine) dihydrochloride (AIBA) as an hydrosoluble alternative to AIBN, used with organic solvents. [27], [30] Using cetyltrimethylammonium bromide (CTAB) as surfactant, polymerization of ethylene could be conducted in water successfully generating PE latex particles. These studies have been of paramount importance to the present work since they were set as benchmarks. They allowed us to sort out the reactor work up very quickly, by comparing our experimental polymerization procedures and the resulting data to these references experiments. They were also valuable to evaluate the data obtained from the experiments with macroRAFT agents.

Another field of great interest and largely studied at C2P2 was the control of macromolecular architectures by living polymerization techniques. The milder polymerization conditions of ethylene played a major role in the feasibility of alternatives to the current methods used to control the growth of the chains, and obviously in the properties of the final material. The work of *C. Dommanget* was possible due to these mild polymerization conditions, reporting the first case of controlled radical polymerization of ethylene through reversible addition-fragmentation chain transfer in the presence of xanthates.

Combining the fields of knowledge previously mentioned, a surfactant-free emulsion polymerization of ethylene using RAFT as control technique to produce PE-based nanoparticles revealed itself a relevant study to be developed. The subject is the aim of this work.

Hence, this chapter reports the results associated to the study, their treatment and the conclusions drawn from these data. The chapter is divided into several parts, starting by a focus on the synthesis of the PEG-X macroRAFT agent (a polyethylene glycol end-functionalized with xanthate) and its characterization. The second section presents the different polymerizations carried out in this work and analyse of the resulting products' characteristics. This section of the chapter ends with a comparison between the behaviour of the different kinds of polymerization. Next, a study was then undertaken to evaluate the influence of the macroRAFT amount used in the polymerization system (for a constant initiator amount). The last part of this chapter presents a kinetic study of ethylene polymerization performed in the presence of the macroRAFT agent. The experiment was performed at either 100 or 200 bar, allowing to draw further conclusion on the effect of pressure in these systems.

2 – Synthesis of the macroRAFT agent – PEG-X

As mentioned in the literature review chapter, the RAFT process is probably the most versatile method for providing control to the polymerization of both more-activated and less-activated monomers (LAM) such as ethylene. [55] The core reactions of this technique were explained in the first chapter (see section 2.6.2). Nevertheless, it is important to notice that the polymerization control in this method is established by the use of thiothiocarbonylated compounds as chain transfer agent (CTA). The RAFT agent (CTA) has a great influence in the control of the polymerization and consequently it has to be carefully chosen. A particular class of RAFT agents that have proven to be very efficient for the controlled polymerization of less activated monomers are xanthates. In this case, the process can also be called MADIX (*Molecular Design by Interchange of Xanthates*).

To apply the PISA process to the synthesis of PE particles (which would be ideally constituted of PEG-*b*-PE amphiphilic block copolymers), the study first focused on the synthesis of a xanthate-functionalized PEG macroRAFT agent. However, this kind of polymer could obviously not be obtained by polymerization in water, preventing the set-up of one pot process (see section 3, chapter I). Its preparation from post-modification of a commercial PEG and its characterization are shown below.

2.1 - PEG-X synthesis

From previous works, it is known that a suitable way of obtaining PEG-based macroRAFT agents is to perform the post-modification of an existing polymer by introducing a xanthate extremity. These PEGs can be prepared via anionic polymerization and have one or two hydroxyl end functionalities (PEG-OH or HO-PEG-OH) that can be further modified into end-functionalized xanthate PEGs (PEG-OH→PEG-X).

As reported in the experimental chapter, the process that led to the production of the macroRAFT PEG-X (Figure 40) used in this work was a sequence of two steps. Herein, are reported the results of this process.

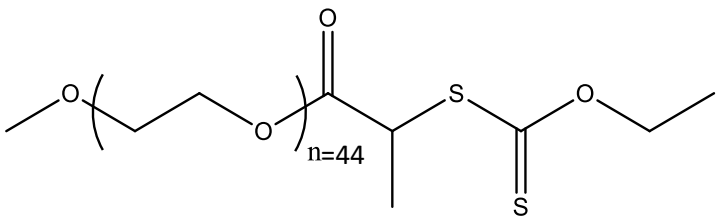

Figure 40 - PEG-X macroRAFT structure (n=44).

To evaluate the structure of the macroRAFT and confirm the correct end-functionalization the PEG-X was analysed by ^{1}H NMR, using deuterated chloroform ($CDCl_3$) as solvent and trioxane was used as internal reference. The obtained spectrum is present in Figure 41.

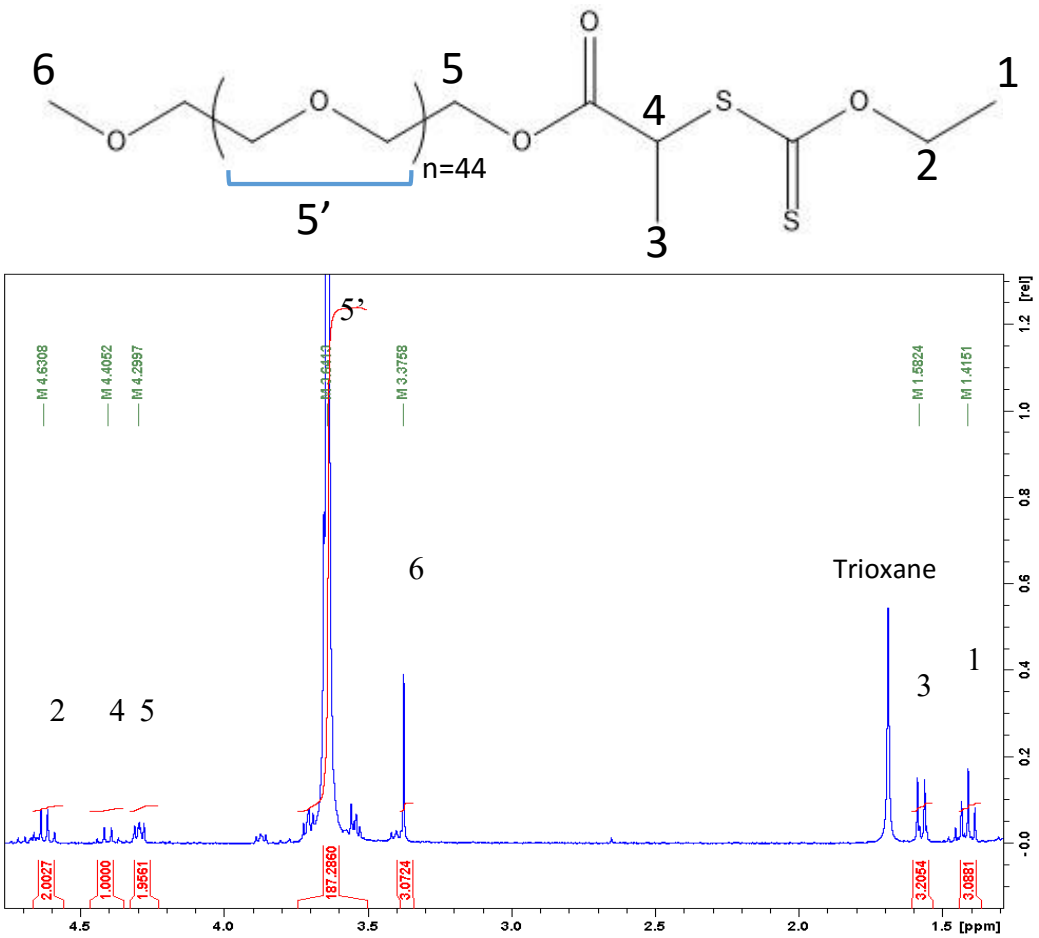

Figure 41 - ^{1}H NMR of PEG-X in $CDCl_3$.

The NMR spectrum of the PEG-X revealed that the obtained structure for this molecule was consistent with the data from other studies where this macroRAFT was synthesized. [62] The integration of the resonances and the respective chemical shifts of the ^{1}H spectrum allowed identifying the groups and structure according to the figure above. Additionally, based on the integration of the resonances, the molar mass of the polymer was estimated 2300 g mol^{-1}, in good agreement with the expected value. These values compared well with that obtained by the SEC analysis.

The Size Exclusion chromatography (SEC) was performed in THF and the resulting elution curve can be seen in Figure 42. This analysis permitted to obtain the molar mass of the macroRAFT agent and its dispersity, being respectively, 2300 g mol^{-1} and 1.03. Once again, these values were similar to

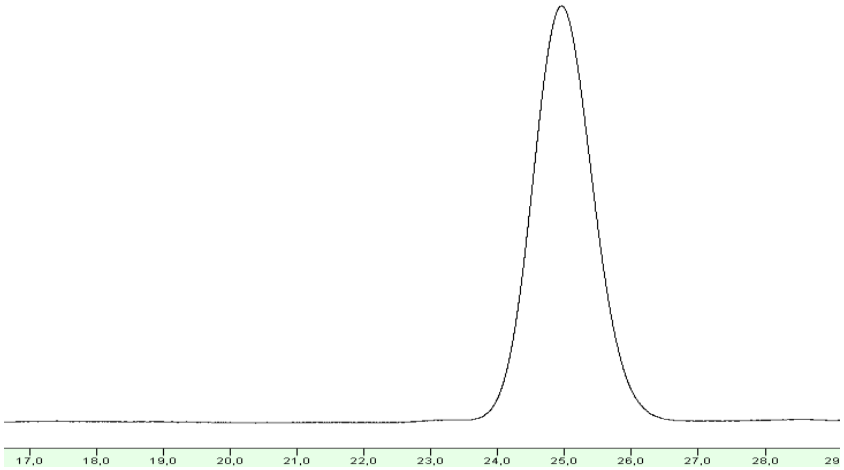

Figure 42 -Retention volume curve of PEG-X from SEC analysis in THF (M_n ≈2300 g mol^{-1} and Đ≈1.03).

the ones reported in previous studies, which meant that this macroRAFT was suitable for the second part of this work. [62]

Parameters such as crystallinity and melting temperature influence the particle morphology and the properties of the final product. The polyethylene glycol end-functionalized with the xanthate group was thus analysed by Differential Scanning Calorimetry. This technique allows the evaluation of the melting temperature, T_m, and the crystallization temperature, T_c, as well as the crystallinity values (X_c and X_m). As seen in Figure 43, the crystallization was identified in the exothermic curve and the melting temperature was identified in the endothermic curve. It was observed a rather high crystallinity, around 47 %, and a T_m of around 50°C, a value very close to the one that characterizes polyethylene glycol methyl ether, 52°C.

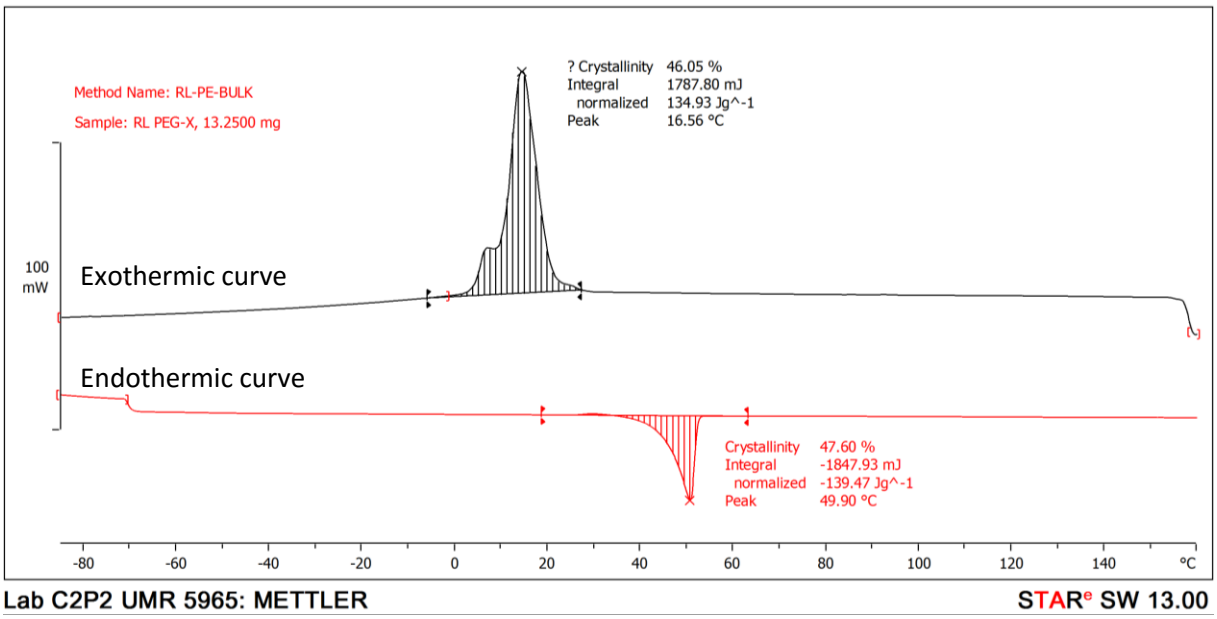

Figure 43 -DSC analyses of PEG-X.

In summary, this work led to the synthesis of a macroRAFT agent, by using a common methodology in this type of syntheses - the end-functionalization of an existing polymer chain, in this case polyethylene glycol, with a xanthate group that will play a major role in the control of the polymerization process. After the synthesis, the resulting product was submitted to a number of analyses that validated the procedure, in good agreement with data from previous syntheses. The free radical emulsion polymerization of ethylene is now depicted in the following section.

3 - Free radical emulsion polymerization of ethylene

3.1 - Comparison between different types of polymerization

As said in the introduction of this chapter, the first sets of experiments were performed in order not only to verify the experimental methodology but more importantly to establish references to the experiments performed in the presence of the PEG-X macroRAFT agent. The reference experiments thus include polymerizations carried out in water 1) with the initiator only, 2) with both initiator and surfactant, and 3) with initiator and the commercial PEG (PEG-OH). The major features that characterize each of these polymerization systems are compared with that observed for the polymerization performed in the presence of initiator and PEG-X. All the resulting polymeric products (both the latex and the dried polymer) were deeply characterized (gravimetry, thermal analyses and electronic microscopy). Finally, the possible conclusions that could be drawn from these polymerization are presented.

The polymerization conditions were selected according to the knowledge developed at the C2P2 laboratory for studies in systems that led to this work. [27], [31] Indeed, works on free radical emulsion polymerization of ethylene showed that a cationic initiating and stabilizing system was suitable. 2,2'-azobis(2-methylpropionamidine) dihydrochloride (AIBA, Figure 44 - [2]) and cetyltrimethylammonium bromide (CTAB, Figure 44 - [1]) were thus selected as water-soluble initiator and surfactant (if used), respectively.

Ethylene pressure was fixed to 100 bar at the beginning of the process and maintained with small addition of ethylene into the reactor as it was consumed during the reaction (4h for each type of polymerization). The stirring rate was set to 250 rpm and the temperature at 70°C, being sufficient to allow the decomposition of the initiator, AIBA, and to guarantee a decomposition rate that ensured a reasonable reaction rate (AIBA, $k_d = 1{,}9 \times 10^{-3} s^{-1}$ in water at 69°C). [63] AIBA was charged initially into a *Schlenk* with around 50 mL of deionized water. Depending on the desired polymerization process, others species could be added to the initial solution, such as the surfactant CTAB, PEG-OH or PEG-X. The added masses of each species depended on its function and intrinsic characteristics:

- The chosen quantity of CTAB was selected to be three times (concentration of 1 g L^{-1}) above the value of the *Critical Micelle Concentration (CMC*, 0,8 mmol L^{-1} or 0,3 g L^{-1}*)*.

- As mentioned above, it was found relevant to perform the free radical emulsion polymerization of ethylene under the standard polymerizations conditions but with the commercial PEG-OH (Figure 44 - [3]). This procedure allowed us to set a reference to evaluate the activity of the chain end, that is, the influence of the xanthate chain-end in the polymerization of ethylene.

- As will be seen in the following section, the quantity of the PEG-X was varied to study the characteristics of the resulting polymer.

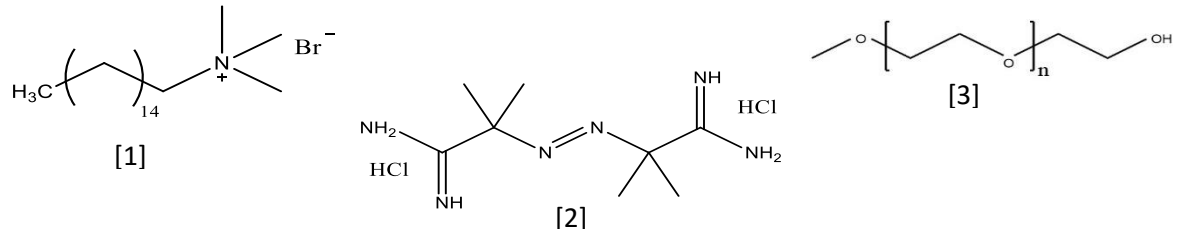

[1] [2] [3]

Figure 44 – [1] - CTAB (concentration 1 g L^{-1}); [2] – AIBA; [3] - PEG-OH;

The references of the four representative experiments to be compared are:

- RL-PE 18 selected as the blank experiments (performed only with AIBA initiator);

- RL-PE 20 for the polymerizations performed with AIBA and surfactant (CTAB);

- RL-PE-14 for the polymerizations performed with AIBA and PEG-OH;

- RL-PE 09 for the polymerizations performed with AIBA and PEG-X.

3.1.1 - Comparison between the appearance of the different types of polymerization

In the first place, the appearance of the latexes obtained by experiments in emulsion polymerization of ethylene was observed to evaluate their stability. Indeed, the recovered latexes from the four different polymerizations revealed to be stable for the standard polymerization conditions. According to the similar aspect of the produced latexes they were divided in two groups of experiments.

The ethylene polymerization performed only with the initiator yielded a milky stable white latex, as observed in Figure 45–[1], which had the same appearance of the latex produced in the polymerization performed with PEG-OH (Figure 45–[3]). On the other hand, the polymerization with surfactant, CTAB, (Figure 45–[2]) gave rise to latexes with a translucent aspect, which were very similar to the ones obtained in the presence of PEG-X (Figure 45–[4]). The appearance of the obtained latexes can be an indicator of the particles size present in the samples. Thus, a milky latex aspect usually indicates the presence of large particle (≈100 nm) and a translucent one, as obtained from the polymerizations with CTAB and PEG-X is an indicator of the presence of smaller particles size (≈20 nm).

[1] [2] [3] [4]

Figure 45 - Latexes obtained by FREPE (1- Blank; 2 - CTAB; 3 - PEG-OH; 4- PEG-X) (4h, 50 mg AIBA, 250 rpm, T=70°C, and $P_{ethylene}$≈100 bar).

3.1.2 - Comparison between the yield of the four types of polymerization

The yield was the first polymer characteristic to be measured. The value of the yield was calculated from the polymer content of the samples.

Table 2 presents the yields of the different types of polymerization for the same polymerization time, 4 hours (blank, with surfactant, PEG-OH and PEG-X) sorted by increasing order of values.

Table 2 -Comparison of yields for the different types of polymerizations (4h, 50 mg AIBA, T=70 °C, and Pethylene≈100 bar).

Polymerization Type	Name of sample	Quantity (1)	Yield (g)/PC (%)
Polyethylene Glycol Xanthate **(PEG-X)**	RL-PE 09	0.3 g	0.5/0.9
Without surfactant **(Blank)**	RL-PE 18	--	0.6/1.2
Polyethylene Glycol **(PEG-OH)**	RL-PE 14	1 g	0.6/1,2
With surfactant **(CTAB)**	RL-PE 20	50 mg	2.6/5.0

(1) - Mass of the referenced compounds introduced in the initial solution (CTAB, PEG, PEG-X).

The highest achieved yield was the one corresponding to the polymerization carried out in the presence of surfactant, CTAB, obtaining, as expected, similar to the ones reported in previous studies (*G. Billuart and E. Grau*) [64]. In addition, the surfactant-free polymerization also presented similar values to the ones from former studies. This indicated a good reproducibility for the polymerization methodologies.

The surfactant-free experiment and the one performed with PEG-OH, which presented a similar aspect (milky white latex), also showed very close yields. The presence of PEG-OH in the initial solution does not seem to significantly affect the course of the polymerization as the production of polyethylene was similar (0.6 g).

At last, the polymerization process in the presence of the macroRAFT agent was the one that achieved the lowest yield. However, this was the polymerization (RL-PE 09) that had the highest yield from the polymerizations performed with PEG-X (Study presented later in section 3.2). The first experiments of this type involved a larger amount of PEG-X in the initial solution, and lead to a very low yield (almost no PE formed). This can be possibly explained by the initial molar ratio between the initiator and the macroRAFT agent (PEG-X/AIBA=2.3), which would not be in the optimal range for obtaining the maximum yield (PEG-X/AIBA=0.6). The influence of the PEG-X/AIBA ratio will be discussed below (section 3.2), by varying the quantity of PEG-X in the system while keeping the same quantity of AIBA in the initial solution.

3.1.3 - Comparison of the particle morphology for the different types of polymerization

The morphology of the PE particles in the latexes was analysed by Transmission Electron Microscopy (TEM). Due to the low contrast characteristic of PE, it was very difficult to obtain clear pictures by TEM. In some cases, to investigate the original structure of the PE particles in the latex, a special type of TEM was employed, Cryogenic Transmission Electron Microscopy (cryo-TEM). In this method, the particles are imprisoned in amorphous ice, which allows them to keep their original morphology. The TEM pictures also allowed to evaluate particle size and particle populations, which were compared to the results obtained by Dynamic Light Scattering (DLS). The TEM pictures that characterize each type of latex are presented below in Figure 46 - TEM of PE particles: [1] – Blank; [2] – CTAB; [3] – PEG-OH; [4] – PEG-X.

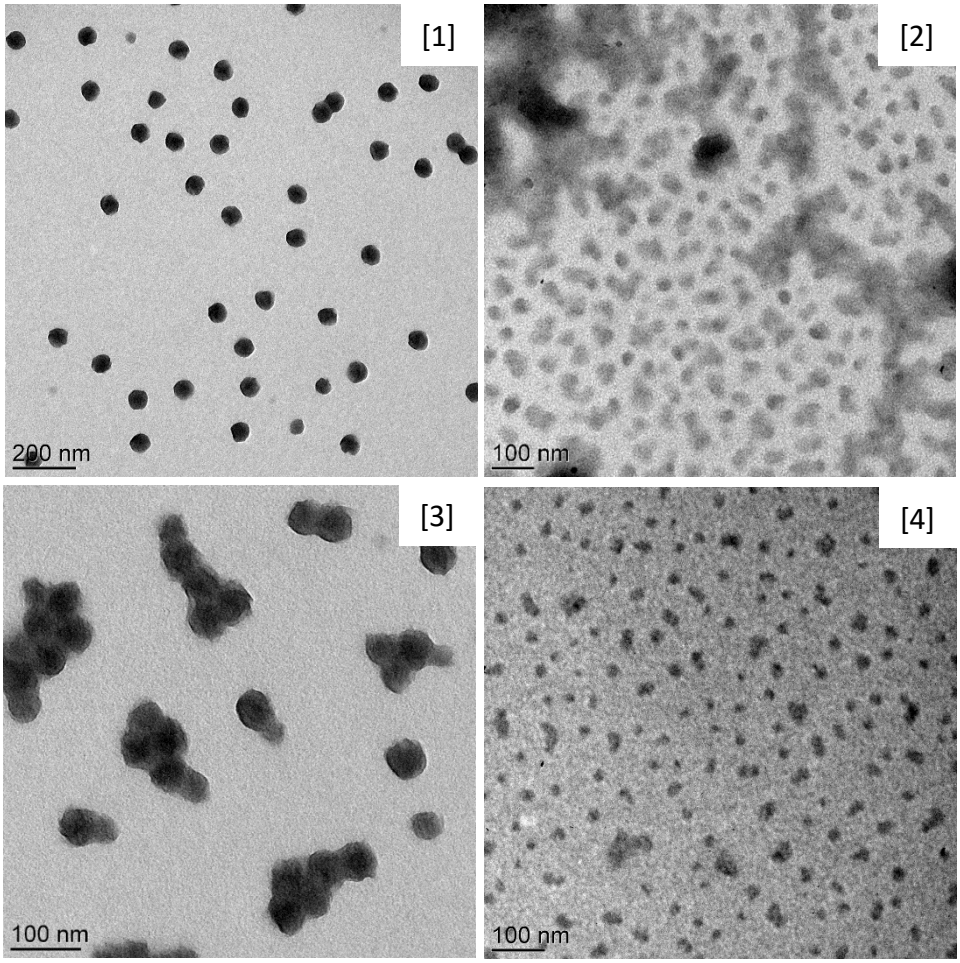

Figure 46 - TEM of PE particles: [1] – Blank; [2] – CTAB; [3] – PEG-OH; [4] – PEG-X.

As seen in Figure 46, the TEM pictures support the conclusions drawn out from the characterization data obtained above. The resemblance between two groups of polymerizations (blank and PEG-OH versus CTAB and PEG-X) rises again in these analyses.

The experiments performed only with initiator yielded relatively large spherical particles (Figure 46 [1]), in the range around 75 nm, which also happened with the polymerization carried out in the presence of PEG-OH. The latter generated PE particles that were also spherical of around 75 nm, although in this case they seemed to have a higher tendency to agglomerate. These results are in line with the similar appearance of these latexes (stable and milky).

The second group to be approached in this study was the one that involves the small particle sizes, that is, the polymerizations carried out with surfactant or in the presence of PEG-X. Both originated a population of particles with a diameter around 25 nm. As in the first group, the particle size observed in these analyses confirmed the conclusions drawn from the appearance of both latexes.

In the case of the polymerization in the presence of the CTAB surfactant, a very large number of particles appeared to be rather non-spherical or disk-like shaped. As a matter of fact, in previous works with experiments including the same surfactant in the same conditions, the observed particles had a disk-like shaped morphology. These unusual kinds of structures were attributed to the crystallinity of the polymer that seemed to prevent the formation of spherical particles. [30], [31]

The polymerization with the macroRAFT agent seemed to produce a large number of particles with non-spherical or disk-like morphologies. However, the TEM and cryo-TEM pictures of this sample evidenced the presence of other structures, such as "cylindrical" particles as seen in the following Figure 47. In some figures it seems that a portion of the small particles has the tendency to agglomerate and another to remain dispersed or attached in very small domains. The Cryo-TEM process, which is supposed to preserve the morphology of the samples show particles sizes at a very small scale, around 20 nm as observed in standard TEM pictures. However, it was observed that the particles had a higher tendency to agregate into larger structures when compared to the pictures taken in the TEM process. These phenomena of agglomerations have to be studied in more details to conclude on their orgin (probably during the sample prepartion).

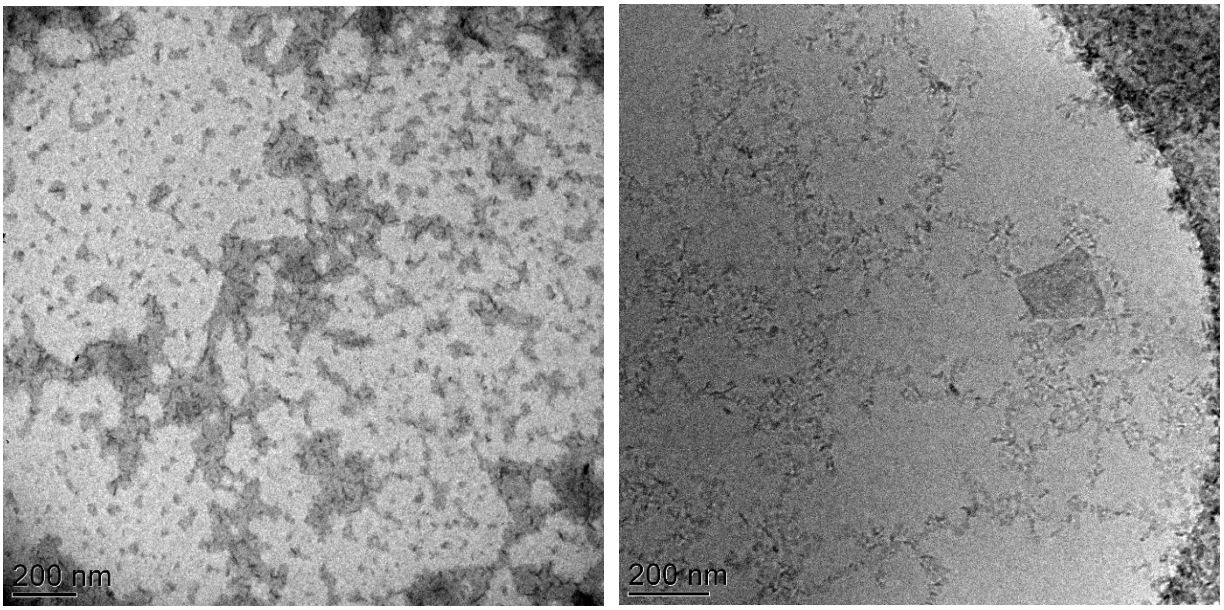

Figure 47 – TEM (left) and Cryo-TEM (right) of PE particles performed with PEG-X (RL-PE 09) (200nm).

Morphologies different from the spherical one can be obtained in the frame of the PISA process. [60] Polyethylene particles could have disk-like or cylindrical shapes due to PE crystallinity, which affects the particle morphology.

3.1.4 - Comparison of the Dynamic Light Scattering data

The four latexes were analysed by Dynamic Light Scattering (Table 3). This analysis provided as main results the hydrodynamic particle size, Z_{av}, and also the polydispersity index (PDI), which usually gives an indication of the "homogeneity" of particle size distribution. Again the polymerizations can be divided into two groups, according to the acquired data.

Table 3 -Comparison of particle sizes and PDI of the four polymerizations. (4h, 50 mg AIBA, T=70 ℃, and Pethylene≈100 bar).

Polymerization Type	Name of sample	Quantity(1)	Z_{av}(nm) [*PDI*]
Polyethylene Glycol Xanthate **(PEG-X)**	RL-PE 09	0.3	20 [0.249]
With surfactant **(CTAB)**	RL-PE 20	50 mg	25/865(2)
Without surfactant **(Blank)**	RL-PE 18	--	75 [0.02]
Polyethylene Glycol **(PEG-OH)**	RL-PE 14	1 g	72 [0.02]

(1) – mass introduced in the initial solution (CTAB, PEG-OH, PEG-X); (2) -Two particle populations.

The “large particle size group” constituted by the latexes obtained from the polymerizations without surfactant or with PEG-OH yielded the same particle size, around 75 nm and had a very low particle size distribution value, around 0.02, as seen in Figure 48. Corroborating the results from transmission electron microscopy, the particle morphology was spherical. DLS analyses perform well with this kind of morphology. The PDI values remained low and reflected a monomodal particle size distribution. The characteristics obtained by DLS were another indicator of the resemblance between these two polymerizations and the lack of influence by the PEG backbone on the ethylene polymerization. The particle size distribution by its intensity is showed in the following figure.

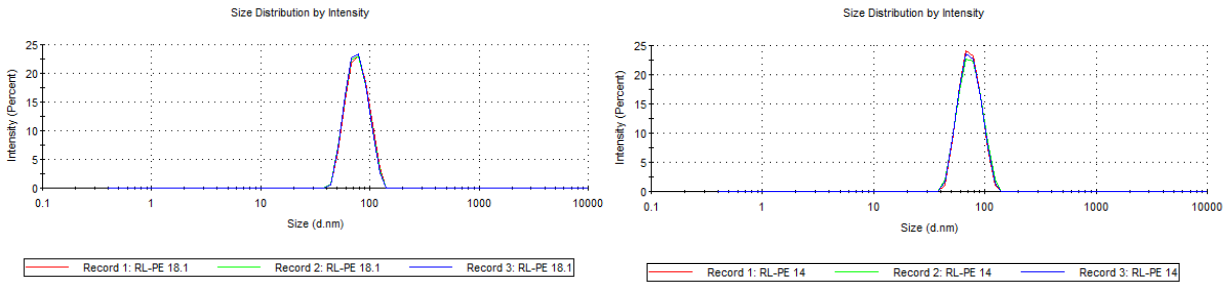

Figure 48 - Particle size distribution by Intensity (RL-PE 18, blank - left) (RL-PE 14, blank - right) (4h, 50 mg AIBA, 250 rpm, T=70 ℃, and Pethylene≈100 bar).

In the “group with lower particle sizes” we find again, like in TEM, the polymerization performed with the macroRAFT agent and the one performed with surfactant (CTAB). As observed by TEM the first one yielded a main population with the characteristic particle size around 25 nm with a high polydispersity (0.25), which was interpreted as a deviation from the spherical morphology that this analytical methodology is design to cope with, and the inadequacy of the DLS measurements in this case. One can also notice the presence of bigger objects, in agreement with TEM observations (Figure 48). Based on the theory associated with DLS it was assumed that the number of the smaller particles surpassed greatly the number of the particles from the larger size population, having a signal much more intense (proportional to radius of the particle - $\approx r^6$). This is evidenced in the following figure that shows the particle size distribution by its intensity.

The second polymerization type in this group, performed with CTAB, yielded a two particle population. The population of small particle size around 25 nm was predominant because the intensity (proportional to radius of the particle - $\approx r^6$) of this population (≈64%) surpasses greatly the one of the population with large particles (≈36%), turning these results comparable with those for the polymerization with the macroRAFT. However, the large objects present in this sample may be large PE particles, but also objects formed of CTAB, such as vesicles, as previously reported. [64]

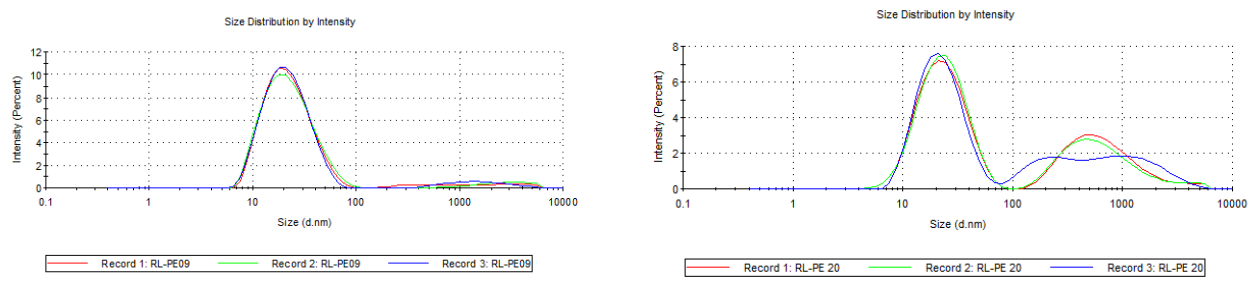

Figure 49 - Particle size distribution by Intensity (RL-PE 09[PEG-X], left) (RL-PE 20[CTAB]- right) (4h, 50 mg AIBA, 250 rpm, T=70 ℃, and $P_{ethylene}$≈100 bar).

3.1.5 – Comparison of Differential Scanning Calorimetry (DSC) data

The samples obtained from the four different types of polymerization were analysed by DSC. The method was employed to a small dried fraction of the latex, and the melting temperature of the sample (T_m), the crystallization temperature (T_c) and crystallinity from crystallization and melting curves (X_c and X_m) were determined (Table 4).

Table 4 - Comparison of DSC values for the different types of polymerizations (4h, 50 mg AIBA, 70°C, and $P_{ethylene}$≈100 bar).

Polymerization Type	Name of sample	T_m(°C)	T_c(°C)	X_c(%)	X_m(%)
Without surfactant **(Blank)**	RL-PE 18	96	76	16	10
With surfactant **(CTAB)**	RL-PE 20	93	72	26	16
Polyethylene Glycol **(PEG-OH)**	RL-PE 14	52/96	24/79	21/6	27/3
Polyethylene Glycol Xanthate **(PEG-X)**	RL-PE 09	96	81	16	12

The blank experiments yielded a polyethylene, with very low crystallinity, lower than the expected (23%). However, the melting temperature was in agreement with the same system by *G. Billuart* (93°C) and lower than the usual T_m of commercial LDPE (≈ 100°C). The polymerization with surfactant was more consistent with the studies previously performed with CTAB, with the crystallinity and the melting temperature being in the same range and in-line with other studies (23% and 93°C, respectively) (*G. Billuart*). [64]

The *DSC* analysis of the product from the polymerization with PEG-OH revealed two peaks in each curve (Figure 50). This situation was interpreted as the existence of two different polymer species in the sample, possibly one related to the polyethylene glycol and the other to polyethylene, with the melting temperatures (52°C [63] and 95°C, respectively) near the ones reported for each.

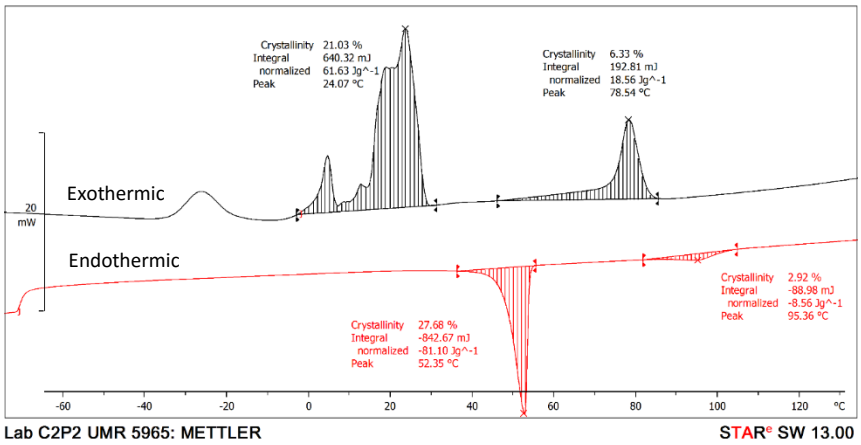

Figure 50 - DSC analyses of RL-PE 14 sample (1 g PEG-OH, 4h, 50 mg AIBA, 250 rpm, T=70°C, and $P_{ethylene}$≈100 bar).

At last, the DSC analysis of the product isolated from the polymerization carried out with PEG-X showed some interesting characteristics. As seen in Figure 51, a very broad peak appears both on melting and crystallization curves. The temperature range is similar to the one obtained by the surfactant-free process. The existence of just one broad signal can be an indicator that the PEG-X (DSC in Figure 43) is not free anymore, but trapped in a block copolymer structure.

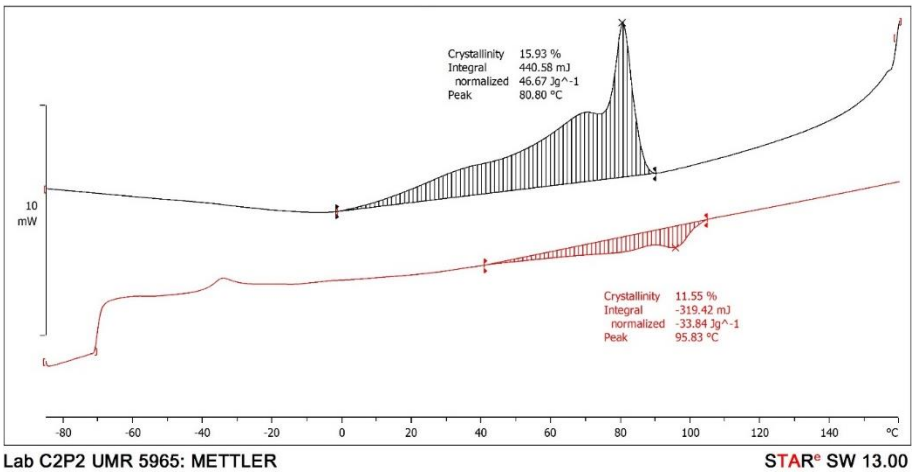

Figure 51- DSC analyses of RL-PE 09 sample (0.3 g PEG-X, 4h, 50 mg AIBA, 250 rpm, T=70 °C, and Pethylene≈100 bar).

3.1.6 – Comparison between polymer molar masses

The last property to be compared in this section is the molar mass of the samples, determined by size exclusion chromatography (SEC) at high temperature (150°C) in TCB. Figure 52 shows the obtained chromatograms and Table 5 gathers the M_n and dispersity values.

Table 5 -Comparison of M_n and Đ for the different types of polymerizations (4h, 50 mg AIBA, 250 rpm, T=70 °C, and Pethylene≈100 bar).

Polymerization Type	Name of sample	M_n (gmol^{-1})	*Dispersity (Đ)*
Polyethylene Glycol Xanthate **(PEG-X)**	RL-PE 09	2800	8.6
Without surfactant **(Blank)**	RL-PE 18	2700	5.1
Polyethylene Glycol **(PEG-OH)**	RL-PE 14	2800	5.6
With surfactant **(CTAB)**	RL-PE 20	5000/2,7× 10^5	5.6/1.2

The first three polymerizations (namely the blank experiment and the ones carried out with PEG-OH and PEG-X) gave rise to rather low and very similar values for the molar masses of the sample (Table 5). When comparing the blank experiment with the polymerization with PEG-OH, the proximity of the obtained values can be explained by the low effect that PEG-OH has on the behaviour of the polymerization, resulting in practical terms on a polymerization mainly dictated by the presence of the cationic initiator, which ensures the stabilization of the systems with positively charged fragments at the chain-ends (even if PEG-OH may participate to the stabilization due to transfer reactions on the PEG-OH backbone, leading to the formation of a graft polymer which can be anchored onto the particle surface). Both blank and PEG-OH samples have dispersities around 5 that might be related to the lack of control in these systems.

The product obtained from the polymerization in the presence of PEG-X presented a rather low molar mass, in the same range of the first two cases. Although the dispersity is even broader (8.6), likely related to the lack of control in these systems, it does not mean that the PEG-X does not influence

the polymerization. As observed from the other characterization (DSC, TEM and DLS), the PEG-X, namely the xanthate chain-end, has an effect on the process, possibly leading to the *in situ* formation of block copolymers and thus participating to the particle stabilization.

It is worth mentioning that if unreacted PEG-OH and PEG-X (M_n≈2000 g mol^{-1} and M_n≈2300 g mol^{-1}) were present in the samples they would be probably contained in the broad signals around 2800 g mol^{-1} obtained from SEC analyses (Figure 58).

The polymerization with surfactant was intrinsically different from the other types given that, as seen before, it yielded two different particle sizes. From previous studies of polymerization in the presence of CTAB (realized by *E. Grau* and *G. Billuart*) it was already expected that it would also give rise to two different molar mass populations, one with very low M_n and another with very high molar mass, which indeed happened (Table 3 and Figure 58). The low M_n population had its value around 5000 gmol^{-1} and the higher at 2.7× 10^5 gmol^{-1}. It is worth noting, however, that these values are significantly different from the ones obtained in the studies with the same system (≈2700 and 1,1× 10^6 gmol^{-1}), although in both populations, the $Đ$ was narrower (5.6 and 1.2 for the low and high M_n, respectively) than expected from the previous studies (15.3 and 2.7, respectively). [30], [64]

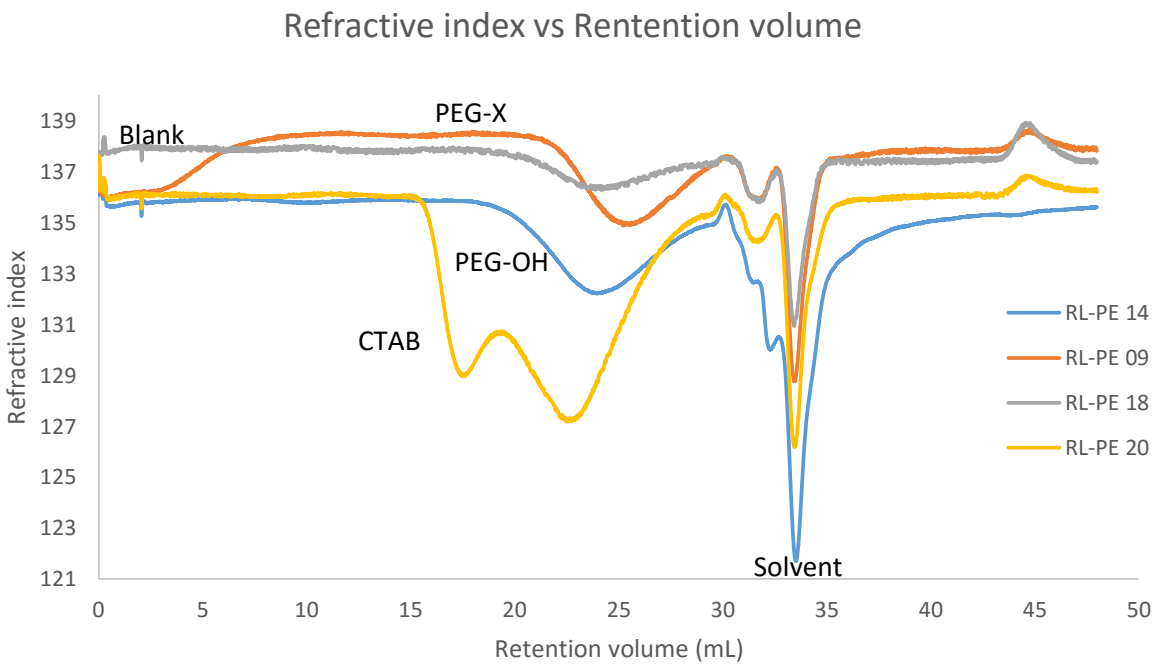

Figure 52 – Chromatogram of the samples RL-PE 09 (PEG-X); RL-PE 14 (PEG-OH); RL-PE 18 (Blank); RL-PE 20 (CTAB) (4h, 50 mg AIBA, 250 rpm, T=70 ºC, and Pethylene≈100 bar).

In summary, from the characterizations performed in this section it is possible to draw some conclusions. The reference polymerizations showed that the procedures were reproducible by comparison to former studies. There are two groups of polymerizations that had very similar characteristics. The first group included the surfactant-free process and the polymerization with PEG-OH. The second group was formed by the polymerization with surfactant (CTAB) and the one performed in the presence of PEG-X. The reference studies allowed to evaluate the effect of the presence of the xanthate chain-end. Indeed, from this section it is possible to conclude that the PEG-X influences the polymerization. The presence of a xanthate chain-end affects the polymerization given that the characteristics of the products obtained from the polymerizations with PEG-X are different from the ones with PEG-OH. Possibly, block copolymers formed in situ, helping the stabilization of the particles.

3.2 – Effect of the macroRAFT (PEG-X) amount on polymerization

The first polymerizations with PEG-X revealed that the obtained PE yield was strongly related to the quantity of macroRAFT agent, the polymerization being almost inhibited in some cases (molar ratio PEG-X/AIBA=2.3). Therefore, a study to evaluate the effect of polymerization conditions on the resulting latexes was carried on. A set of polymerizations were performed maintaining the same reaction conditions, that is, pressure (100 bar), temperature (70°C), stirring rate (250 rpm) and quantity of initiator (50 mg AIBA), while the concentration of PEG-X the quantity of PEG-X introduced in the initial solution and the PEG-X/AIBA ratio were varied.

For a standard polymerization time of 4 hours, three sets of experiments were performed with the following quantities of PEG-X of: ≈1 g, 0.5 g and 0.3 g. The recovered latexes were all stable and translucent.

The plot below shows a linear relation between the amount of PEG-X and the resulting yield (and polymer content).

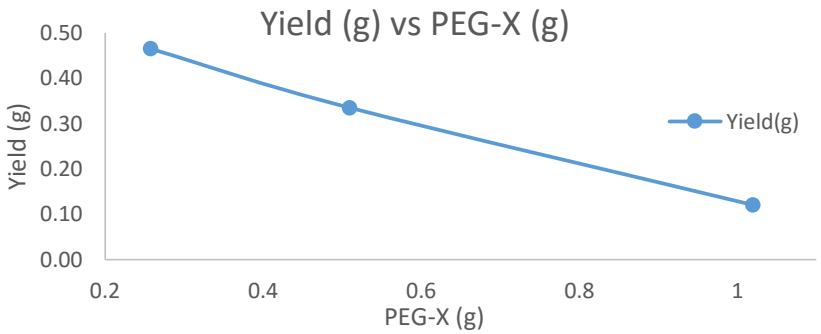

Figure 53 - Yield (g) vs. PEG-X (g) for the standard polymerization conditions ([1 g, 0.5 and 0.3 g of PEG-X], 4h, 50 mg AIBA, T=70°C, and $P_{ethylene}$≈100 bar).

As the quantity of PEG-X decreased, and consequently the ratio between PEG-X and AIBA increased, the polymer content of the samples increased significantly as seen in Table 6.

Table 6 –Yields, Z_{av} and PDI of the polymerizations performed with different quantities of PEG-X. ([1 g, 0.5 and 0.3 g of PEG-X], 4h, 50 mg AIBA, T=70°C, and $P_{ethylene}$≈100 bar).

Name of sample	PEG-X (g)	Molar ratio (PEG-X/AIBA)	Yield (g) / PC (%)	Z_{av} (nm)	*PDI*
RL-PE 07	1	2.3	0.1 (0.2)	25	0.272
RL-PE 08	0.5	1.2	0.3 (0.6)	19	0.189
RL-PE 09	0.3	0.6	0.5 (0.9)	20	0.249

Like the latex obtained from the experiment performed with 0.3 g of PEG-X (Figure 49), the latexes prepared with higher quantity of PEG-X (1 g, RL-PE 07 and 0.5 g, RL-PE 08) were also analysed by DLS (Table 6 and Figure 54-55).

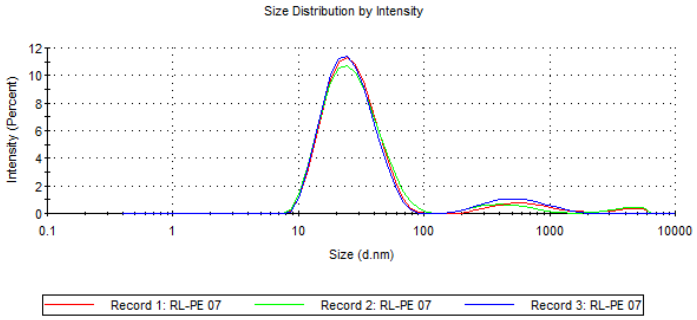

Figure 54 - Particle size distribution by Intensity (RL-PE 07) (1 g PEG-X, 4h, 50 mg AIBA, 250 rpm, T=70 ℃, and Pethylene≈100 bar).

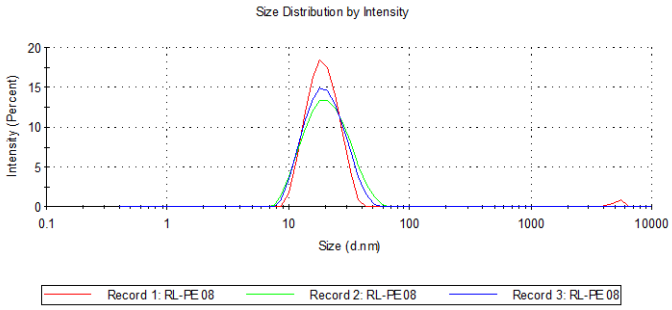

Figure 55 - Particle size distribution by Intensity (RL-PE 08) (0.5 g PEG-X 4h, 50 mg AIBA, 250 rpm, T=70 ℃, and Pethylene≈100 bar).

As present in Table 6 these two samples were characterized by having a low particle size and *PDI* values. The effect of the concentration of PEG-X on the particle size appears to be minimal in these polymerizations, with the Z_{av} of the three samples being around 20 nm and the PDI in the range of 0.2 to 0.3. These high values may be attributed to the deviation from the spherical particle morphology and the inadequacy of the DLS measurements in this case. As previously mentioned, it was assumed that the stronger intensity signal because the number of the smaller particles surpassed greatly the number of the particles from the larger size.

DSC analysis of the dried latex of these samples. (RL-PE 09 in section 3.1.5) from the experiment carried out with 1 g of PEG-X (RL-PE 07, PEG-X/AIBA=2.3) revealed that there was almost no polyethylene in that sample. The obtained T_m, T_c and crystallinity values are close to the ones obtained in the DSC analysis of PEG-X.

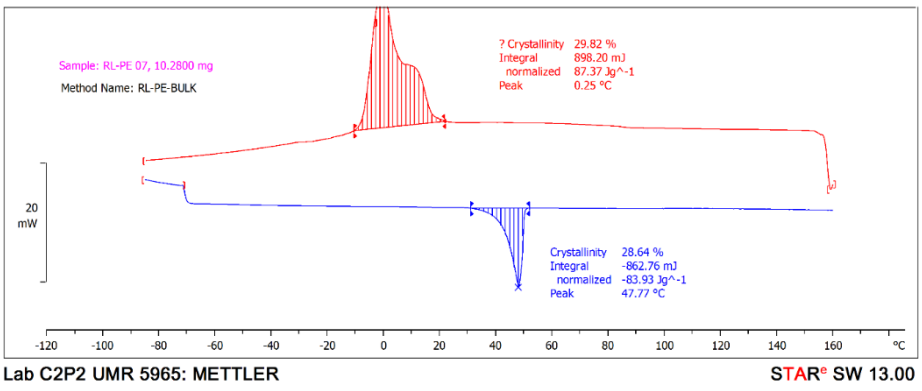

Figure 56 -DSC analyses of RL-PE 07 sample (1 g PEG-X, 4h, 50 mg AIBA, 250 rpm, T=70 ℃, and Pethylene≈100 bar).

The molar masses and molar mass dispersities were also determined for these experiments by performing SEC at high temperature (150°C) in TCB. The corresponding chromatograms (refractive index versus retention volume) are shown in Figure 57.

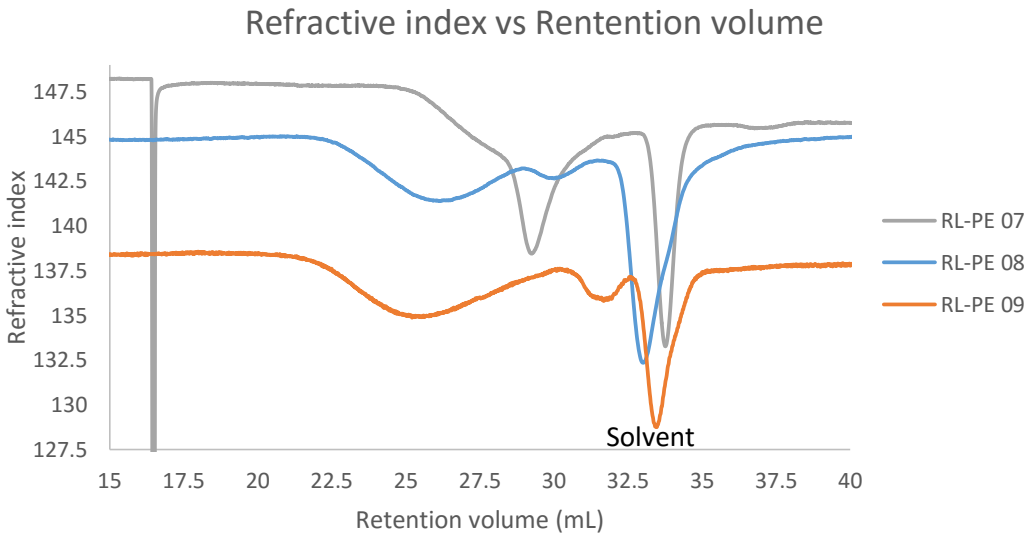

Figure 57 - Chromatogram of the samples RL-PE 07; RL-PE 08; RL-PE 09(4h, 50 mg AIBA, T=70°C, and $P_{ethylene}$≈100 bar).

As seen in Figure 57, the molar mass increases slightly as the quantity of PEG-X decreases in the system (from RL-PE 07 to RL-PE 09). Also, the broadness of the molar mass distribution seemed to be larger (Table 7).

Table 7 - M_n and Đ (RL-PE 07;08; RL-PE 09) ([1 g, 0.5 and 0.3 g of PEG-X], 4h, 50 mg AIBA, T=70°C, and $P_{ethylene}$≈100 bar).

Name of sample	PEG-X (g)	M_n (gmol^{-1})	Đ
RL-PE 07	1	≈2600	1.9
RL-PE 08	0.5	≈2800	4.4
RL-PE 09	0.3	≈2800	8.6

In summary, this group of experiments revealed the influence of the quantity of the macroRAFT agent (polyethylene glycol end-functionalized with a xanthate). It seems that this parameter has a strong effect on the yield obtained in the different polymerizations; the yield decreasing when the quantity of PEG-X increases. The mass of PEG-X also appeared to affect the melting temperature and crystallinity of the polymer. The molar masses remained in the same range for the three experiments (2600 to 2800 g mol^{-1}), although the dispersity was largely broadened as the quantity of PEG-X was reduced.

3.3 – Kinetic study on the polymerization of ethylene in the presence of PEG-X

The last section of this chapter concerns the kinetic study of the polymerizations performed in the presence of the macroRAFT agent. In order to follow the course of these polymerizations with time, several polymerizations were carried in the same reaction conditions (of pressure, temperature, stirring rate) and around 0.3 g of PEG-X was employed in each polymerization. Given that the polymerization apparatus did not allowed the withdrawal of samples at high pressure, the kinetic study was performed by carrying out the identical reactions at different polymerization durations (1, 2, 4 and 8 hours). This study was performed at two different pressures, 100 and 200 bar, and thus also allowed a further understanding of the system.

3.3.1 – Polymerizations of ethylene in the presence of PEG-X at 100 bar

The kinetic study was carried out at 100 bar of pressure of ethylene, at 70°C and at stirring rate of 250 rpm. In these polymerizations, whatever the reaction duration the recovered latexes were stable and had a translucent aspect as seen in Figure 58 (RL-PE 26).

Figure 58 - Polymerization sample of FREPE (RL-PE 26) (1h, 100 bar, 50 mg AIBA, 0.3 g PEG-X, 250 rpm, T=70°C).

The yield of these experiments was obtained by gravimetric analysis similarly to the RL-PE 09 sample (Table 8).

Table 8- Yields of FREPE at 100 bar in the presence of PEG-X (1h, 2h, 4h, 8h) (50 mg AIBA, 0.3 g PEG-X, 250 rpm, T=70°C).

Name of sample	Time (h)	Yield (g) / PC (%)
RL-PE 26	1	0.08/0.16
RL-PE 29	2	0.21/0.42
RL-PE 09	4	0.47/0.88
RL-PE 27	8	0.53/1.01

The yield increased along with the polymerization time as expected. However, for higher polymerization times, from 4 hours on, the yield on polyethylene seemed to attain a plateau (increasing from 0.4 g after 4 hours to 0.53 g after 8 hour reaction time). This evolution is present in the Figure 59. Very low yields were obtained.

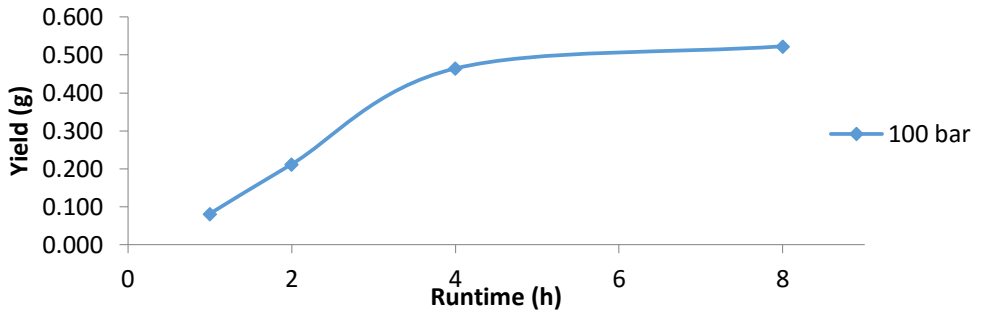

Figure 59 – Yield as function of time in FREPE with PEG-X. (1h, 2h, 4h, 8h) (100 bar, 50 mg AIBA, 0.3 g PEG-X, 250 rpm, T=70°C).

The particle sizes were determined by DLS analyses of the samples (RL-PE 26, RL-PE 27 and RL-PE 29) as for the RL-PE 09 sample (section 3.1.4).

The RL-PE 26 corresponds to the polymerization with a duration of 1h. As seen in Figure 60, two populations of particles are present. A smaller particle population with diameter around 19 nm and a larger one with a diameter at around 83 nm, the last one corresponds to of the higher intensity signal (65%).

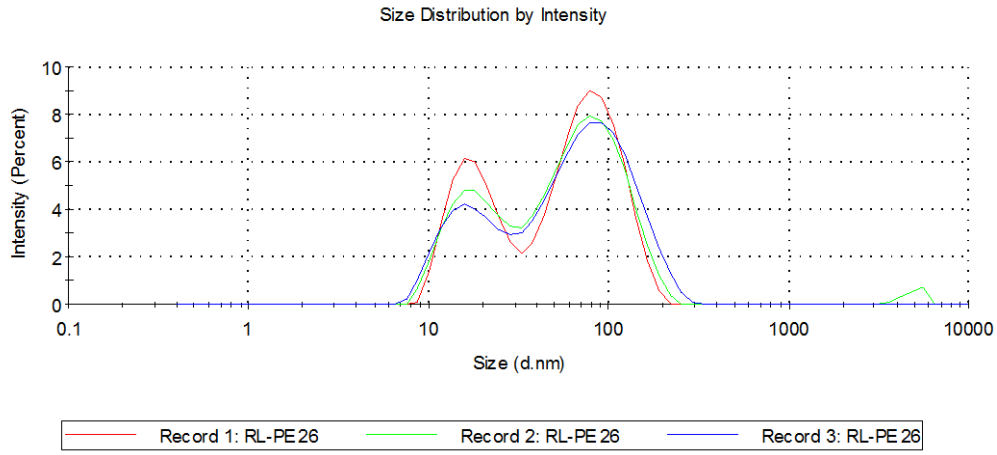

Figure 60 - Particle size distribution by Intensity (RL-PE 26) (1h, 100 bar, 50 mg AIBA, 0.3 g PEG-X, 250 rpm, T=70°C).

The RL-PE 29 had an average particle size of 26 nm and a PDI value of 0.30. Apparently, as seen in Figure 62 after two hours of polymerization (RL-PE 29 sample) the population with higher particle size was practically not detected by DLS. A similar phenomenon was previously reported by *E. Grau* during the kinetic study of the polymerization performed with surfactant, this was explained by shattering of the larger particles into smaller ones under heating and the presence of CTAB. [30] However, in his work on the same system, *G. Billuart* stated that probably the extinction of the larger particles population did not take place. Instead, it was shown that the former DLS apparatus was not efficient in detecting the two populations. Based on the theory associated with DLS it was assumed that the number of the smaller particles surpassed greatly the number of the particles from the larger size population (that might remained the same number or decreased), having a signal much more intense. Although the interpretation of these phenomena is not trivial, this might be a possible explanation for this system.

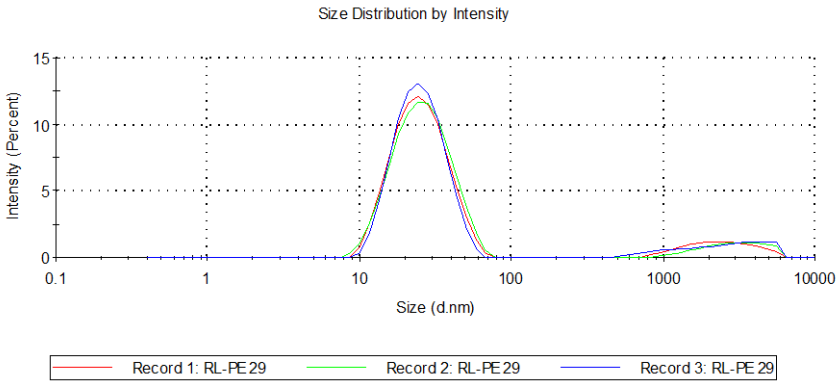

Figure 62 - Particle size distribution by Intensity (RL-PE 29) (2h, 100 bar, 50 mg AIBA, 0.3 g PEG-X, 250 rpm, T=70℃).

The 4 hour experiment, RL-PE 09, was already reported above with the Z_{av} around 20 nm and the corresponding PDI being 0.25. The polymerization with duration of 8 hours is represented by the RL-PE 27 sample. Basically, as seen in the following figure, almost the totality of the intensity signal corresponds to the small particle population, a very low intensity of the residual large particle size being identified as well. The average particle size obtained for this experiment is 17 nm for a PDI value of 0.20.

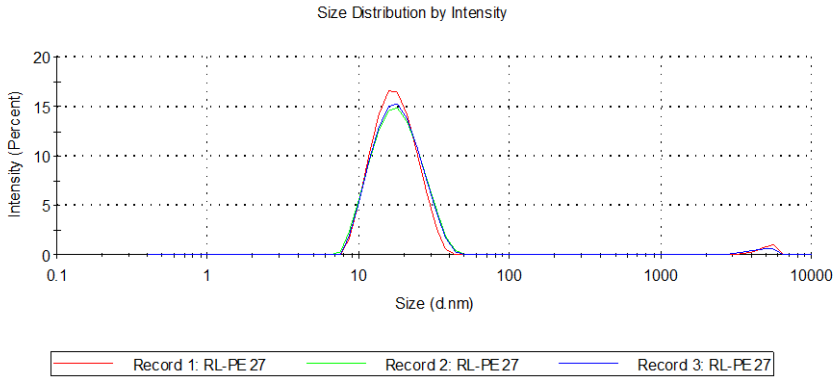

Figure 61 - Particle size distribution by Intensity (RL-PE 26) (2h, 100 bar, 50 mg AIBA, 0.3 g PEG-X, 250 rpm, T=70℃).

The graph showing the evolution of the average particle size along time for the experiments performed under 100 bar of pressure of ethylene and 0.3 g of PEG-X is presented in the Figure 63. The particle size tends to decrease as the polymerization proceeds and to reach a plateau after long polymerization time. In all of these experiments the PDI value are very high being probably justified, as previously said, by heterogeneity of the particle sizes and non-spherical morphology.

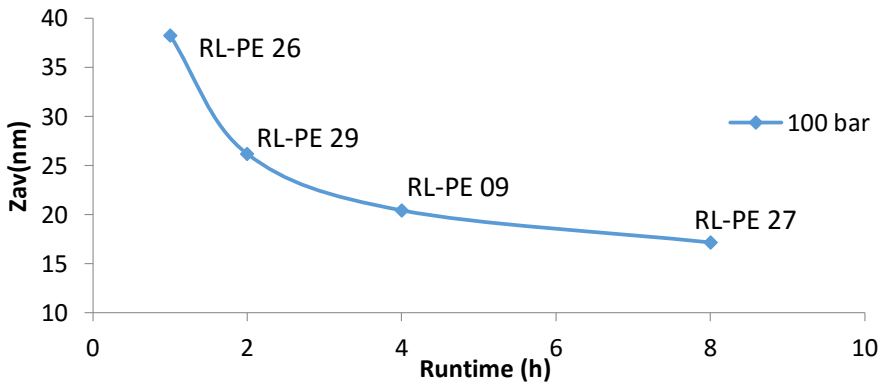

Figure 63 - Z_{av} as function polymerization time in FREP of ethylene using PEG-X (100 bar, 50 mg AIBA, 0.3 g PEG-X, 250 rpm, T=70℃).

Cryo-TEM analysis was performed for the sample RL-PE 27 (8 hour polymerization). Very small particles were consistently observed in the 20 nm range, which seem to have a disk-like morphology. As seen in the previous section this led to the inadequacy of the DLS analysis for this sample.

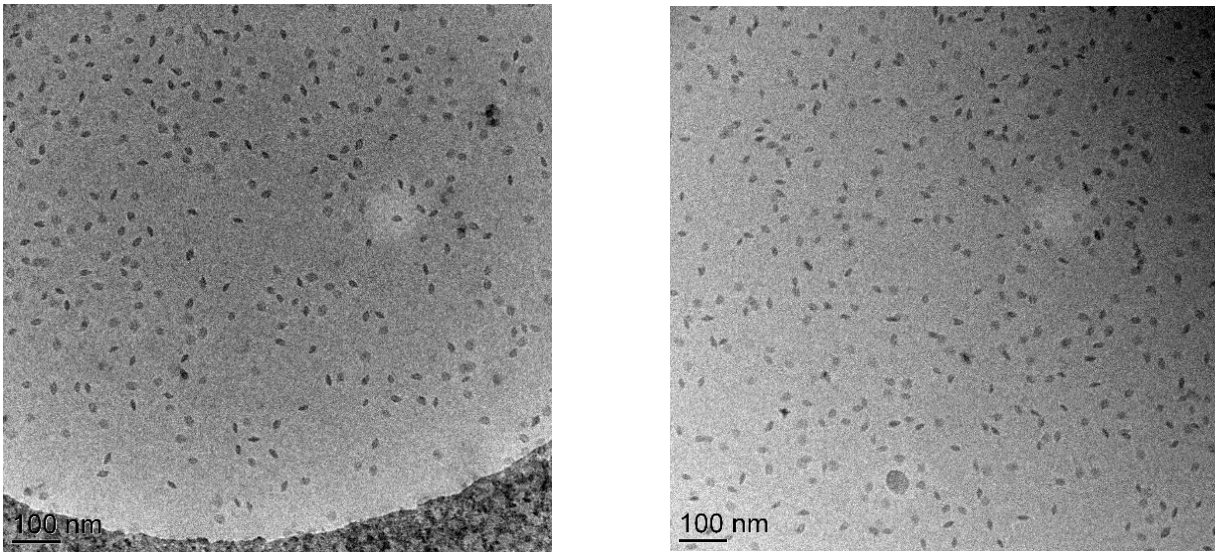

Figure 64 -TEM RL-PE 27 (100 nm, left) and Cryo-TEM (100 nm, right) (8 h, 100 bar, 50 mg AIBA, 0.3 g PEG-X, 250 rpm, T=70 ℃).

The molar masses of these polymerization samples were also determined by SEC analyses at high temperature (150°C) in TCB. The values of M_n and of dispersity obtained from these analyses are in Table 9.

Table 9 - Mn and Đ of FREP of ethylene at 100 bar and with PEG-X (50 mg AIBA, 0.3 g PEG-X, 250 rpm, T=70°C).

Name of sample	Time (h)	M_n (g mol^{-1})	*Dispersity (Đ)*
RL-PE 26	1	2500	4.0
RL-PE 29	2	2700	2.3
RL-PE 09	4	2800	8.6
RL-PE 27	8	2800	5.8

As seen in Table 9 and Figure 65 the molar mass slightly increased with time in these polymerizations. The molar mass distribution is very large for most of the experiments, and being noticeably higher at longer polymerization times.

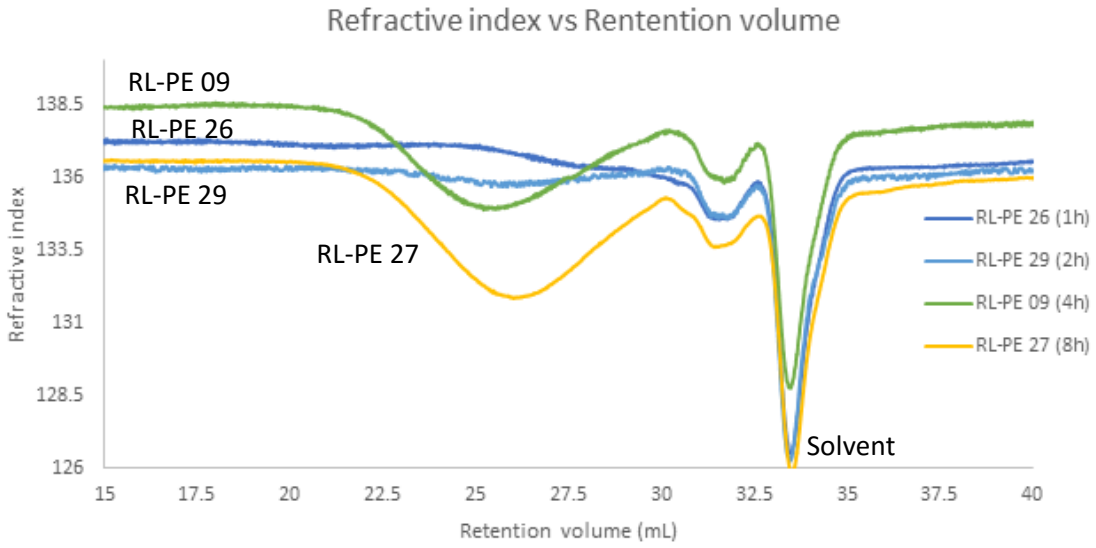

Figure 65 - Chromatogram of the samples RL-PE 26 (1h); RL-PE 29 (2h); RL-PE 09 (4h); RL-PE 27 (8h) (50 mg AIBA, 70 ℃, Pethylene≈100 bar).

The graph of the Figure 66 shows the evolution of the molar masses with yield for the experiments performed at different polymerization times. The M_{peak} increased with the polymerization time and yield, this is a possible indicator of some control of the block copolymer synthesis.

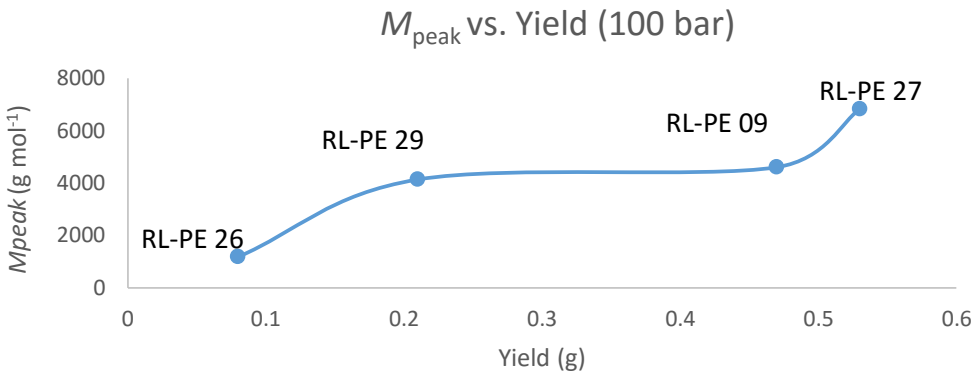

Figure 66 -M_{peak} vs. Yield in FREPE using PEG-X – samples RL-PE 26 (1h); RL-PE 29 (2h); RL-PE 09 (4h); RL-PE 27

In summary, this group of experiments depict the evolution of emulsion polymerization of ethylene mediated by PEG-X with time. In the polymerizations performed at 100 bar, the recovered latexes were stable and had a translucent aspect. From the gravimetric analyses it was observed that the yield increased with time and tends to reach a plateau, after 4 hours of duration. The size of the particles in these latexes were measured by DLS, and two particle populations were observed after 1 hour of reaction. After two hours, the large particles were practically not detected anymore. This phenomenon was mainly attributed to the outnumbering of the larger particles population by the smaller ones (around 20 nm). Particle sizes remained low (>20 nm) for the rest of the polymerization and relatively high dispersities were observed. The molar masses of these samples increased marginally during the polymerizations and the dispersity was high for most of the samples, being noticeably higher at longer times. The *molar masses* increased with the polymerization time and yield, being a possible indicator of some control of the block copolymer synthesis.

3.3.1 – Polymerizations of ethylene in the presence of PEG-X at 200 bar

The same kinetic study was then performed at 200 bar in the presence of the macroRAFT agent. Similarly to the polymerizations performed at 100 bar, this set of polymerizations was carried out with different reaction durations (1, 2, 4, and 8 hours) under the same conditions (70°C, 250 rpm and 50 mg of AIBA) and with the same quantity of PEG-X introduced in the initial solution, 0.3 g.

The recovered latexes were noticeably less stable than the ones recovered at 100 bar. The experiments performed for the shortest times (1 and 2 hours) yielded latexes with a translucent appearance similarly to the former ones (Figure 67). However, the polymerizations with a duration of 4 and 8 hours seem to exhibit larger particle sizes (milky aspect) and what appeared to be some coagulum on the walls of the sample flask was observed (Figure 67, right). These observations were confirmed by the values of particle size and particle size distribution later obtained DLS (see further on).

Figure 67 - Latex produced via FREPE with 0.3 g of PEG-X (RL-PE 28, 2h)(left); (RL-PE 32, 8h)(right) (200 bar, 50 mg AIBA, 250 rpm, T=70 ℃).

As from the samples recovered at 100 bar, the yield of these reactions was obtained through gravimetry analyses and the value of the yield and PC are given in Table 10.

Table 10 - Yields of FREP of ethylene at 200 bar and in the presence of PEG-X (1h, 2h, 4h and 8h) (50 mg AIBA, 0.3 g PEG-X, 250 rpm, T=70℃).

Name of sample	Time (h)	Yield (g) / PC (%)
RL-PE 31	1	0.24/0.47
RL-PE 28	2	0.61/1.17
RL-PE 30	4	1.08/2.12
RL-PE 32	8	2.71/3.70

It is possible to see in Table 10 and in Figure 68 that, in resemblance to the former set of polymerizations at 100 bar, the yield increased along the polymerization time as expected. In this case, the overall yield was higher than the latter for the same polymerization time. It is possible to see from the graph and the table above that the yield increases from the first hour to the standard polymerization time, 4 hours, at almost the same rate as the procedures at 100 bar, that is, doubling between experiments (from 1h to 2h and from 2h to 4h). However, instead of plateauing, the yield almost tripled between 4h and 8h but some coagulation occurred in the latter case.

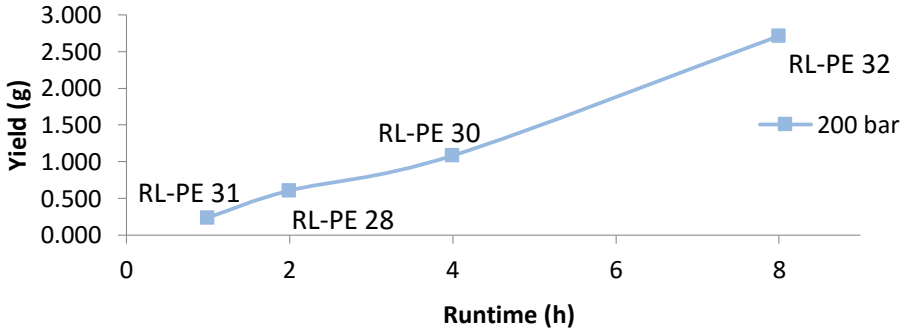

Figure 68 -Yield vs. polymerization time in FREPE using PEG-X (1h, 2h, 4h, 8h) (200 bar, 50 mg AIBA, 0.3 g PEG-X, 250 rpm, T=70 ℃).

TEM observation was performed on sample RL-PE 28 (2 hour polymerization). It was very difficult to obtain a clear image of the particles because of the low contrast (cryoTEM has to be performed). However it is possible to observe in the following figures the presence of a very large number of small non-spherical particles and also the presence of larger particles, also detected by DLS, as shown below.

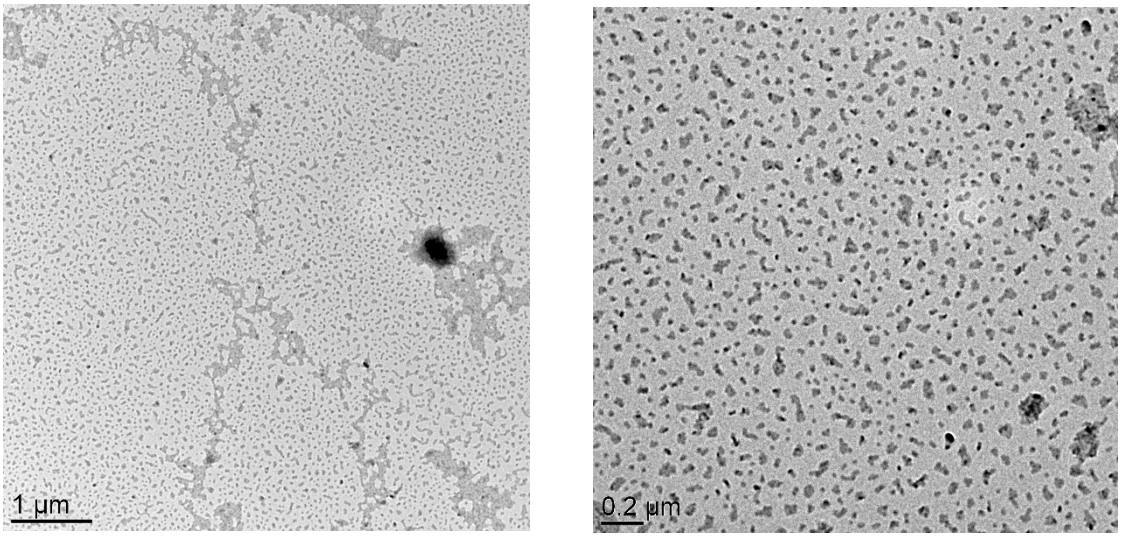

Figure 69 -TEM RL-PE 28 (1 µm, left) and (200 nm, right) (2h, 200 bar, 50 mg AIBA, 0.3 g PEG-X, 250 rpm, T=70 °C).

The four latexes were analysed by DLS. As seen in the following figures, the population with lower particle sizes represented majority of the intensity signal for the samples analysed (RL-PE 31, RL-PE 28, RL-PE 30 and RL-PE 32). A second population of large particle size is systematically observed. The next figure shows the size distribution by intensity for the four experiments.

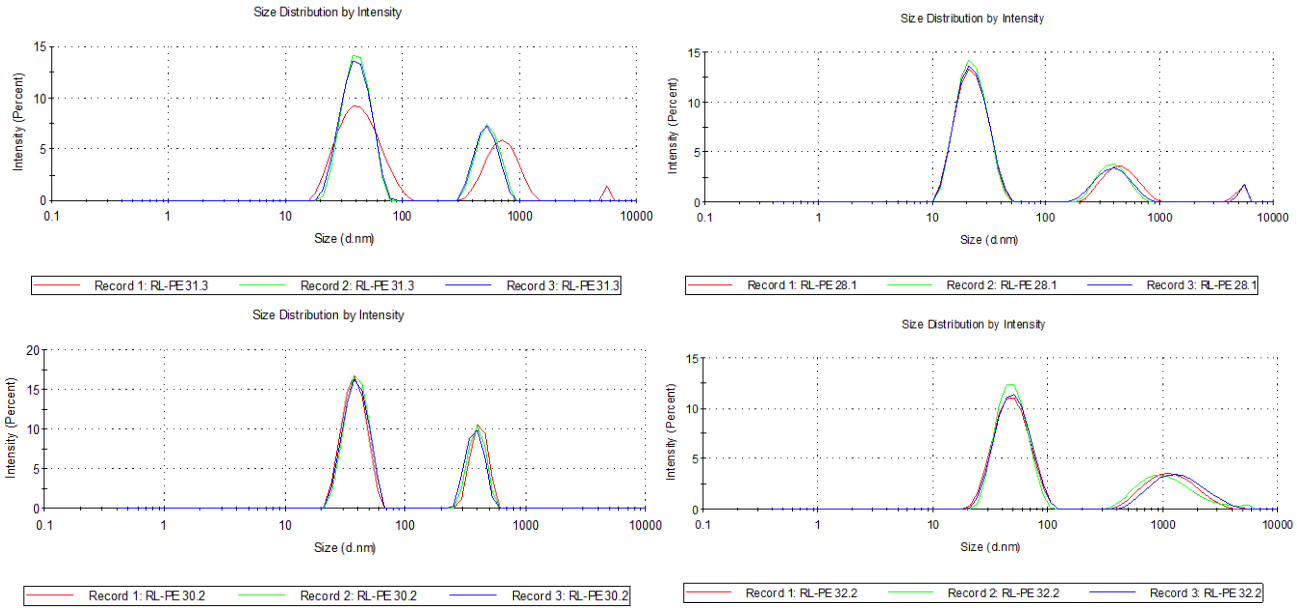

Figure 70 - Particle size distribution by Intensity (RL-PE 31, 1h), (RL-PE 28, 2h), (RL-PE 30, 4h), (RL-PE 32, 8h) (200 bar, 50 mg AIBA, 0.3 g PEG-X, 250 rpm, T=70 °C).

The sample from first hour of polymerization has shown a particle size around 40 nm for the small particle size population and around 500 nm for the large particle. The RL-PE 28 showed two populations, a small particle size population around 20 nm and a larger particle size one at 460 nm.

In the RL-PE 30 sample the two populations continued to coexist, the size of the small particle size population seemed to increase in relation to the former to the 40 nm range and the larger size population continued to decrease to the 410 nm range. At last, The RL-PE 32 sample had higher values than the previous polymerization time, with the small particles having its size around 50 nm and the larger one at 1300 nm with a higher dispersity value.

The values for both types of populations were plotted as a function of polymerization time (Figure 71). The size of the circles is proportional to the intensity percentages of each population obtained by DLS. Unlike the results of the experiments at 100 bar that tend to lower particle sizes, at this pressure the particle size of the small particle population appeared to decrease from the first to the second hour of polymerization, but increased from the 2h experiment to the 8h. Similarly to the first case, the particle size of the large particle population decreased from the 1h experiment to the 4h one, but increased from the last to the 8h run, probably due to the lack of stability of the latex at higher polymerization times.

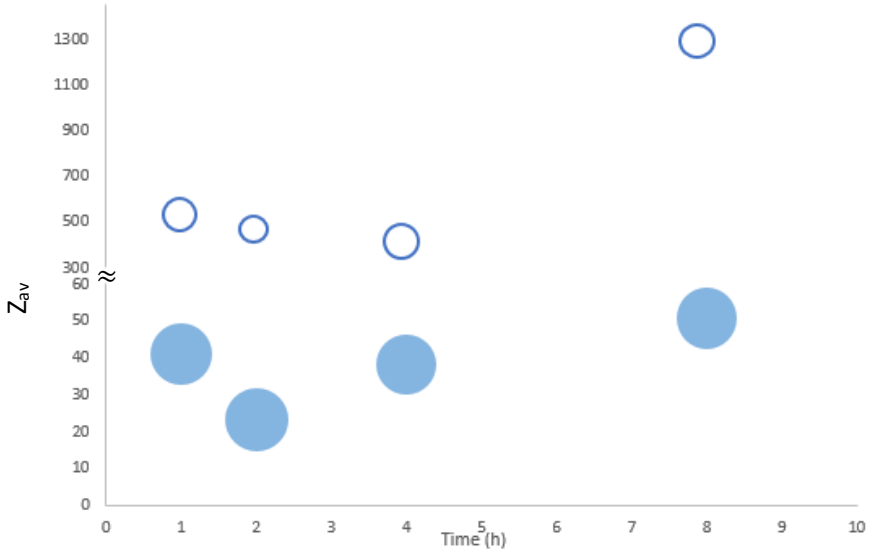

Figure 71 – Particle size as a function of time for small and large particle size populations (circle proportional to the intensity signal) in FREPE (RL-PE 31, 1h), (RL-PE 28, 2h), (RL-PE 30, 4h), (RL-PE 32, 8h) (200 bar, 50 mg AIBA, 0.3 g PEG-X, 250 rpm, T=70 ºC).

The molar masses of the experiments performed at 200 bar were determined by performing SEC analysis to the samples at high temperature (Figure 72). As seen from the Table 11, the values of M_n and of the molar mass distribution obtained for these samples were higher than the equivalent experiments at 100 bar.

Table 11 - M_n and dispersity of FREPE (1h, 2h, 4h and 8h) (200 bar, 50 mg AIBA, 0.3 g PEG-X, 250 rpm, T=70 ºC).

Name of sample	Time (h)	M_n(g mol^{-1})	*Dispersity (Đ)*
RL-PE 31	1	3100	8.7
RL-PE 28	2	4400	8.7
RL-PE 30	4	5100	13.0
Rl-PE 32	8	7200	17.6

From the table above and as seen in the following figure, the values of molar mass seem to increase with the polymerization time. The dispersity increased along the polymerization time being very high for the 4 hour and the 8 hour runs.

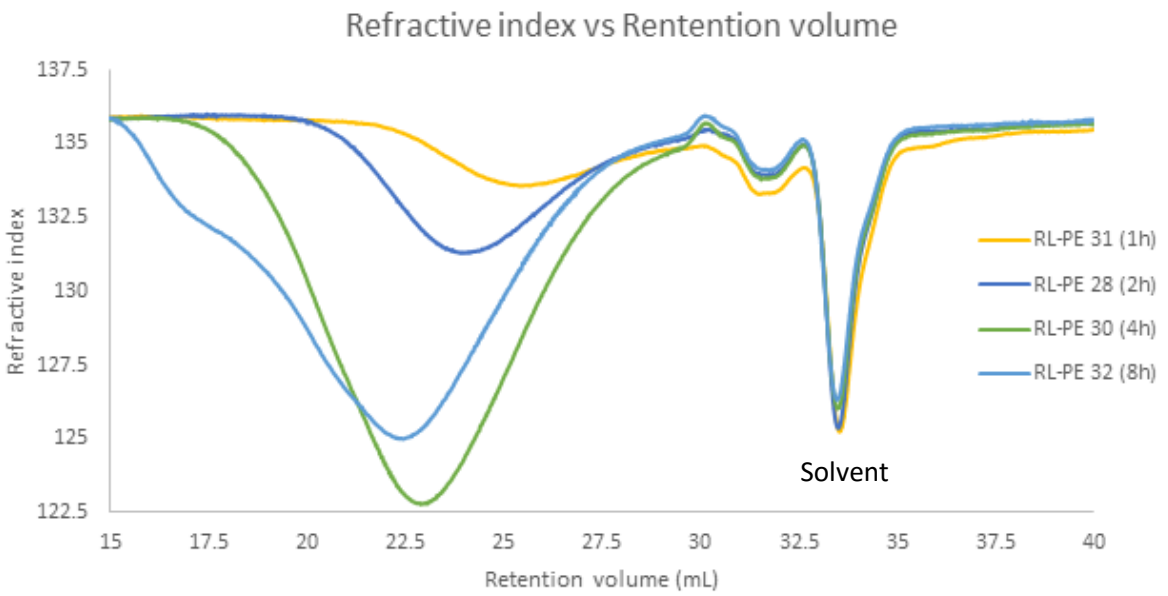

Figure 72- Chromatogram of the samples (RL-PE 28, 1h); (RL-PE 30, 2h); (RL-PE 31, 4h); (RL-PE 32, 8h) (200 bar, 50 mg AIBA, 0.3 g PEG-X, 250 rpm, T=70 ℃).

The graph of the Figure 73 shows the evolution of the molar masses with yield for the experiments performed at 200 bar for the different polymerization times. The M_{peak} increased with the polymerization yield linearly, this is a possible indicator of some control of the block-copolymer synthesis.

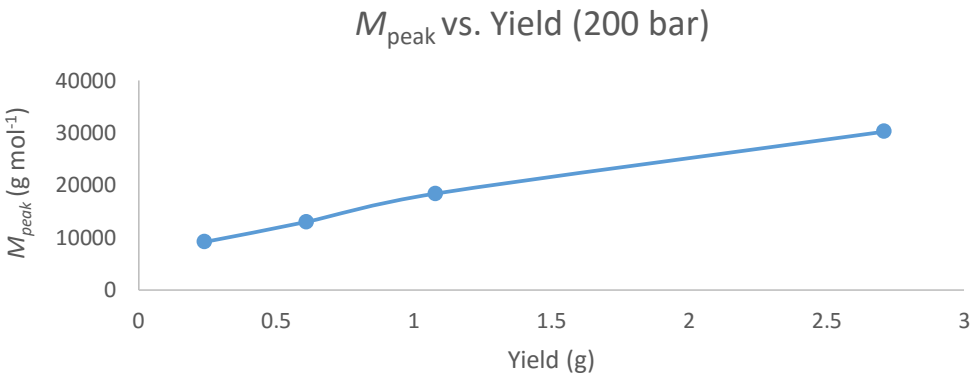

Figure 73 –M_{peak} vs. Yield in FREP of ethylene using PEG-X (200 bar, 50 mg AIBA, 0.3 g PEG-X, 250 rpm, T=70 ℃).

In summary, the procedures performed at 200 bar showed the evolution of the polymerization yield and of the polymer features along with time at this pressure. The recovered latexes were stable at short polymerization times (1 and 2 hours) and had a translucent aspect. After 4 h of polymerization, the latexes seemed to be less stable, having a milky aspect and some coagulum was observed in the samples. Contrary to the polymerizations at 100 bar, the yield increased along with the polymerization time up to 8h.

The TEM analyses showed a very large population of small particles that appeared to have a non-spherical morphology. The size of the particles was measured by DLS, although being inadequate, two particle populations were observed for all the four experiments, although the small particle size population (between 20 and 50 nm) represented the majority of the particles, having a larger intensity signal.

The molar mass of these samples, unlike the polymerizations at 100 bar that showed a marginal increase of the dispersity, increased through all the experimental procedures (from ≈3000 to 7000 $gmol^{-1}$). The dispersity values of the samples were high (≈9), increasing to higher values at longer polymerization times.

Conclusions and perspectives

The primary aim of the present work was the implementation of the RAFT polymerization of ethylene in a surfactant-free emulsion process to obtain, from water-soluble functional polymers, aqueous dispersions of PE-based nanoparticles by the polymerization-induced self-assembly of amphiphilic block copolymers (PISA process). It relied on the knowledge developed at the C2P2 laboratory, on the possibility of performing free radical emulsion polymerization of ethylene under mild conditions ($T<100^{\circ}C$ and $P<250$ bar) and the controlled radical polymerization (CRP) of ethylene via RAFT. In addition the concepts developed at C2P2 for the synthesis of block copolymers produced by emulsion polymerization according to the PISA process were also considered, and relied on the chain extension of a preformed hydrophilic polymer produced by RAFT by a hydrophobic monomer in water. This was presently tentatively applied to the case of ethylene.

The first part of this work consisted in the synthesis of the hydrophilic macroRAFT agent, produced before the polymerization of ethylene. For that purpose, a commercially available polyethylene glycol (PEG-OH) prepared via anionic polymerization was used. The hydroxyl chain end can be further end-functionalized with a xanthate, producing xanthate-functionalized PEGs (PEG-X). These xanthate based molecules are well-suited for the RAFT polymerization of ethylene. [57] The characterization of the PEG-X was performed by SEC, and by ^{1}H NMR .The molar masses obtained by both techniques were in good agreement, close to 2300 g mol^{-1}.

The second part of this work focused on the free radical emulsion polymerization of ethylene. At first, there was the need to establish benchmarks experiments. Thus, a set of four different reactions was performed. In the first place, the polymerization was carried out uniquely in the presence of a cationic initiator (AIBA). In the second one, the experiment was performed in the presence of both AIBA and a cationic surfactant, CTAB. Two more experiments were performed with either the commercial PEG-OH or with the macroRAFT agent PEG-X. PEG-OH was used in order to evaluate the activity of the xanthate chain-end. The main results from these polymerizations were compared afterwards.

In terms of visual aspect it was possible to set two groups of latexes: ethylene polymerization carried out only with AIBA yielded a stable and milky white latex. The same observation could be made for the latex produced in the presence of PEG-OH. This suggested the presence of relatively large size particles (around 100 nm). On the other hand, the second group is formed by the stable translucent latex synthesized either in the presence of surfactant (CTAB) or in the process with PEG-X. The translucent aspect suggested the presence of small size particles (around 25 nm) in the latexes. The size range was confirmed by other analyses.

Indeed, cryo-TEM observations allowed estimating both the size and the morphology of the particles. The polymerization performed only with initiator showed relatively large spherical particles (around 75 nm), which also occurred with the polymerization in the presence of PEG-OH. The similarity between the two experiments would indicate that PEG-OH had no influence in the polymerization of ethylene. For the polymerizations carried out with surfactant and the ones performed with PEG-X it was observed a vast majority of small size particles ($\approx$25 nm). As expected, the morphology of the particles from the latexes obtained in the presence of CTAB was disk-like shaped. In the case of the polymerization with PEG-X, other morphologies were observed: a large number of particles appeared to be disk-like shaped but cylindrical shapes were also observed. These unusual kinds of structures can be of obtained by the PISA process. The crystallinity may favour the formation of such non-spherical

particles. The aspect of the latexes and the TEM pictures revealed a striking difference between the polymerization performed in the presence of PEG-OH and PEG-X.

DLS analysis supported TEM observations. Polymerizations performed with only initiator or in the presence of PEG-OH yielded relatively large spherical particles (around 75 nm) and had a low *polydispersity index,* PDI (0.02 for both). The polymerization with PEG-X yielded a single particle size population (≈25 nm) with a high PDI, which was interpreted as a deviation from the spherical morphology (DLS was inadequate in such case).

The yield was determined for the four polymerizations after the same reaction time (4h). The polymerization only with initiator and the one in presence of PEG-OH had the same yield, supporting the conclusions drawn above on the role of PEG-OH. The lowest yield was obtained for the polymerization conducted in presence of the macroRAFT agent and the influence of the quantity of the macroRAFT agent in the polymerization of ethylene was further studied.

DSC analyses of the PE obtained with AIBA and with AIBA and CTAB showed crystallinity and melting temperature values similar to those reported in previous studies for similar systems. In the case of PEG-OH, two peaks were observed, which was correlated with the presence of two polymer species in the sample, probably PEG-OH and PE. On the other hand the DSC of the product obtained from the polymerization with PEG-X revealed a broad signal with no evidence of isolated PEG-X, which could be interpreted as the formation of a block copolymer structure, together with PE homopolymer.

The main conclusions brought by these analyses are the following: The presence of PEG-OH did not influence the process of polymerization. On the other hand, the polymerizations performed with PEG-OH and PEG-X showed different behaviour, indicating that the xanthate-functionalized PEG chains participated to the free radical process.

The first polymerizations with PEG-X yielded a very low amount of PE. Thus, the influence of the quantity of macroRAFT agent on the resulting latexes characteristics was studied. This study showed that this parameter has a great effect on the yield obtained - As the quantity of PEG-X increased the yield decreased. On the other hand, the amount of PEG-X had no or little effect on the particle size, with the Z_{av} remaining around the 25 nm for the three samples, or on the molar masses, which remained in the same range for the three experiments (2600 to 2800 g mol^{-1}). The dispersity however increased as the quantity of PEG-X was reduced.

At last, a kinetic study was made with polymerizations in the presence of the PEG-X. The withdrawal of samples being not possible, several experiments were carried out in the same conditions but with different durations (1, 2, 4, and 8h). This study was performed at two different pressures, 100 and 200 bar, allowing to study the influence of the pressure in these systems. At 100 bar, the recovered latexes were stable and had a translucent aspect. However, after 1 hour of polymerization two particle populations were observed. After two hours they were no longer observed. This phenomenon was mainly attributed to the outnumbering of the larger particles population by the smaller ones (Z_{av}≈20 nm). The molar masses increased with yield, although not completely linear, a possible indication of some control of the block copolymer synthesis.

At 200 bar the recovered latexes were stable at short polymerization times (1 and 2 hours) and had a translucent aspect. After 4 h, the latexes appeared to be less stable, having a milky aspect and some coagula were observable. In resemblance to the polymerizations at 100 bar, the yield increased along with the polymerization time, but were higher than in the first system. The molar mass increased linearly with the polymerization yield, which again could be an indicator of some livingness of the polymerization.

With all the acquired data it is possible to conclude that indeed, the aim of this project was achieved. The emulsion polymerization of ethylene mediated by a xanthate macroRAFT can lead to the formation of PE-based nanoparticles by a PISA process. The block copolymers formed in situ would provide the stabilization of particles.

Future studies could continue on the characterization of the particles obtained in the polymerizations with PEG-X, focusing on the morphology of the non-spherical particles and their formation mechanism. Additionally, the use of other macroRAFT agents could be interesting to study, and compared to the polymerizations performed in the presence of PEG-X, and open an opportunity to increase the number of applications for this process.

References

[1] E. Segel, "Polyethylene Global Overview," 2012. [Online]. Available: http://www.ptq.pemex.com/productosyservicios/eventosdescargas/Documents/Foro%2.pdf. [Accessed 20 June 2015].

[2] A. J. Peacock, em *Handbook of Polyethylene. Structures, Properties and Applications*, New York, Marcel Dekker, Inc., 2000, 1-42.

[3] C. F. Cordeiro, F. P. Petrocelli, em *Encyclopedia of Polymer Science and Technology*, John Wiley & Sons, Inc., 2002, 412-441, vol. 2.

[4] C. F. Cordeiro, F. P. Petrocelli, *Encyclopedia of Polymer Science and Technology*, John Wiley & Sons, Inc., 2002, pp. 382-482, vol. 2.

[5] Y. Tokiwa, B. P. Calabia, C. U. Ugwu e S. Aiba, " Biodegradability of Plastics" *International Journal of Molecular Science,* 3722-3742, vol. 10, 2009.

[6] G. ODIAN, em *Principles of Polymerization*, New Jersey, JOHN WILEY & SONS, INC., 2004, 301.

[7] J. K. Th. Meyer, *Handbook of Polymer Reaction Engineering*, Weinheim, Germany, WILEY-VCH Verlag GmbH & Co, 2005, 1-15.

[8] H. R. Kricheldorf, O. Nuyken e G. Swift, *Handbook of Polymer Synthesis*, New York, Marcel Dekker, 2005, 12-39.

[9] B. Poling, J. M. Prausnitz e J. P. O'Connell, *Properties of Gases and Liquids, Fifth Edition*, New York, McGraw-Hill Education, 2001.

[10] J. A. Peacock, *Handbook of Polyethylene Structures, Properties and Applications*, New York, Marcel Dekker, Inc., 2000, 43-66.

[11] E. Bamberger e . F. Tschirner, ""Ueber die Einwirkung von Diazomethan auf β-Arylhydroxylamine"," *Berichte der Deutschen chemischen Gesellschaft zu Berlin,* 955-959, 1900.

[12] A. J. Peacock, *Handbook of Polyethylene Structures, Properties and Applications*, New York, Marcel Dekker, 2000, 27-40.

[13] E. W. Fawcett, R. O. Gibson e M. W. Perrin, "POLYMERIZATION OF OLEFINS". US Patente 2,153,553, 1939.

[14] J. T. M. Keurentjes, *Handbook of Polymer*, Weinheim, WILEY-VCH Verlag GmbH & Co. KGaA, 2005, 1-15.

[15] A. H. Muller, K. Matyjaszewski, *Controlled and Living*, Weinheim, WILEY-VCH Verlag GmbH & Co. KGaA, 103-156, 2009

[16] K. Matyjaszewski, T. P. Davis, *Handbook of Radical Polymerization*, Hoboken, John Wiley & Sons, Inc., vii-x., 2002

[17] K. Matyjaszewski e T. P. Davis, em *Handbook of Radical Polymerization*, Hoboken, John Wiley & Sons, Inc, 2002, pp. 1-76.

[18] K. S. Whiteley, T. G. Heggs, H. Koch, R. L. Mawer e W. Immel, em *Ullmann's Encyclopedia of Industrial Chemistry, Seventh Edition*, Wiley-VCH Verlag GmbH & Co., 2002.

[19] E. Segel, " "Polyethylene Global Overview,"," 2012. [Online]. Available: http://www.ptq.pemex.com/productosyservicios/eventosdescargas/Documents/Foro%2.pdf.. [Acessed 20 June 2015].

[20] C. F. Cordeiro and F. P. Petrocelli, *Encyclopedia of Polymer Science and Technology, vol. 2*, John Wiley & Sons, Inc., 2002, 382-482.

[21] C. BARNER-KOWOLLIK, P. VANA e T. P. DAVIS, "The Kinetics of Free radical" *Handbook of Radical Polymerization*, Sydney, John Wiley & Sons, Inc., 2002, 187-262.

[22] G. A. Mortimer, "Fundamentals of the Free radical Polymerization", *Advances in Polymer Science, Vol. 7*, New york, Springer, 1970, 386-448.

[23] H. Knuuttila, A. Lehtinen, A. Nummila-Pakarinen, "Controlled Material Properties", *Advanced Polyethylene Technologies*, Porvoo, Finland, Springer-Verlag Berlin Heidelberg, 2004, 16-22.

[24] J. K. T. Meyer, em *Handbook of Polymer Reaction Engineering*, Weinheim, WILEY-VCH Verlag GmbH & Co. KGaA, 2005, 17-18.

[25] A. Leblanc, E. Grau, J.-P. Broyer, C. Boisson, R. Spitz e V. Monteil, *Macromolecules,* 44, 3293–3301, 2011.

[26] T. Suwa, H. Nakajima, M. Takehisa e S. Machi, "Preparation of emulsifier-free polyethylene latecies by radiation polymerization," *Journal of Polymer Science: Polymer Letters Edition,* 13, 369–375, 1975.

[27] E. Grau, J. Broyer, C. Boisson, R. Spitz e V. Monteil, "Free Ethylene Radical Polymerization under Mild conditions: the impact of the solvent," *Macromolecules, 42,* 7279–7281, 2009.

[28] E. Grau, J.P. Broyer, C. Boisson, R. Spitz e V. Monteil, "Unusual activation by solvent of the ethylene free radical polymerization," *Polymer chemistry,* 2, 2328–2333, 2011.

[29] C. Dommanget et. al., "Enhanced Spin Capturing Polymerization of Ethylene", *Macromolecules, 46,* 29-36, 2013.

[30] E. Grau, P.-Y. Dugas, J.-P. Broyer, C. Boisson, R. Spitz e V. Monteil, *Angew Chem. international ed,* 122, 6962–6964, 2010.

[31] G. Billuart, E. Bourgeat-Lami, M. Lansalot e V. Monteil, *Macromolecules, 47,* 6591-6600, 2014.

[32] C. Barner-Kowollik, *Handbook of RAFT polymerization*, Weinheim, WILEY-VCH Verlag GmbH & Co. KGaA, 2008, 285-295.

[33] K. T. Meyer, *Handbook of Polymer Reaction Engineering*, Weinheim, WILEY-VCH Verlag GmbH & Co. KGaA, 2005, 249-312.

[34] C. D. Anderson, E. S. Daniels, em *Emulsion Polymerisation and Applications of Latex*, Shropshire, Rapra Technology Limited, 2003, 3-10.

[35] W. Harkins, "Theory of the mechanism of emulsion polymerization," *Journal of the American Chemical Society,* 1947, 69, 1428–1444.

[36] M. G. I. L. G. Khaddazh, "*An Advanced Approach on the Study of Emulsion Polymerization: Effect of the Initial Dispersion State of the System on the Reaction Mechanism, Polymerization Rate, and Size Distribution of Polymer-Monomer Particles"*, InTech, 2012, 164-200.

[37] G. T. Russell, R. G. Gilbert e D. Napper, "Chain-length-dependent termination rate processes in free radical polymerizations. 1. Theory," *Macromolecules,* vol. 25, 2459–2469, 1992.

[38] H. Heinrich, G. Siebert, "Process for the production of polymerization products". Patent US2334195 A, 1943.

[39] H. Heinrich, C. W. Rautenstrauch, G. Siebert, "Production of polymerization products from ethylene". Patent US2342400 A, 1944.

[40] H. K. Stryker, A. F. Helin, G. J. Mantell, "Emulsion polymerization of ethylene. II. Effect of recipe on particle size and distribution," *J. Appl. Polym. Sci.,* 10, 1214, 1966.

[41] H. K. Stryker, A. F. Helin, G. J. Mantell, "Emulsion polymerization of ethylene III - factors afecting the stability of polyethylene latexes," *J. of Applied Polymer Science,* vol. 10, 81-96, 1966.

[42] G. J. Mantell, H. . K. Stryker, A. F. Helin, D. R. Jamieson, C. H. Wright, "Emulsion polymerization of ethylene. IV. Effect of recipe and polymerization conditions on polymer properties," *Journal of Applied Polymer Science, vol.* 10 (12), 1845–1862, 1966.

[43] S. Senrui, T. Suwa, K. Konishi, M. Takehisa, *J. Polym. Sci. Polym. Chem.,* vol. 12, 83–92, 1974.

[44] T. Suwa, H. Nakajima, M. Takehisa, S. Machi, *Polym Lett Ed,* 1975.

[45] S. Machi, S. Kise, M. Hagiwara, T. Kagiya, *J. Polym. Sci.,* vol. 4, 585–588, 1966.

[46] A. L. German, P. A. Weerts, R. G. Gilbert, "Kinetic aspects of the emulsion polymerization of butadiene," *Macromolecules,* 24, 1622–1682, 1991.

[47] J. Wu, J. P. Tomba, J. K. Oh, M. A. Winnik, R. Farwaha, J. Rademacher, "Synthesis of Dye-Labeled Poly(vinyl acetate- co-ethylene) (EVA) Latex and Polymer Diffusion in their Latex Films," *Journal of polymer science, Part A, Pol. chem.,* 43, 5581–5596.

[48] J. K. Th. Meyer, "Living Polymerization in Emulsion," *Handbook of Polymer Reaction Engineering*, Weinheim, WILEY-VCH Verlag GmbH & Co. KGaA, 2005, 275-285.

[49] A. Muller, K. Matyjaszewski, *Controlled and Living Polymerizations*, Weinheim, WILEY-VCH Verlag GmbH & Co., 2009, xv-xvii.

[50] J. C. et. al., "Living Free radical Polymerization by Reversible Addition-Fragmentation Chain Transfer: The RAFT Process," *Macromolecules, 31,* 5559-5562, 1998.

[51] C. Barner-Kowollik, *Handbook of RAFT polymerization*, Weinheim, WILEY-VCH Verlag GmbH & Co. KGaA, 2008, 235-284.

[52] A. H. Muller, K. Matyjaszewski, *Controlled and Living Polymerization*, Weinheim, WILEY-VCH Verlag GmbH & Co., 2009, 126-155.

[53] J. CHIEFARI, E. RIZZARDO, *Handbook of Radical Polymerization*, Hoboken, John Wiley and Sons, Inc., 2002, 629-690.

[54] M. Hill, R. N. Carmean, B. S. Sumerlin, *Macromolecules,* 48, 5459−5469, 2015.

[55] D. J. Keddie, G. Moad, E. Rizzardo, S. H. Thang, "RAFT Agent Design and Synthesis" Macromolecules, 2012, 45 (13), 5321–5342

[56] M. Benaglia, J. Chiefari, Y. K. Chong, G. Moad, E. Rizzardo, S. H. Thang, "Universible (switchable) RAFT agents," *J. Am. Chem. Soc. ,* 131, 6914–6915, 2009.

[57] C. Dommmanget, F. D'Agosto, V. Monteil, "Polymerization of Ethylene through Revirsible Addition-Fragmentation Chain Transfer (RAFT)," *Angewandte Chemie int. ed., 53,* Wiley-VHC verlag GmbH & Co., 2014.

[58] B. Charleux, G. Delaittre, J. Rieger e F. D'Agosto, "Polymerization-Induced Self-Assembly: From Soluble Macromolecules to block copolymer Nano-Objects in one Step," *Macromolecules,* 45 (17), 6753-6765, 2012.

[59] Szwarc, M., *Nature (London),* 178, 1168, 1956.

[60] M. Lansalot, J. Rieger, F. D'Agosto, ""Polymerization-Induced Self-Assembly: the Contribution of Controlled Radical Polymerization to the Formation of Self-Stabilized Polymer Particles of Various Morphologies" em *Macromolecular self-assembly*, Wiley, 2016- in press.

[61] M. Lansalot, J. Rieger, F. D'Agosto "Polymerization-Induced Self-Assembly: The contribution of Controlled Radical polymerization to the formation of Self-Stabilized Polymer Particles of various Morphologies," 2016- in press.

[62] S. Binauld, L. Delafresnaye, B. Charleux, F. D'Agosto, M. Lansalot, *Macromolecules, 47 (10),* 3461-3472, 2014.

[63] Sigma-Aldrich, "sigmaaldrich.com," [Online]. Available: http://www.sigmaaldrich.com/content/dam/sigma aldrich/docs/Aldrich/General_Information/thermal_initiators.pdf. [Acedido em 2015].

[64] G. Billuart, PhD Thesis -Free radical emulsion polymerization of ethylene, 2015.

[65] M. Szwarc, M. Levy, R. Milkovich, *J. Am. Chem. Soc.,* 78, 2656, 1956.

[66] T. P. Davis, *Handbook of Radical Polymerization*, Hoboken, John Wiley & Sons, Inc, 2002, pp. 775-785.

[67] E. Grau, P.-Y. Dugas, J.-P. Broyer, C. Boisson, R. Spitz, V. Monteil, *Angew Chem. international ed.*, 49 (38), 6810–6812, 2010.

[68] S. P. Armes, N. J. Warren, “Polymerization-Induced Self-Assembly of Block Copolymer Nanoobjects via RAFT Aqueous Dispersion Polymerization,” *Journal of the American Chemical Society,* 136 (29), 10174-10185, 2014.

[69] A. L. German, P. A. Weerts e R. G. Gilbert, “Kinetic aspects of the emulsion polymerization of butadiene,” *Macromolecules,* 24, 1622–1682.

SIGMA-ALDRICH®

sigma-aldrich.com

3050 Spruce Street,Saint Louis,MO 63103,USA
Website: www.sigmaaldrich.com

Email
USA:

techserv@sial.com
Outside USA: eurtechserv@sial.com

Product Specification

Product Name:
4,4'-Azobis(4-cyanovaleric acid) - ≥75%

Product Number:	**118168**
CAS Number:	2638-94-0
MDL:	MFCD00002799
Formula:	C12H16N4O4
Formula Weight:	280.28 g/mol
Storage Temperature:	2 - 8 °C

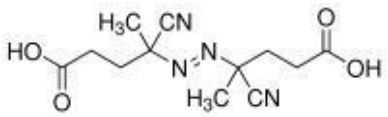

TEST	Specification
Appearance (Color)	White
Appearance (Form) Powder or Chunks	Conforms to Requirements
Infrared spectrum	Conforms to Structure
Purity (Titration by NAOH)	≥ 75.0 %
Water (by Karl Fischer)	≤ 25.0 %

Specification Date : 06/21/2010

3050 Spruce Street, Saint Louis, MO 63103, USA
Website: www.sigmaaldrich.com

Email
USA:

techserv@sial.com
Outside USA: eurtechserv@sial.com

Product Specification

Product Name:
Poly(ethylene glycol) methyl ether – average M_n ~2,000, flakes

Product Number:	**202509**
CAS Number:	9004-74-4
MDL:	MFCD00084416
Formula:	CH3(OCH2CH2)nOH

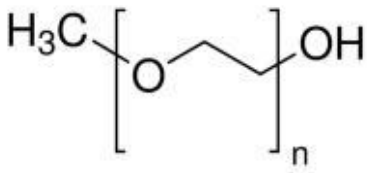

TEST	Specification
Appearance (Color)	White to Off-White
Appearance (Form)	Flakes
Infrared spectrum	Conforms to Structure
Molecular Number	1800 - 2200
pH C=5%, H2O at 25 Degrees Celsius	4.5 - 7.5

Specification: PRD.1.ZQ5.10000017243

3050 Spruce Street,Saint Louis,MO 63103,USA
Website: www.sigmaaldrich.com

Email
USA:

techserv@sial.com
Outside USA: eurtechserv@sial.com

Product Specification

Product Name:
Triethylamine ≥99.5%

Product Number:	**471283**
CAS Number:	121-44-8
MDL:	MFCD00009051
Formula:	C6H15N
Formula Weight:	101.19 g/mol

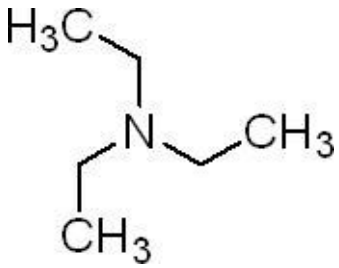

TEST	Specification
Appearance (Color)	Colorless
Appearance (Form)	Liquid
Infrared spectrum	Conforms to Structure
Purity (GC)	99.50 %
Water (by Karl Fischer)	0.1 %

Remarks:
Specification Date : 11/24/2010